



Escuela Universitaria de
Ingeniería
Técnica Industrial
Universidad Zaragoza



Universidad Zaragoza

PROYECTO FINAL DE CARRERA
Seismic and vibration signal analysis
and monitoring using LabVIEW

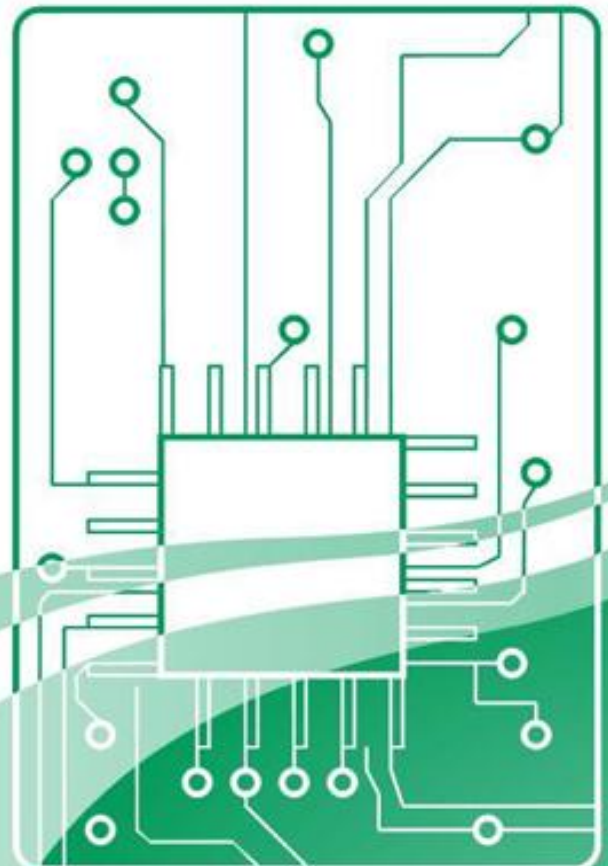
AUTOR
Mariano Martínez

Desarrollado en programa de
intercambio en:



University of Central Lancashire

DIRECTOR
Simon Platt(UCLAN)
SUPERVISOR UNIV.ZARAGOZA
Antonio Bono
ESPECIALIDAD
Electrónica
CONVOCATORIA
Junio 2012



School of Computing, Engineering
and Physical Sciences

MARIANO MARTINEZ
**SEISMIC AND VIBRATION SIGNAL
ANALYSIS AND MONITORING
USING LabVIEW**
(EL3990)

Submitted in partial satisfaction of the
requirements for the degree of

Bachelor of Engineering (with Honours)
in
1. Electronic Engineering
April 2012

I declare that all material contained in
this report, including ideas described in
the text, computer programs and
drawings, is my own work except
where explicitly and individually
acknowledged.

Signed

Date

Abstract

Every year there are around 20 earthquakes of magnitude 7 or above (PREPA.R.E, 2008). This kind of seismic events are potentially destructive and can cause several structural damage, economic and human loss. In order to perform an efficient risk management and prevention work geophysics must be equipped with suitable software and hardware tools. Seismic studies comprise not only risk management but earth structure studies that are useful in gas and oil prospections. Vibration monitoring has also turned in a very useful scientific approach to deal with structural safety and maintenance. Among these devices, MEMS accelerometer combines great performance with low costs, characteristics that have made it one of the most popular devices when it comes to this task. (Santoso, 2010).

Seismic analysis software has been developed using LabVIEW. The software decodes SAC data files and retrieves important seismic parameters like arrival wave times, location and magnitude. The precision and performance reached is acceptable for the scope of this project and it could be used as a domestic seismic analyser but not for its use in a professional seismic station. The seismic data for the system evaluation was retrieved from IRIS database. (IRIS, 2011)

A vibration DAQ and monitoring module has been designed and implemented. It successfully measures and monitors acceleration versus time and the signal's spectra. Zooming options were included in order to make easier the background noise and ambient vibration study (Attri R. K., 2004). An instant and maximum earthquake intensity gauge was programmed to give an idea of the experienced event potential danger. The user can selectively save acceleration time responses in LVM format.

An analogue output was implemented. It is capable of reading acceleration versus time responses saved in LVM and SAC files and output them using a DAQ card analogue output function. This voltage can be seen in an oscilloscope or input to other devices.

In order to acquire and save the analogue waveforms created with the previous function an analogue input was included as an initial objective in the Scheme of Work. However, it was dropped in the final implementation because it was considered that its function was too similar to the vibration DAQ module and it did not have enough practical application.

Acknowledgements

I would like to take this opportunity to express my gratitude to all the academic staff that has helped me during the development of this final project. Particularly to Simon Platt for sharing his knowledge, the orientation, material lent and the doubts solved. I'd also like to express my gratitude to David Heys in whose SIC tutorial sessions I sometimes had project related enquiries. I would like to show my appreciation to the Stores staff for their kindness, good work and also for the patience showed the busy laboratory days. I wouldn't like to forget University of Zaragoza professors, as the knowledge obtained in their lessons were essential to bring this project into a conclusion. I would like to show my appreciation to the UCLAN instruction for giving me the opportunity of studying here this year and the budget assigned to buy the materials I needed for the project execution. Many thanks to the Google team as their search tool has saved me enormous amounts of time being a key tool during the great amount of background information I had to research.

Table of contents

Abstract.....	3
Acknowledgements.....	4
Table of contents	5
List of tables	7
List of equations.....	7
List of figures.....	8
List of abbreviations.....	11
1. Introduction	12
1.1 Motivation.....	12
1.2 Aim and objectives	13
1.3 Scope.....	14
1.4 Literature review	15
2. Background	18
2.1 Vibration Monitoring Instrumentation Systems	18
2.1.1 Introduction and applications.....	18
2.1.2 Instrumentation Systems for Data Acquisition	18
2.1.3 Vibration transducers	19
2.1.4 Accelerometers.....	20
2.1.5 Acceleration, intensity and damage	20
2.2 Seismological data analysis	22
2.2.1 Introduction to earthquakes and seismic waves	22
2.2.2 Measuring and recording seismic data.....	24
2.2.3 Seismic Data	25
2.3.4 Seismic Data in LabVIEW. SAC format	25
2.3.5 Earthquake parameters computation overview	26
2.3.6 Processing timing parameters	28
2.3.7 Processing location parameters	30
2.3.8 Processing magnitude parameters	31
3. Vibration Monitoring System Design	35
3.1 Hardware.....	35
3.1.1 Accelerometer choice.....	35
3.1.2 DAQ selection.....	37
3.1.3 Data acquisition structure.....	39
3.1.4 Signal conditioning	40

3.1.5 ADXL203EB Evaluation board	43
3.1.6 Enclosure and mounting.....	43
3.1.8 PCB	45
3.1.9 EMI/EMC considerations	46
3.2 Software	47
3.2.1 Global software framework	47
3.2.2 DAQ.....	47
3.2.3 Axis calibration.....	47
3.2.4 Earthquake intensity and danger	48
3.2.5 Display characteristics and saving options	49
4. Seismological data analysis software design	50
4.1 Introduction and Specifications	50
4.2 Data format selection	50
4.3 Global software framework	51
4.4 Reading SAC files.....	51
4.5 Frequency analysis and optional filtering	52
4.6 Arrival times	52
4.6.1 Introduction.....	52
4.6.2 Automatic picking.....	52
4.6.3 Manual picking	55
4.7 Coda length	55
4.8 Distance to the epicentre.....	56
4.9 Magnitude	58
5. Analogue output design.....	60
6. Vibration monitoring system construction and implementation	61
6.1 Hardware.....	61
6.2 Software	62
7. Seismological data analysis software implementation.....	64
8. Analogue output software implementation	69
9. Dataflow and Interface	70
10. System evaluation and results	72
10.1 Vibration DAQ evaluation	72
10.2 Seismic analysis evaluation	75
10.3 Analogue output evaluation	86
11. Future work: Potential improvements and modifications.....	87

12. Conclusion.....	89
Appendix A: Detailed Seismic analysis software.....	91
Appendix B: Detailed Vibration DAQ software	106
Appendix C: Detailed analogue output software.....	110
Appendix D: Brief Instructions for use	113
Appendix E : Planning documents	117
Appendix F: DAQ Circuit and PCB plans	119
Appendix G: DAQ hardware components list	126

List of tables

Table 2.1: Mercalli intensity scale relationship with PGA (PREPA.R.E, 2008).....	22
Table 2.2 Seismic data global computation	27
Table 2.3: Approximate Magnitude vs Size equivalence	32
Table 3.1: Input range and resolution for NI 6221	38
Table 10.1 Software magnitude calculations evaluation. Comparison with magnitude of different data retrieved from ISIS	78
Table 10.2 Coda magnitude characteristics verification.....	79
Table 10.3 Threshold determination for different earthquakes	81
Table 10.4: Automatic and manual picking comparison	82
Table G.1 DAQ hardware component list	126

List of equations

Equation 2.1: STA and LTA equations	28
Equation 2.2: Distance formulas.....	31
Equation 2.3: Local magnitude	32
Equation 2.4: Coda/duration magnitude	32
Equation 3.1: Anti-aliasing condition	38
Equation 3.2: Satisfactory conversion time demonstration	38
Equation 3.3: Cut-off frequency and added capacitors relationship (Analog Devices, 2011)	41
Equation 3.4: Accelerometer noise.....	41
Equation 4.1: STA/LTA ratio equations	52
Equation 4.2: Coda length.....	56

List of figures

Figure 1.1: Software main structure	13
Figure 1.2: Global software specifications	15
Figure 2.1: DAQ general structure	18
Figure 2.2: Earthquake origin. Image by Taiwanese Central Weather Bureau (Central Weather Bureau, 2012).....	23
Figure 2.3: P waves Figure 2.4 S waves.....	24
Figure 2.5: STA LTA algorithm illustration (Han, 2010).....	29
Figure 2.6: Coda length illustration.....	30
Figure 2.7: Generic depth distance travel time dependence and epicentre plotting (Havskov & Ottemöller, 2010)	31
Figure 2.8: Coda Magnitude parameters in different areas of the world (Havskov & Ottemöller, 2010)	33
Figure 2.9: Magnitude scale conversion table (Havskov & Ottemöller, 2010)	34
Figure 3.1: Hardware block diagram	39
Figure 3.2: Schematics design	40
Figure 3.3: Connection scheme used	42
Figure 3.4: BNC 2120 GS input	42
Figure 3.5: ADXL Evaluation board.....	43
Figure 3.6:1591XXMS Dimensions	44
Figure 3.7:1591XXMS 3D model.....	44
Figure 3.8:PCB artwork	45
Figure 3.9: PCB 3D model.....	46
Figure 3.10: Vibration DAQ software framework	47
Figure 3.11: Calibration subroutine flowchart.....	48
Figure 3.12: Magnitude and danger calculator subroutine	48
Figure 4.1 Seismic analysis software specifications.....	50
Figure 4.2: Global computation framework (Attri R. K., 2005).....	51
Figure 4.3: Read data flowchart.....	51
Figure 4.4: Automatic Arrival time picking global flowchart	53
Figure 4.5: STA/LTA ratio implementation subroutine flowchart	54
Figure 4.6: STA/LTA one sample subroutine flowchart	55
Figure 4.7: Pick arrival times subroutine	55
Figure 4.8: Coda length subroutine algorithm.....	55
Figure 5.1: Analogue output specifications	60
Figure 5.2: Analogue output flowchart.....	60
Figure 6.1 Vibration sensor device without the lid and header on which the evaluation board is mounted.....	61
Figure 6.2: Complete vibration sensor module.	61
Figure 6.3 code section comprising DAQ assistant and calibration VI.....	62
Figure 6.4: Vibration DAQ front panel	62
Figure 6.5: "Intensity and danger Display" VI in the vibration DAQ main code	63
Figure 7.1Seismic analysis VI front panel.....	64
Figure 7.2Code sections where the mentioned SubVIs are used	65

Figure 7.3 Seismogram and its spectra	65
Figure 7.4 Filtering options in the seismic analysis front panel.....	66
Figure 7.5 : STA LTA ratio and Pick arrival times VIs in the main seismic code	66
Figure 7.6 STA/LTA ratio VI front panel. The figure shows an earthquake seismogram, the STA/LTA ratio and the STA and LTA waves for specific L1 and L2 window lengths	67
Figure 7.7 Cursors and controls for manual picking in the seismic analysis VI front panel(left) and the loop that actualises coda length and S-P when the use modifies arrival times.	68
Figure 7.8 "Coda length" VI in the main seismic code	68
Figure 7.9: Distance to the epicentre subVI placed in the seismic analysis code.....	69
Figure 7.10: Magnitude controls and indicators in the front panel.....	69
Figure 8.1: <i>Analogue output</i> VI front panel	70
Figure 9.1: Example of the event structure continuously used in the software. The External loop keeps it running. The shift registers and local variables can be seen.....	71
Figure 9.2: Main menu interface	71
Figure 10.1: Hardware system distribution for vibration DAQ and output testing	72
Figure 10.2: Accelerometer voltage outputs when tilted so that the two axes support different accelerations	72
Figure 10.3: DAQ front panel when running.....	73
Figure 10.4: Light table hitting (Y axis) time and frequency responses	73
Figure 10.5: Strong enclosure hitting (X axis) time responses.....	74
Figure 10.6: Strong shaking time and frequency responses.....	74
Figure 10.7: Heavy shaking time and frequency responses	75
Figure 10.8 Software distance calculations compared to USGS Distance vs S-P time table	77
Figure 10.9: STA/LTA ratio VI front panel	80
Figure 10.10: Averaged threshold.....	82
Figure 10.11: Coda length calculator problem	84
Figure 10.12: Non- filtered seismogram	85
Figure 10.13: Seismogram spectra.....	85
Figure 10.14: Filtered seismogram. Low cut-off = 0. 01 Hz. High cut-off =1 Hz.....	85
Figure 10.15: Analogue output front panel running and reading a SAC file.....	86
Figure 10.16: LVM vibration file reading and analogue output.....	86
Figure 10.17: SAC file reading and analogue output	87
Figure A. 1: Seismic analysis VI front panel.....	91
Figure A. 2: Seismic analysis VI global structure. Timeout event.	91
Figure A. 3: Seismic analysis VI. Read file event	92
Figure A.4 Seismic analysis VI. Automatic picking event	92
Figure A. 5: Seismic analysis VI .Frequency analysis event	93
Figure A. 6:Seismic analysis VI.Filter event.....	93
Figure A.7: Seismic analysis VI. Calculate distance event	94
Figure A.8: Seismic analysis VI. Calculate magnitude event	94
Figure A..9: Seismic analysis VI. Stop event.	95
Figure A.10: Read SAC VI icon	96
FigureA.11: Retrieve properties VI block diagram.....	97
Figure A.12: STA LTA ratio front panel.....	98
Figure A.13: STA LTA ratio VI Start event and global VI structure	99

FigureA.14:STA LTA ratio VI BACK event.....	99
FigureA.15: STA LTA one sample VI icon.....	100
Figure A.16:STA LTA one sample block diagram.....	100
Figure A.17: Pick arrival times VI icon.....	101
Figure A.18: Pick arrival times VI block diagram.....	101
FigureA.19: Frequency analysis VI icon.....	102
FigureA.20: Frequency analysis VI front panel	102
FigureA.21: Frequency analysis VI block diagram.....	103
Figure A.22: Distance to the epicentre icon	103
Figure A.23: Distance to the epicentre block diagram	103
Figure A.24: Distance to the epicentre case structures.....	104
Figure A.25 Coda length meter	104
FigureA.26: Coda length meter VI block diagram.....	104
Figure A.27: Gather signals below a threshold VI icon	105
Figure A.28: Gather signals below a threshold block diagram (NI Instructors, 2011)	105
Figure B.1: Vibration DAQ VI front panel.....	106
Figure B.2: Vibration DAQ event structure. Timeout.....	106
Figure B.3: Vibration DAQ VI. Acquire event	107
FigureB.4: Vibration DAQ VI Main menu event	107
FigureB.5: Vibration DAQ VI pause event	108
FigureB.6: Axes calibration VI icon.....	108
FigureB.7: Axes calibration VI block diagram.....	108
FigureB.8: Intensity and danger display VI icon.....	109
Figure B0.9: Intensity and danger display VI front panel.....	109
FigureC.1: Analogue output VI front panel.....	110
FigureC.2: Analogue output VI .Timeout event	110
Figure C.3: Analogue output VI. Read file event.	111
Figure C.4: Analogue output VI. Start output event.	112
Figure C. 5: Analogue output VI. Back event	112
Figure D.1: Seismic analysis main window instructions.....	113
Figure D.2: STA LTA ratio VI front panel instructions	114
Figure D.3: Vibration DAQ VI instructions	115
Figure D.4: Analogue output VI instructions.....	116
Figure D.1: Gantt diagram.....	117
Figure D.2: Risk register	118

List of abbreviations

ADC – Analogue to digital conversion

AO – Operational amplifier

BGS – British Geological Survey

BNC – British Naval Connector

COSMOS –The Consortium of Organizations for Strong-Motion Observation Systems

CSMIP – California Strong Motion Instrumentation Program

DAQ – Data acquisition

GSEC – Group of Scientific experts

IEPE – Integral Electronics Piezoelectric

IRIS – Incorporated Research Institutions for seismology

K-NET – Kyoshin Net

LCC – Leadless chip carrier

LTA – Long-time average

LVM - LabVIEW Measurement file

MEMS – Microelectromechanical systems

MMIS – Modified Mercalli Intensity Scale

NIED – National Institute for Earth Science and Disaster Prevention

PCB – Printed circuit board

PGA – Peak Ground Acceleration

SA – Spectra acceleration

SAC – Seismic Analysis Code

SCEDC – The Southern California Earthquake data center

SEED – The Standard for the Exchange of Earthquake Data

SNR – Signal to noise ratio

STA – Short time average

USGS – US geological Survey

VI – Virtual instrument (LabVIEW)

1. Introduction

1.1 Motivation

Last spring, on March 11th of 2011 immediately after the earth shook in Japan there were alarms throughout their entire east coast warning people to head towards highest places. Furthermore, the trains and underground of Tokyo actually stopped before the dangerous surface waves reached the city to prevent derailments. Meanwhile, the passengers were warned some seconds before the trains started to swing. Most of the buildings that compound Tokyo's skyline were swaying instead of collapsing since sooner or later a large earthquake was expected. These preventing actions were possible thanks to a well-developed science that is lately making huge steps thanks to the new technologies to detect signals and store, analyse and monitor data efficiently so that the specialists can work fast and precisely. It is not necessary to go to Japan to experience earthquakes, here in Britain microseisms occur every year and although hardly perceptible by human, they are used by the experts to study the earth structure (British Geological Survey, 2012). There are no more tremors now than 100 years ago. Nevertheless, due to the increasing population in the globe the effects have become devastating and the human and structural loss unacceptable. Geophysics and structural engineers need modern tools to face this challenge, and this was the central stimulus to focus my work on this issue (Attri R. K., 2004). The analysis of seismological events also allows the geophysics to determine the earth structure; they perform a key role in the detection of cavities and therefore are essential to obtain data on oil and gas prospection.

The acquisition of seismic data involves complex DAQ systems, proper locations, infrastructure and expensive sensors like seismometers, geophones or special accelerometers. (Turk et al, 2011). The monitoring and assessment of the vibrations that affect structures during an earthquake, other events or just the study of noise level vibration are essential to save lives, minimize damage as well as to aid with the maintenance of a structure and detect possible failures. Usually, traditional instrumentation systems to monitor structure and noise level vibration are complex and expensive. There is an increasing demand of better and cheaper monitoring systems and the low cost signal-conditioned MEMS accelerometers are among the devices that possibilities these features in a system. (Wenzel & Pichler, 2005) (Santoso, 2010)

LabVIEW is a comprehensive graphic programming language and development environment established by National Instruments which is loved among engineers that can see the flow of the data rather than text based programming. LabVIEW is industry standard software for

instrumentation, signal processing and control. In terms of employability LabVIEW knowledge is highly valued by managers because it helps to improve and accelerate productivity (Haugen, 2008).

The final project is the last step before jumping into the engineering job environment, therefore, while selecting the requirements of the tasks there has been both functional and training considerations. The specifications have been selected so that at the end of the project usual functions of LabVIEW have been mastered and work on instrumentation, analogue input, signal processing and analogue output has been performed.

1.2 Aim and objectives

The monitoring and analysis of vibrations and Earthquake seismic signals are crucial to deal with structural, industrial and safety problems, as well as to tackle geological issues.

The aim of this project was to develop a useful monitoring system to provide experts of those fields useful information to work with.

To accomplish this, the objectives were:

1. To develop a vibration monitoring system using a MEMS accelerometer
2. To create software to analyse and monitor earthquake seismic data to display the main parameters of these events.
3. Output of voltage simulated seismic signals based on existing data.

The software was developed using LabVIEW in a personal computer.

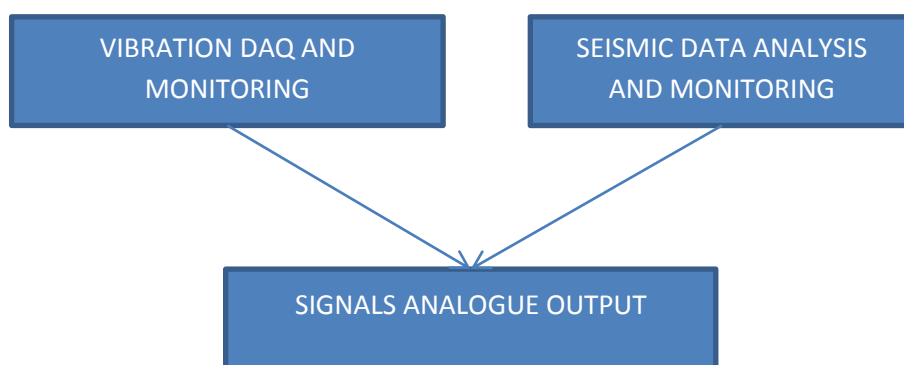


Figure 1.1: Software main structure

1.3 Scope

It is obvious that in a seismological project the sense of real seismic waves would have been preferable. The measurement of seismic signals in Britain is extremely challenging due both to its rare nature and the cost of the installation of proper sensors as seismometers, geophones or special accelerometers (Turk et al, 2011), far above the resources available. Taking this into account the measurement of general vibration was selected as more suitable.

The device is intended to be appropriate to measure ambient vibration of ground and walls in a building, detecting also the potential damage of those tremors for building up to about 7 stories (see 2.1.5 Acceleration, intensity and damage). Notice that to accurately identify large structures condition, several data from different points are required. The DAQ developed meets the requirements to categorise the condition in very small structures, a network with a master-slave structure is needed if the area of study is significant. It is not the purpose of this project to develop such network, it will be suggested as a future widening of the work though.

Nowadays most of the seismic stations capture data in different channels. Sensors are distributed through different places to cover the all the axis the best way possible, some of the relevant parameters of a seismic event –as the important phase picking – are computed using several of these channels to prevent faults and improve the reliability and precision (Havskov & Ottemöller, 2010). That task involves advance software that is out of the reach with the time and resources accessible. However, although the precision and reliability are not going to be the same, the earthquake parameters can be obtained from a single channel (Attri R. K., 2005). What is more, these computations are often the first step before going beyond and often can be good enough to contribute with important information. Hence, the scope of the project is going to extract relevant information from one single channel at a time.

The analogue output of the NI PCI-6221 DAQ card has been used to generate voltage simulated seismic and vibration signals based on existing data. These outputs signals can be for example displayed in an oscilloscope or input in other devices. For example, it could be a starting point to develop a shaking-table that simulates the earth movement during an event. The signals are not synthetic but based on existing data from seismic data bases in the interned or vibration data measured and recorded previously.

To clarify the scope of the project the following table display the functions that have been developed:

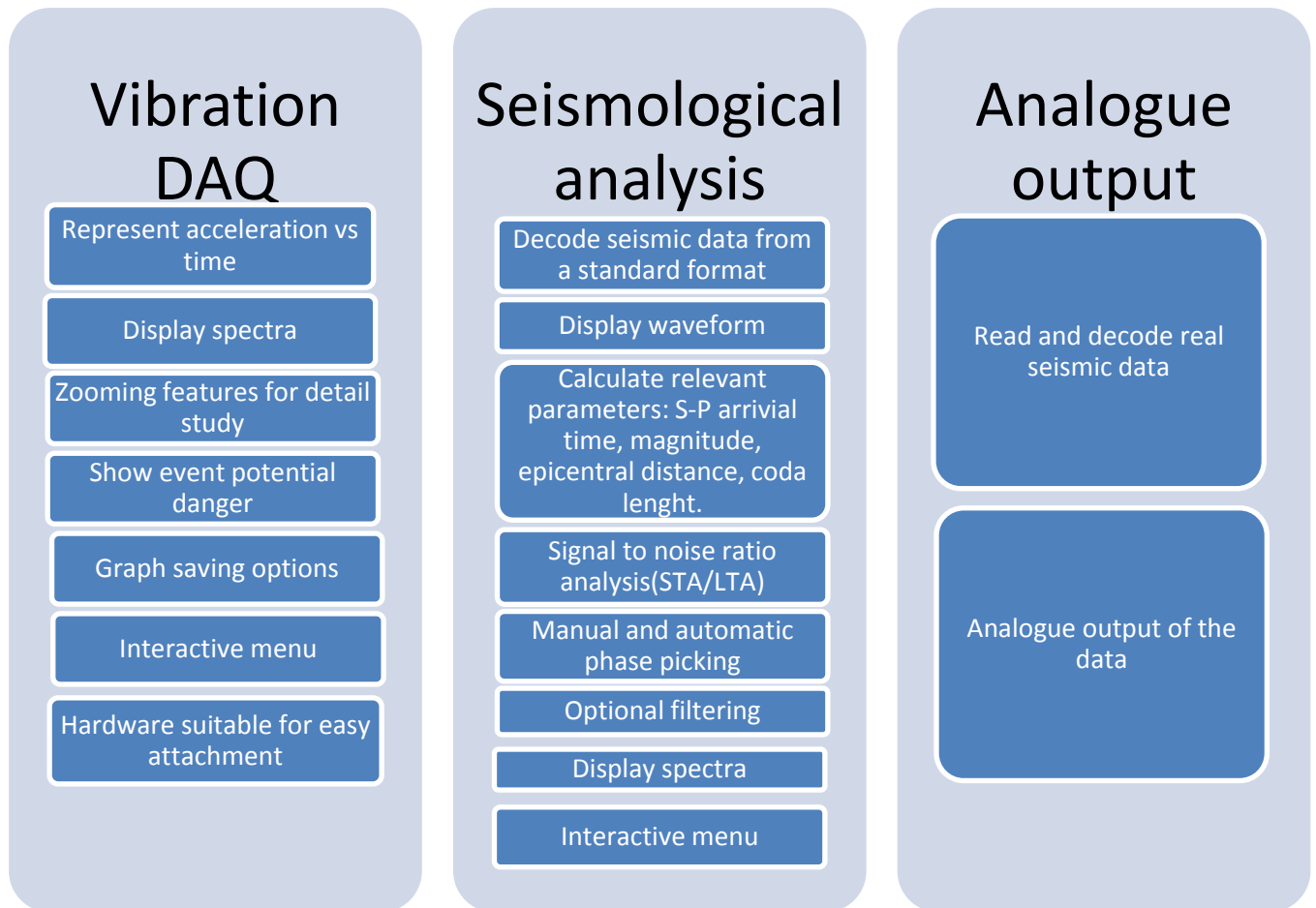


Figure 1.2: Global software specifications

1.4 Literature review

The literature search and study has been very intense and important in this work in order to acquire the necessary background knowledge and abilities. With no previous geophysics and geo-instrumentation knowledge, the time prior the design start was longer than expected. The advanced internet searching tools and free resources available from various institutions and webpages had a central role to gather the required material. It is doubtful that the same results would have been achieved without these tools. The relevant literature for the design understanding is summarized in chapter 2, in this section a critical analysis about the information sources handled is going to be performed.

Regarding the seismic wave origins, Havskov & Ottemöller (2010) make a very detailed description of the processes and elements that cause the seismic signals. The description presented has been considered too exhaustive to be included in the background(Chapter 2) Alternative sources as Attri R. K (2004) or the British Geological Survey (2011) have been

estimated as more suitable. The British institution was chosen for being a local organization, its significance and the clear and simple explanations that it provides.

Routine data processing in earthquake seismology (Havskov & Ottemöller, 2010) is one of the key books that have been used. It offers an impressive amount of relevant information, some of it at advanced geo-physical level but always oriented to readers that not necessarily have previous knowledge about the topic. Its most notable contributions were the seismic signal measuring and processing, data formats and seismic parameters. Although seismic data format descriptions were found in different sources it was the only resource that gathered all them together and discussed differences and applications.

Concerning the data sources, the amount of websites of institutions supplying this information has been greater than expected but only the ones with a clear interface have been pre-selected [(British Geological Survey, 2012) (European Strong-Motion Database, 2000) (IRIS, 2011) (NIED, 1996) (SCEDC, 2011)]. Some of these pages presented a poor and unclear retrieval display and explanations about the data available. Therefore, they have been discarded. The final data has been retrieved from IRIS and the British Geological Survey. However, after further analysis BGS data exhibited too much noise, probably because most of its sources are non-professional stations located in schools. The small magnitude of the earthquakes in this part of the world sure has contributed to the noisy seismograms.

There is a lack of information about the management of earthquake signals with labVIEW, to deal with this kind of data there are standard specific programs and these are more used by the experts of this field. It is not easy to find an earthquake strong motion project developed with LabVIEW in the internet. The development of an analysis program using labVIEW has been measured interesting particularly in two points. As a standard in industry and science it is a key ability in the formation of an engineer so one of the aims of the project is to master this important tool. Also, creating an analysis program using an industry standard like LabVIEW can be a good contribution to the existing tools as it will make this field more accessible to engineers and scientifics that are not directly related with the world of seismic events.

Attri R.K(2005) offers a good approach to the single wave seismic parameters computation. Nevertheless, the occurrence and arrival times computation methods are barely sketched and it is impossible to develop the software from that information. One of his references (Munro K. , 2004) details the STA/LTA averaging method and is the thread to a couple of thesis

where different types of arrival pickings techniques as well as other signal processing and analysis procedures are described and evaluated in detail. (Munro K. A., 2005) (Han, 2010).

Wenzel et al (2005) explain ambient vibration based methods for structure assesment. Nevertheless, the instrumentation used, approaches and structures assessed are beyond the scope of this project. The accerometers cited measure μg , no low cost accelerometers with that resolution were found. UCLAN discovery gave access to a convenient paper that deals with structural low cost vibration monitoring system (Santoso, 2010). It also provides useful information about MEMS accelerometers.

The literature about specifications and usage of accelerometers in this field has been abundant. The most valuable information has been retrieved from practical tips in some internet magazines and private companies notes comprising mounting and parameter description (Endevco, 2006) (Barnes, 2011) (Lent, 2009).

The US geological Survey webpage publish important educational material which has been handled for testing – arrival times vs distance tables. It was also the base along with another paper (PREPA.R.E, 2008) to retrieve the earthquake intensity and danger information that was later implemented in the vibration DAQ software. USGS excels giving simple but precise earthquake related parameter definition while the paper provides a worthwhile acceleration-intensity relationship.

2. Background

2.1 Vibration Monitoring Instrumentation Systems

2.1.1 Introduction and applications

Monitoring and sensing are key processes when investigating or evaluating vibration exposure in scientific, industrial or structural fields. The vibration is originated in the object of study due to its work conditions as for example a bridge while cars are crossing it or some equipment while working with engines attached to them. Sensors are needed to measure this signals.

When the input vibration origin is not fully known the tremors are called ambient vibration and the study of the –mostly – noise level produced has a margin of uncertainty. Many man-made structures have what is called a “vibration signature”, behaviour which, if appropriately measured and analysed, can report important data about the load-bearing or damage of a structure (Wenzel & Pichler, 2005). Efficient and economic systems and sensors are increasingly on demand to perform vibration based maintenance and safety monitoring, analysis and evaluation.

2.1.2 Instrumentation Systems for Data Acquisition

An instrumentation system for data acquisition (DAQ) that senses, conditions and translates to digital the measured information is needed so that the signal is properly applied to the processing system. The fundamentals of DAQ can be seen in the following chart:

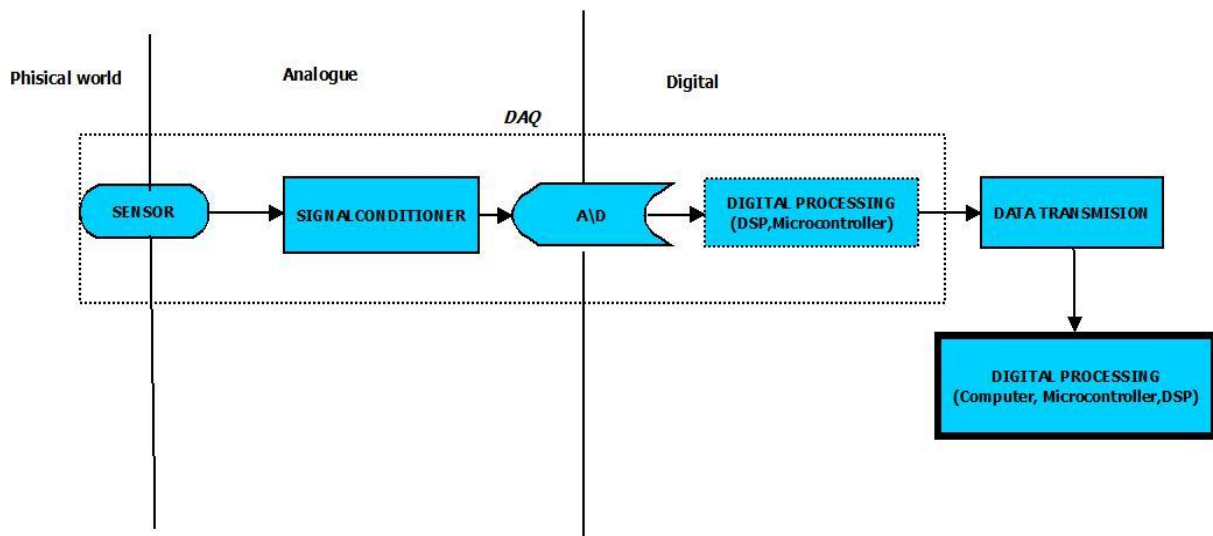


Figure 2.1: DAQ general structure

- **Sensors:** A sensor translates a physic magnitude into an electric signal that can be read by the commonly used instrumentation. There are common parameters to all of them like range or span, accuracy, precision, tolerance and sensitivity. Linear and non-linear sensors are available in the market; in almost all circumstances linear sensors are preferred because of its easy handling. Therefore, a linearization process is often carried out on non-linear devices. Several physic magnitudes can be sensed nowadays. More information in 2.1.3 Vibration .
- **Signal Conditioning:** In this stage, the electrical signal measured by the sensor is turned into a signal easier to treat, store, convert to digital or displayed on a screen.
- **A/D Conversion:** The signals in the physic world are analogue, however, today almost all of the processing systems are digital. A circuit that performs the translations is required.
- **Digital Processing:** Depending on the processing, the systems can be classified as centralised, decentralised and distributed. While centralised systems just require one processing stage – and hence, just one computing device – the other two involve a previous processing phase before sending the data to the main computational system. The processing hardware that can handle these includes DSP (Digital Signal Processors), microcontrollers, automatons and even personal computers.
- **Data Transmission:** Frequently, the signal acquired by the DAQ has to be sent a certain distance for its process, display or storage. The common techniques include Electromagnetic waves (radio, infrared...), Laser (fibre optics) and Electrical signals. The signal can be encoded using voltage, current or frequency patterns and can be either digital or analogue.

2.1.3 Vibration transducers

There are several motion transducers (motion sensors) that are used in industry for mechanical vibrations measurements. This large set includes:

- **Potentiometers:** Displacement transducers. The output voltage is related to the displacement; $V_0 = kx$. Where k is a constant and x the displacement.
- **Variable inductance transducers:** They are based on the following principle. When a flux linkage changes within an electrical conductor a voltage is generated. If the flux change is caused by motion, the mechanical energy is converted into electrical energy and hence, motion parameters are related with electrical magnitudes.

- **Self-induction transducers:** Based on the change of self-inductance when moving a ferromagnetic object in a magnetic field.
- **Variable capacitance transducers:** Transducers where displacement, velocity or acceleration depend on a capacitance.
- **Piezoelectric transducers:** Uses the piezoelectric characteristic of some materials. These materials generate an electrical charge that implies potential difference when exposed to mechanical stress.

(De Silva, 2007)

2.1.4 Accelerometers

Accelerometers are transducers of acceleration into a proportional voltage.

The most usual technologies are:

- Piezoelectric accelerometers
- Piezoresistive accelerometers
- Variable capacitance accelerometers

Except for extremely low frequency seismic measurements, piezoelectric accelerometers are the most popular for vibration and seismic sensing. The characteristics that make them suitable are a large bandwidth, high sensitivity and resolution along with their easy use. Among the piezoelectric accelerometers nowadays the IEPE is dominating the market. Due to its incorporated charge amplifier, it just requires normal wire connections without external components. (Lent, 2009)

It is difficult to find a piezoelectric accelerometer for less than £100 or £200. The last decade advances in MEMS technology have made possible to manufacture compact low cost MEMS accelerometers with a great performance and accuracy (Buckari, 2000). Nowadays, this technology is highly on demand in order to develop high-sensitive low cost structural vibration monitoring systems. It is available in different types and different axes can be measured with the same device. (Santoso, 2010)

2.1.5 Acceleration, intensity and damage

A particle attached to the earth will irregularly vary its acceleration when an earthquake occurs on the surface. The horizontal component of this acceleration is particularly interesting for the topic in study as the building codes define how much horizontal force a building can resist. Force is related to acceleration. The peak ground acceleration (PGA) is the maximum

acceleration that a particle suffers during the event. PGA is associated to the earth surface movement and it is a suitable danger indicator for short buildings up to seven floors; hazard for higher buildings can be measured by other parameters like SA (Spectral Acceleration). PGA is quite a simple parameter while SA depends on the building structure and complicates calculations (U.S. Geological Survey, 2010). While earthquake magnitude parameters are related to the power of an event, intensity parameters measure the effect that an earthquake has on buildings, persons and object. It measures the damage and varies within the affected zone. The Modified Mercalli Intensity Scale is the most widely used intensity scale in US. It is based on PGA (PREPA.R.E, 2008).

Modified Mercalli Intensity Scale

- I. Not felt except by a very few under especially favorable conditions.*
- II. Felt only by a few persons at rest, especially on upper floors of buildings.*
- III. Felt quite noticeably by persons indoors, especially on upper floors of buildings. Many people do not recognize it as an earthquake. Standing motor cars may rock slightly. Vibrations similar to the passing of a truck. Duration estimated.*
- IV. Felt indoors by many, outdoors by few during the day. At night, some awakened. Dishes, windows, doors disturbed; walls make cracking sound. Sensation like heavy truck striking building. Standing motor cars rocked noticeably.*
- V. Felt by nearly everyone; many awakened. Some dishes, windows broken. Unstable objects overturned. Pendulum clocks may stop.*
- VI. Felt by all, many frightened. Some heavy furniture moved; a few instances of fallen plaster. Damage slight.*
- VII. Damage negligible in buildings of good design and construction; slight to moderate in well-built ordinary structures; considerable damage in poorly built or badly designed structures; some chimneys broken.*
- VIII. Damage slight in specially designed structures; considerable damage in ordinary substantial buildings with partial collapse. Damage great in poorly built*

structures. Fall of chimneys, factory stacks, columns, monuments, walls. Heavy furniture overturned.

IX. Damage considerable in specially designed structures; well-designed frame structures thrown out of plumb. Damage great in substantial buildings, with partial collapse. Buildings shifted off foundations.

X. Some well-built wooden structures destroyed; most masonry and frame structures destroyed with foundations. Rails bent.

XI. Few, if any (masonry) structures remain standing. Bridges destroyed. Rails bent greatly.

XII. Damage total. Lines of sight and level are distorted. Objects thrown into the air.

(US Geological Survey, 2009)

MOD. MERCALLI SCALE	PGA(g)
IV	0.03 and below
V	0.03 – 0.08
VI	0.08 – 0.15
VII	0.15 – 0.25
VIII	0.25 – 0.45
IX	0.45 – 0.60
X	0.60 – 0.80
XI	0.80 – 0.90
XII	0.90 and above

Table 2.1: Mercalli intensity scale relationship with PGA (PREPA.R.E, 2008)

2.2 Seismological data analysis

2.2.1 Introduction to earthquakes and seismic waves

Seismic signals recorded by sensors in seismic stations have a regular pattern most of the time, this is called seismic noise. However, time to time there is an event; a seismic wave stands out of the background noise with a particular form easily recognised. The most

common source of seismic waves are earthquakes, these have a usual frequency between 0.001 and 4 Hz and can be detected from a considerable long distance. However, strong motion signals can be produced by man as well. For example, powerful explosions, or earth movements caused for natural gas extractions can cause these elastic waves. Nevertheless, excepting nuclear explosions, the range detection of these phenomena is far smaller than the one of a natural earthquake. (Kennett, 2009) (Havskov & Ottemöller, 2010).

The earthquakes are caused by the energy accumulation in the Earth's crust due to the relative movement of the two sides of a fault – discontinuity in volume of rock. When the stress limit is reached the event can be easily triggered and the rock is fractured around the weak points of the fault. The accumulated energy is suddenly released as an earthquake and seismic waves spread out from the rupture point, if they are very large can be extremely destructing in points near to the epicentre. (British Geological Survey, 2011)

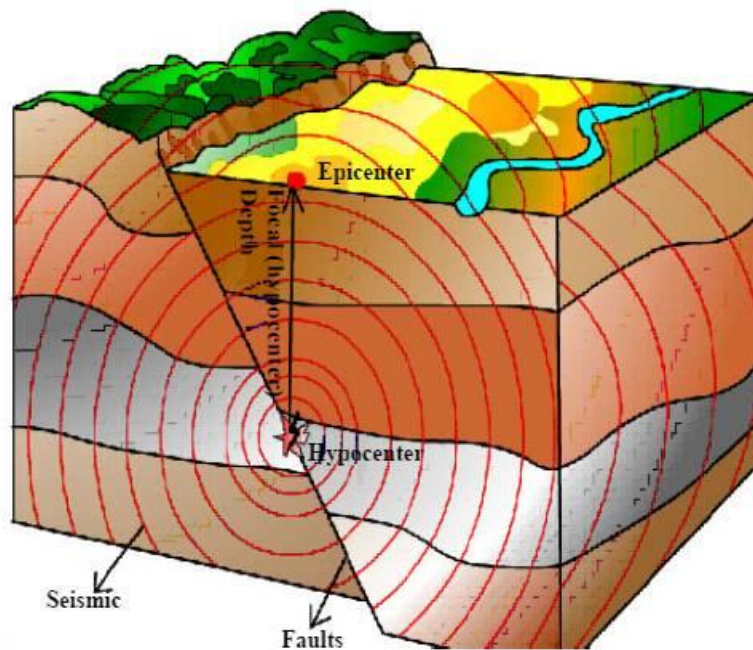


Figure 2.2: Earthquake origin. Image by Taiwanese Central Weather Bureau (Central Weather Bureau, 2012)

The sudden movement of a fault generates different kinds of seismic waves:

- P waves (Primary): Compressional waves. As the name indicates, they are the first to arrive. They feature typical speed values of 6 km/s in depths less than 15 km.
- S waves (Shear or Secondary): Arrive after P. Typical velocity of 3.5 km/s in the same conditions as P waves.

- Surface waves: They are waves that travel through the surface. Combination of S and P waves (Rayleigh waves) and multiply reflected and superimposed S waves (Love waves). Typical velocities between 3.5-4.5 km/s although they always arrive after S waves. (Havskov & Ottemöller, 2010)

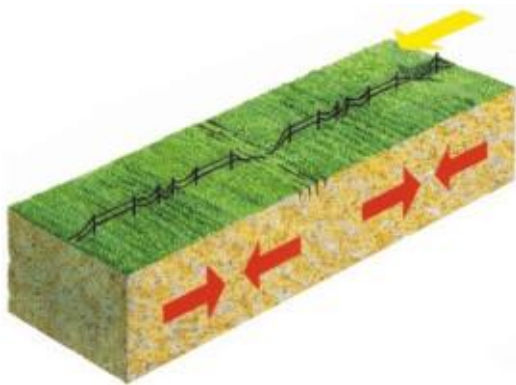


Figure 2.3: P waves

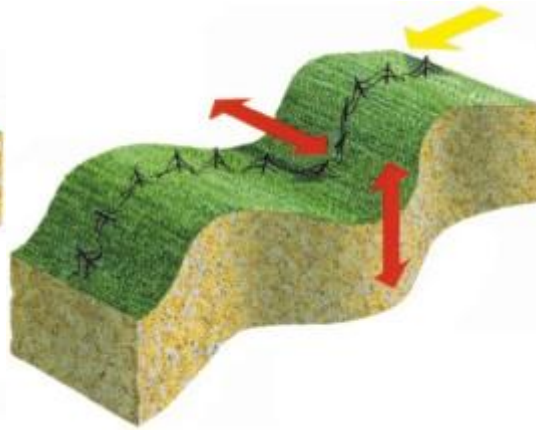


Figure 2.4 S waves

Pictures from British Geological Survey (2011).

2.2.2 Measuring and recording seismic data

The seismic signals can be recorded both locally and globally by seismic instruments. The typical sensors used for acoustic and seismic detection are seismometers, piezoelectric sensors, geophones and capacitive sensors. A seismic sensor outputs voltage proportional to the surface motion. Usually in a seismic station there are 3 sensors, one for each of the 3 axes. Nowadays, the data is stored only digitally after filtering and amplification processes, the use of a GPS at the same time has solved the problem of a proper timing stamp of the records. (Havskov & Ottemöller, 2010)

As a result of the increasing number of stations recording data around the world there is a good amount of this kind data in the internet. Although in most cases after formal request, different governments, universities and scientific organizations supply this data to whoever wants to use it. Examples of these organizations are:

- IRIS (Incorporated Research Institutions for Seismology) (IRIS, 2011)
- British Geological Survey (British Geological Survey, 2012)
- European Strong-Motion Database (European Strong-Motion Database, 2000)
- The Kyoshin Net (K-NET) (NIED, 1996)
- Southern California Earthquake Data Centre (SCEDC, 2011)

2.2.3 Seismic Data

Havskov & Ottemöller(2010) state about waveform formats “*Each channel of seismic waveform data consists of a series of samples (amplitude values of the signal) that are normally equally spaced in time (sample interval). Each channel of data is headed by information with at least the station and component name (see below for convention on component name), but often also network and location code (see below). The timing is normally given by the time of the first sample and the sample interval or more commonly, the sample rate. Some waveform formats (e.g. SAC) can store the timing of each sample.*”

There are several formats for strong motion data; we can classify them in three big groups according to the purpose:

- **Recording formats:** The specific purpose of past data was just to be recorded and saved, these format were not very suitable for processing. Most of the data nowadays have to be able to be processed.
- **Processing formats:** Appropriate for processing without any modification. An example is .SAC of which further details will be given later in 2.3.4 Seismic Data in LabVIEW. SAC format.
- **Data exchange formats:** The data exchange formats are the most complete data available nowadays as all the information is included, the GSE(Group of Scientific Experts) and SEED (Standard for the Exchange of Earthquake Data) are examples. A variant of this last one seems to be becoming the standard both for exchange and processing, miniSEED. (Havskov & Ottemöller, 2010)

The examples above are some of the most common type of data. However, there are a great amount of formats and sometimes even each institution has its own. For example CSMIP (California Strong Motion Instrumentation Program) or COSMOS (Consortium of Organisations for Strong-Motion Observation System).

2.3.4 Seismic Data in LabVIEW. SAC format

Plug--ins for the following data are available for LabVIEW

- COSMOS
- CSMIP
- European Strong-Motion Database Format.
- K-Net Strong Motion Data Format files.

- SAC Strong Motion Data files.
- SMC Strong Motion Data Format files.

(National Instruments, 2011)

A particularly interesting format for this project development is SAC, as it is possible to obtain this type directly and very easily from the biggest database found, IRIS, and the local British Geological Survey also offers data in this format.

IRIS website defines SAC as

“SAC (Seismic Analysis Code), previously SAC2000, is a general-purpose interactive program designed for the study of sequential signals, especially time-series data. Emphasis has been placed on analysis tools used by research seismologists in the detailed study of seismic events. Analysis capabilities include general arithmetic operations, Fourier transforms, three spectral estimation techniques, IIR and FIR filtering, signal stacking, decimation, interpolation, correlation, and seismic phase picking. SAC also contains an extensive graphics capability. Versions are available for a wide variety of computer systems. SAC was developed at Lawrence Livermore National Laboratory and is copyrighted by the University of California. It is currently being developed and maintained by a small group of developers working in cooperation with IRIS.”

(IRIS, 2011))

Its data format -.SAC- works in different platforms as UNIX, LINUX or MAC and the data can be either in binary or ASCII. It is a processing format. (Havskov & Ottemöller, 2010). The amplitude of available data in IRIS and BGS is mostly given in nm/s.

2.3.5 Earthquake parameters computation overview

Seismic software should include a suitable interface along with analytical software to study the seismic signal. The computational process starts with the retrieval of raw analogue data in a PC in which the parameters that are relevant to seismologist are calculated.

The parameters that are of interest to seismologists are:

- Timing parameters
- Location parameters
- Magnitude Parameters
- Intensity parameters

This project is focused on the first three aspects; therefore, background information about them is going to be provided below. Notice that usually, to calculate location parameters, timing parameters are required and, to obtain magnitude, location parameters are also a prerequisite.

The figure underneath describes the computational process that is usually carried out by the specialized software from an analogue seismological raw signal.

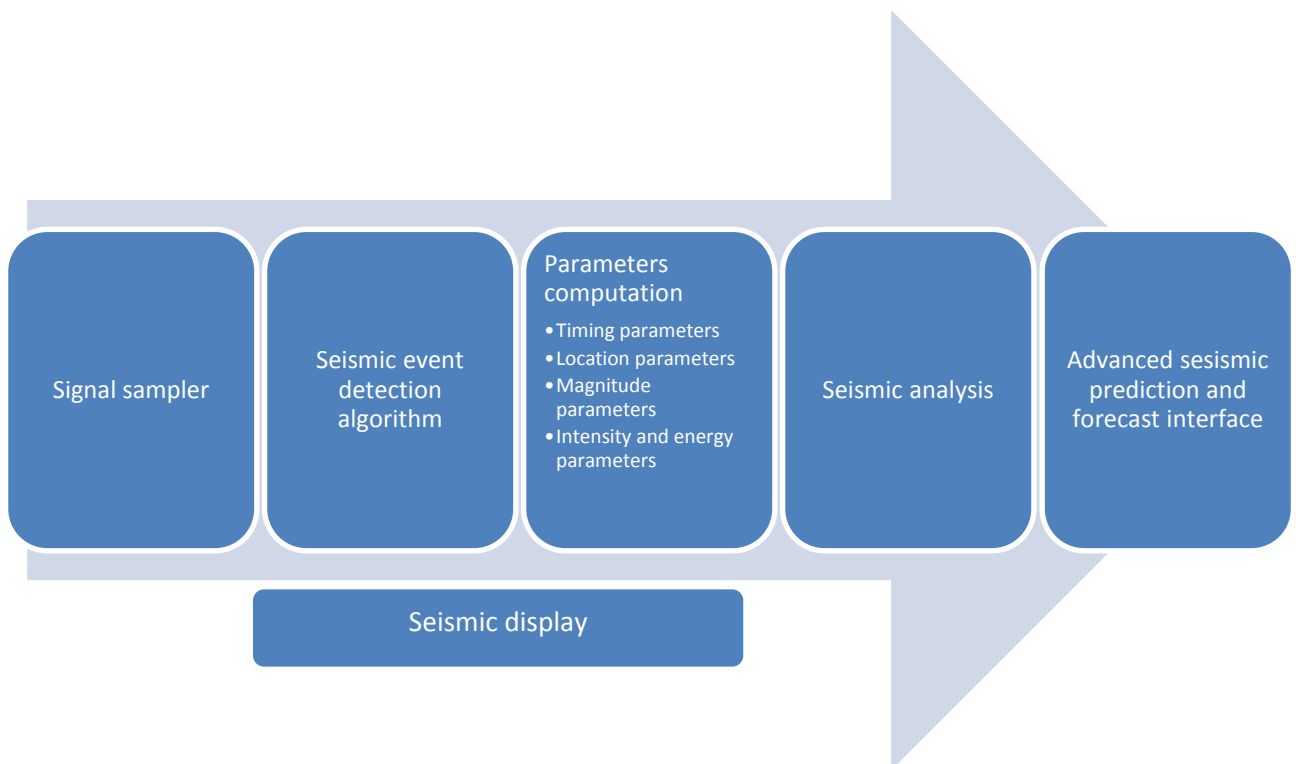


Table 2.2 Seismic data global computation

The event detection triggers when a seismic event has been detected in order to save the incoming data. Nowadays, the digital memory is cheap but it is not unlimited so it is necessary to carefully select the signal that is going to be collected. When parameters are retrieved, advanced software provide complex analytical tools that perform earth structure calculations and work with statistical data to “forecast” earthquakes. A true forecast it is not possible , “precise when” cannot be predicted but statistical calculations allow to forecast where and in which magnitude the events are going to take place establishing danger zones. Obviously, an advanced interface is needed to properly display this data. (Attri R. K., 2005)

2.3.6 Processing timing parameters

2.3.6.1 P and S arrival times

Picking the arrival times of P and S waves has a key role in event location and recognition. (Munro K. , 2004). The S-P time interval is used in formulas or tables to calculate the event distance to the epicentre and, in some approximations, the magnitude of the seism.

Manual picking is sometimes imprecise and very subjective. Not to mention that it is impracticable when continuous huge amounts of data are processed (Han, 2010). Hence, several methods to automatically detect the waves have been developed. (Munro K. , 2004) (Attri R. K., 2005)

These methods include time domain approaches based most of the time on signal energy techniques, amplitude methods, autoregressive methods and procedures based on frequency and S transform (Munro K. , 2004) (Han, 2010). Frequency based algorithms obtain better accuracy than the time domain based but they are more complex and require more computational resources. The project is focused on time domain methods for its easier implementation and because they are still popular among the seismologists (Han, 2010).

Two of the most popular time domain methods – both based in energy theory – are:

- STA/LTA technique
- Modified energy ratio

Further details about the STA/LTA technique are going to be given below as it is the method implemented in this project.

STA/LTA ratio description

The STA/ LTA averaging technique is used mostly for event triggering - occurrence, but correctly implemented it can also approximately calculate the arrival times (Munro K. A., 2005). The software should implement the following equations for the incoming data.

$$STA = \frac{\sum_{j=1}^{i-l_1} grm(i)^2}{l_1} \quad \text{Short-time average}$$

$$LTA = \frac{\sum_{j=1}^{i-l_2} grm(i)^2}{l_2} \quad \text{Long-time average}$$

Equation 2.1: STA and LTA equations

(Han, 2010) (Munro K. , 2004)

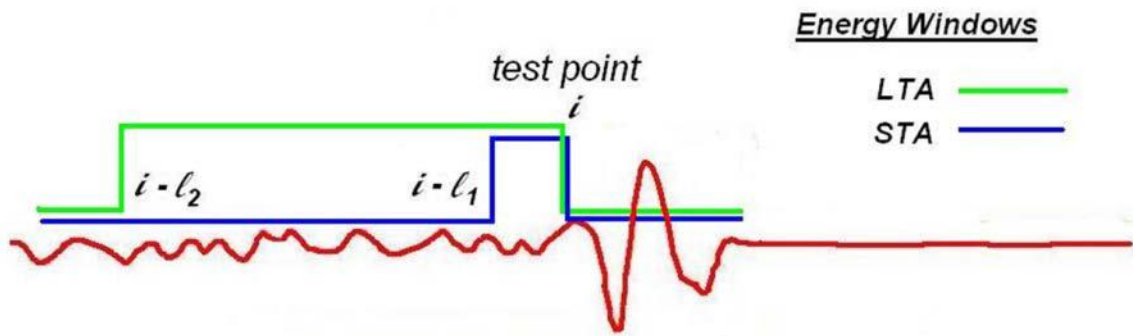


Figure 2.5: STA LTA algorithm illustration (Han, 2010)

Where L_1 and L_2 are the window lengths, $g_{rm}(i)$ the discrete points of the incoming signal and i the testing point index. This algorithm calculates the average energies in a long time and short time windows. Notice that the STA is a signal intensity measurement while LTA measures the background noise. Hence, the STA/LTA ratio is a signal to noise level (SNR) indicator. When a sudden increment of that ratio occurs, implies a seismic occurrence or wave arrival. At the moment that value reaches a threshold, an upcoming P or S wave has arrived and, therefore, the time value when that happened should be saved.

It is important to notice that L_1 and L_2 should be user defined; L_1 is normally two or three times the dominant period of the signal while L_2 is between 5 and 10 times L_1 . The threshold is picked up by the user too. As these parameters depend on the signal expected and the station among others, a calibration process is required. This means that these figures are not fixed, varying from one station to another. (Munro K. A., 2005) (Attri R. K., 2005) (Han, 2010)

There are other expressions for this technique as various modifications have been done to the original algorithm to improve its performance both in accuracy and noise isolation. (Han, 2010) (Munro K. A., 2005) (Munro K. , 2004). Both of these authors apply a different one in their referenced works. But for this project the one above were kept for the reasons explained in 4.6.2.1 Algorithm selection.

2.3.6.2 Coda Length

The Coda length is a measurement of the duration of an event. When the earthquake started and how much did it take until the earth calmed down. It is an important magnitude to estimate the earthquake destruction power. It can be calculated by subtracting the P wave

arrival time to the event end time. The tremor end can be measured by comparing the signal level with the averaged noise level before it arrives. When signal patterns return to a level compared to that noise the earthquake has concluded. (Attri R. K., 2005)

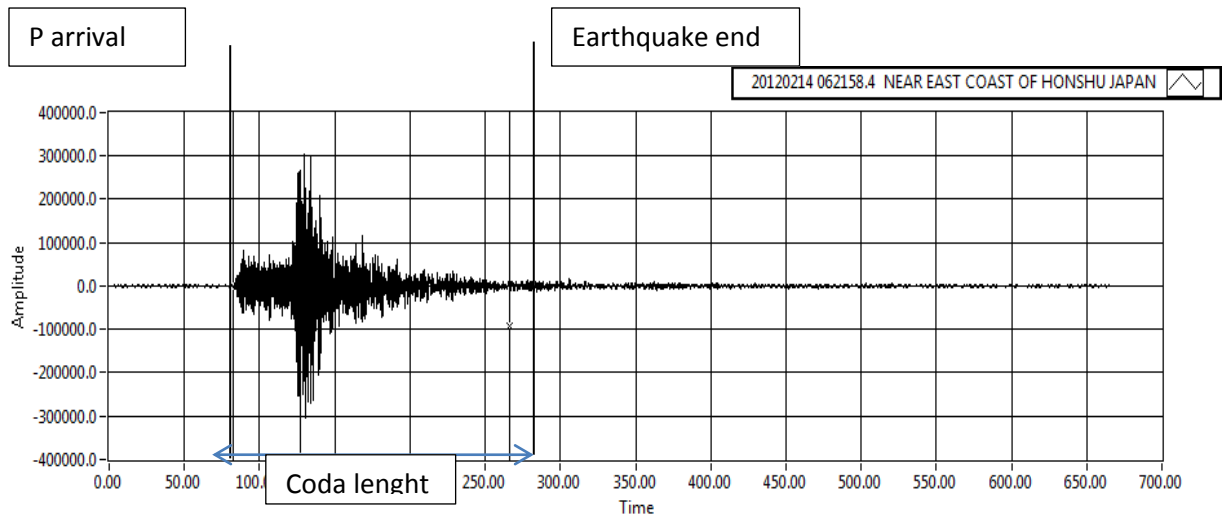


Figure 2.6: Coda length illustration

2.3.7 Processing location parameters

The hypocentre is the exact point where a seismic event happens, the epicentre is the point exactly above on the earth surface (Attri R. K., 2005). Nowadays, the professional stations use complicated computational iterative methods that process the available timing information in different station to, step by step, approach to the exact point where the earthquake was originated. However, there are easier ways –although less precise – to calculate the hypocentre and epicentre distance. (Havskov & Ottemöller, 2010)

The P and S wave velocity in the earth crust is known. Hence, once the arrival times are identified the distance to the station is completely determined. Below are represented different formulas that use this principle to approximate the hypocentre distance.

Their validity depends on the distance:

$$1) \text{ From 0 to 250 km } \Delta(km) = (t_p^{arr} - t_s^{arr}) \frac{v_p v_s}{v_p - v_s}$$

$$v_s = \frac{v_p}{\sqrt{3}}$$

$$v_p = 5.9 \frac{km}{s}; v_s = 3.4 \frac{km}{s}; \text{ for normal crust}$$

$$2) \text{ From 250 km to 2222 km (20°) } \Delta(km) = (t_p^{arr} - t_s^{arr}) * 10$$

$$3) \text{ From 20° } \Delta(^{\circ}) = [(t_p^{arr} - t_s^{arr})min - 2] * 10; [t] = \text{minutes}$$

Equation 2.2: Distance formulas

Where t_p^{arr} and t_s^{arr} are P and S first arrivals respectively and Δ is the distance to the epicentre. (Havskov & Ottemöller, 2010)

Notice that the expressions above can represent an approximation to the distance to the epicentre, especially if the tremors are not too deep. In fact, that was the method used years before the new computational techniques were introduced. In order to solve the depth imprecision, depth dependant time-distance tables or graphs like the one below can be used and integrated in the software (Attri R. K., 2005). The figure also shows how the exact point to the epicentre can be plotted triangulating when the distance from three different stations have been estimated.

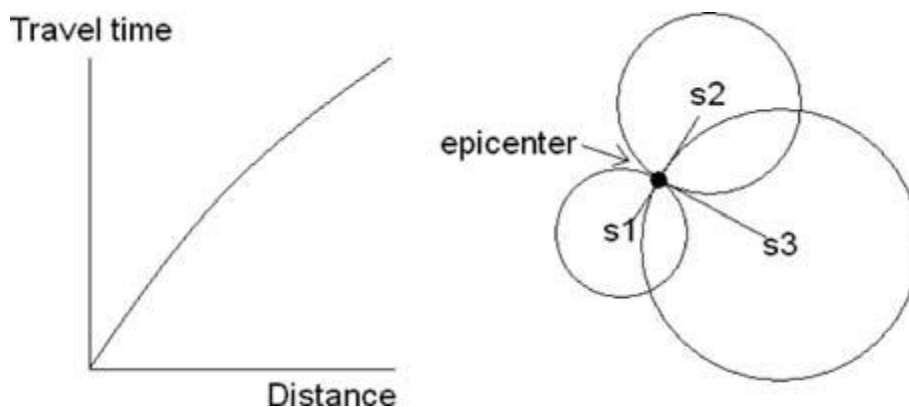


Figure 2.7: Generic depth distance travel time dependence and epicentre plotting (Havskov & Ottemöller, 2010)

2.3.8 Processing magnitude parameters

The magnitude is an arbitrary number proportional to the size of an earthquake. There are several magnitude scales although probably the most widely known among people is the Richter scale. Depending on the seismic network and the distance, one or more may be used. Due to the different ground structure and station position in a location, great magnitude variation among these different stations may occur, proving that magnitude measurement is not an exact discipline. The final magnitude can be revised several times before coming with the final one. Each magnitude scale has an application range and they are suitable for different distances and magnitudes (Havskov & Ottemöller, 2010).

Size	Guidance magnitude
Large	$M > 8$
Great	$M = 6-8$
Medium	$M = 4-6$
Small	$M = 2-4$
Micro	$M < 2$

Table 2.3: Approximate Magnitude vs Size equivalence

Some of the most common scales are:

- Local magnitude M_L . Original magnitude scale, also known as Richter scale. It is defined as

$$M_L = \log A + Q_d(\Delta)$$

Equation 2.3: Local magnitude

A = Maximum amplitude in a Wood-Anderson seismogram (which measures displacements from signals with $f > 2$ Hz)

$Q_d(\Delta)$ =Distance correction function

Δ =Distance to the epicentre [km]

Applicable to events of amplitude less than 6-7, distance below 1500 km and 1-20 Hz frequency band.

The simplest way to calculate the local magnitude is using the coda Magnitude M_c (sometimes called duration magnitude). It is a local magnitude approximation that relates the coda length (event duration) to the earthquake size. It is defined as:

$$M_c = a \log(t_{coda}) + br + c$$

Equation 2.4: Coda/duration magnitude

t_{coda} = coda length

r =distance to the epicentre in km

The a, b and c parameters try to reflect the different attenuation on the earth surface depending on the place, so their values differ depending on the location. The parameters used by Lee et al (1972) (original developers of this method) are sometimes used for locations where no local studies are available. However, the results are not always satisfactory. The usage of this scale

should be restricted to magnitude below 5 and distance below 1500 km. Havskov & Ottemöller in their book *Routine data processing in Earthquake seismology* compile an extremely useful table with this parameter for different localion altogether with a reference list.

Region	a	b	c	Magnitude range	M _c at 50 km	M _c at 300 km	References
California	2.0	0.0035	-0.87	2-5	3.3	4.2	Lee et al. (1972)
Italy	2.49	0.0	-2.31	1.5-4.5	2.7	2.7	Castello et al. (2007)
E. USA	2.74	0.0	-3.38		2.1	2.1	Viret (1980)
California	0.71	0.0	0.28	0.5-1.5	1.7	1.7	Bakun and Lindh (1977)
Norway	3.16	0.0003	-4.28	1.5-5	2.1	2.1	Havskov and Sørensen (2006)
Mexico	2.40	0.00046	-1.59	3-6	3.2	3.3	Havskov and Macias (1983)
East Africa	1.9	0.0004	-1.2	3-5	2.6	2.7	Dindi et al. (1995)

Figure 2.8: Coda Magnitude parameters in different areas of the world (Havskov & Ottemöller, 2010)

- Broadband surface wave magnitude M_S: Takes advantage of the fact that in shallow earthquakes for distances over 600-1000 km surface waves dominate over the rest.

$$MS = \log\left(\frac{V_{max}}{2\pi}\right) + 1.66 \log(\Delta) + 3.3$$

V_{max}= Maximum velocity amplitude (which is usually the surface wave amplitude)

Δ= distance to the epicentre in deg

It is valid for depths under 60 km, a wide range of periods (from 2 to 60 s), distance from 2 to 160 ° and magnitudes between 4 and 9. (British Geological Survey, 2011)

There is a decent concord between M_S and M_L for magnitudes from around 4 to 6.5 (Havskov & Ottemöller, 2010).

Standards tables are available to translate from one magnitude scale to another.

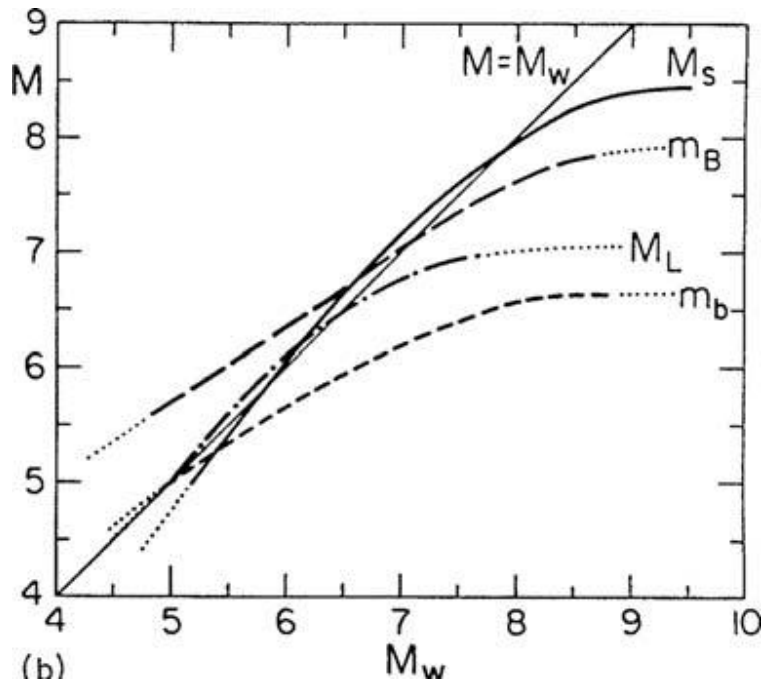
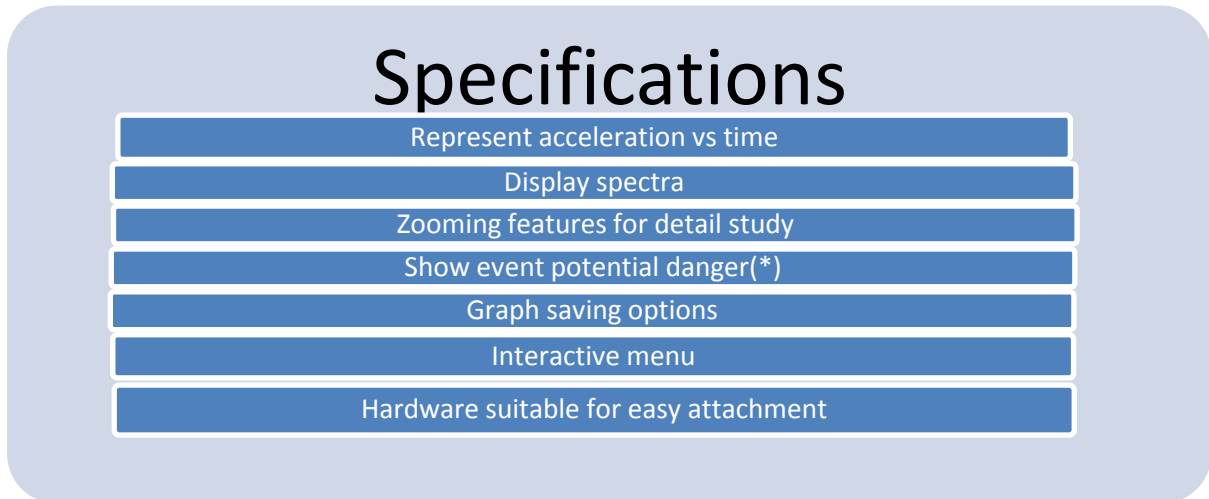


Figure 2.9: Magnitude scale conversion table (Havskov & Ottemöller, 2010)

3. Vibration Monitoring System Design

Before giving top-level details about how the requirements have been fulfilled it is advisable to recall the functions that were agreed in the Scheme of work



(*) **Only for short buildings up to 7 stories.** System based on PGA .See 2.1.5 Acceleration, intensity and damage.

3.1 Hardware

3.1.1 Accelerometer choice

At the first stages of the project it was decided that the vibration sensor to use was going to be an accelerometer. This is due to the fact that recent advances have made possible high-performance, high-accuracy, low-cost accelerometers available on a single monolithic IC (Bukhari, 2000). These characteristics make the technology suitable for the task regarding the resources available.

As stated in the background(2.1.4 Accelerometers), the most popular accelerometer type for vibration and seismic signals is the piezoelectric but, with a market price of around £200 in some of the main online catalogues it exceeded the budget available and, therefore ,a variable capacitance MEMS accelerometer was preferred. This technology provides small size, compact, sensitive lightweight and relatively cheap sensors perfect for the project purpose. (Santoso, 2010)

Once selected the technology the following parameters requirements have been taken into account to select the most suitable accelerometer:

- *Axes:* A dual axes system for both horizontal axes measurements is going to be developed as the horizontal component of the PGA (Peak Ground Acceleration) is

the standard for most building codes and hazard risks. (U.S. Geological Survey, 2010) An additional vertical axis for μg sensing (ambient noise) has been considered but discarded due to economic reasons (see 11. Future work: Potential improvements and modifications)

- *Frequency response*: A bandwidth of 50 Hz will be enough for structural monitoring (Lynch, 2003).
- *Maximum acceleration*: A PGA of 0.9 g causes total damage. Hence, an accelerometer with at least that figure as a maximum is required. (PREPA.R.E, 2008)
- *Weight*: The accelerometer weight not more than 10% of the test or mounting device so that the measurements are not significantly altered.
- *Ground Isolation*: If the test article is conductive and at ground potential, a difference in ground levels could cause measurement problems and therefore a common ground is required
- *Mounting*: Suitable for high sensitivity, adequate attachment.
- *Sensitivity*: The lower the better but according to table 2.1 tens of mg is enough to cover all cases.
- *Resolution*: The lowest level in Mercally Scale (IV) is characterised by a 30 mg acceleration or below. Therefore, this will be the minimum resolution we will be targeting at.
- *Signal conditioning*: Better if signal already conditioned to save costs both of time and money.
- *Power*: Standard 3 to 5 Volts preferred
(Lent, 2009) (Aszkler, 2005)

Considering the requirements and limitations, the accelerometer series that have been selected are the ADXL203. They are high precision, low power, dual axis accelerometers. Their bandwidth can be modified with capacitors to make it fit the application and the output signal is already conditioned.

ADXL203 FEATURES

- High performance, single-/dual-axis accelerometer on a single IC chip
- 1 mg resolution at 60 Hz
- Low power: 700 μ A at $V_S = 5$ V (typical)
- High sensitivity accuracy
- X and Y axes aligned to within 0.1° (typical)
- Bandwidth adjustment with a single capacitor (0.5 to 2500)
- Single-supply operation
- RoHS compliant

(Analog Devices, 2011)

The device is commercialised in a 8 ld LCC package only (8 terminal ceramic Leadless Chip Carrier).

3.1.2 DAQ selection

Among the DAQ cards available the DAQ device selected was the NI6021 from National instruments connected to a BNC-2120 accessory. The factors that backed up this decision were:

- Available, installed and configured in the laboratories
- Provides flexible AI and AO sample and convert timing
- Can perform 32 bit ADC.
- It includes a 5 V power supply, exactly the same that is needed for the accelerometer. It also features a driver supplying current enough.
- Customized analogue input range. The ranges available are ± 10 , ± 5 , ± 1 and ± 0.2 V. The device automatically amplifies or attenuates the signal depending on the input range. This feature is very valuable in order to save signal conditioning circuits. It maximizes the resolution as well.
- It includes a 700 kHz low-pass filter.
- The input channel resolution is, regardless the range used, below 500μ V, which implies, taking into account the accelerometer sensitivity (≈ 1 V/g), that a high resolution is available in any case. See table 3.1
- The BNC-2120 accessory available provides user-friendly interface.

(National Instruments, 2008) (National Instruments, 2007) (National Instruments, 2008)

Input range	Nominal Resolution
-10 V to 10 V	320 μ V
-5 V to 5 V	160 μ V
-1 V to 1	32 μ V
-200 mV to 200 mV	6.4 μ V

Table 3.1: Input range and resolution for NI 6221

The device should be able to gather samples fast enough so those aliasing problems are avoided:

$$f_{smax} = 250 \frac{kS}{s} \text{ per channel} \Rightarrow f_{schan} = 125 \frac{kS}{s} \text{ because we are using two;}$$

$$f_{schan} \gg 2 * f_{3dB}$$

$$125 \frac{kS}{s} \gg 100Hz$$

Equation 3.1: Anti-aliasing condition

(Martin & Bono, 2010)

Where f_{smax} is the DAQ maximum sample rate, f_{schan} is the maximum sample rate per channel and f_{3dB} is the filter's corner frequency.

Hence, there are no problems regarding the aliasing.

The NI 6021 timing resolution is 50 ns, taking this into account the signal frequency should be below a limit or a sample and hold circuit will be required. (National Instruments, 2007)

Considering the signal as a sine superimposition:

$$f \leq 1/(\pi 2^n t_c) ; f_{3dB} \leq \frac{1}{\pi 2^{16} 50ns} ; f_{3dB} \leq 97.14$$

Equation 3.2: Satisfactory conversion time demonstration

(Martin & Bono, 2010)

Therefore, a S&H circuit is not needed.

3.1.3 Data acquisition structure

Selecting a sensor and a data acquisition device was the first step because they are essential hardware. However, the design of a simple block diagram preceded any other advance in the hardware design. A proper structure design determines the rest of the hardware selection clarifying the processes that follow and minimizing modifications later on. The following figure is the block diagram from which the rest of the hardware was built up.

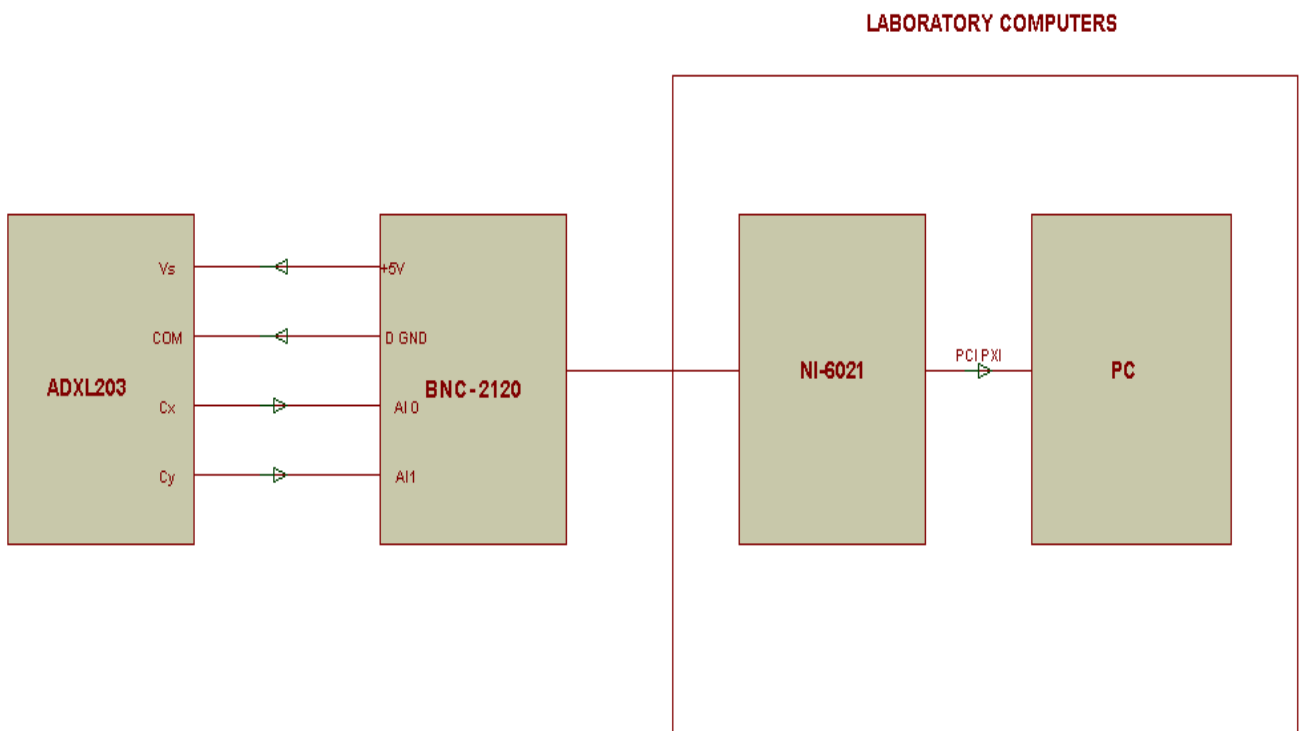


Figure 3.1: Hardware block diagram

Notice that D GND is the same electrical point as AI GND. The type of AI connection selected is reasoned in the next section.

Considering the electronic nature of the device, the next step was a schematic hardware design. Due to the System simplicity, it does not differ much from the block diagram.

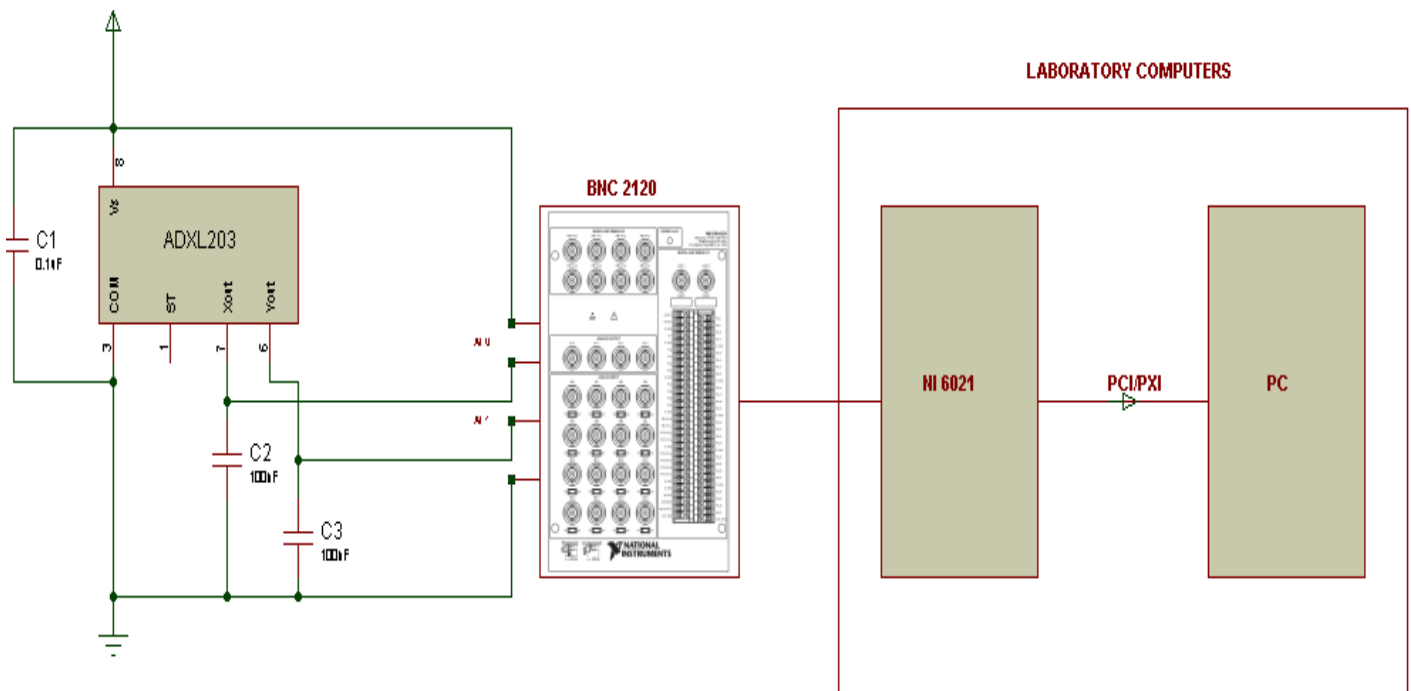


Figure 3.2: Schematics design

As it can be seen, excepting the capacitors C2 and C3 there is not additional signal conditioning. This will be explained with detail in the following subchapter. C1 filters the supply (details on EMI/EMC section). Observe that the computers in the laboratory used already integrate the DAQ card.

3.1.4 Signal conditioning

Amplification and signal levels

The ADXL203 MEMS accelerometer has a typical Zero g bias level of 2.5 V. This offset can be eliminated using software which simplifies considerably the hardware design. The DAQ card used – NI6021 – allows the selection of a customized analogue input range which determines the system resolution. The ranges available are ± 10 , ± 5 , ± 1 and ± 0.2 V. In order to maximize the resolution of the vibration monitoring system the most suitable choice is ± 1 V as the accelerometer resolution is 1000 mV/g. A building structural vibration caused by an earthquake will rarely exceed 1 g, and if it does, the high value of the acceleration assures that the event is potentially destructive so the danger selection is already clear. To achieve this objective a suitable band pass filtering could be used to eliminate the offset and adapt the signal to the input limitations of ± 1 but, is that input resolution needed? Setting the ± 5 range, the resolution will be 160 μ V, which implies an acceleration of 160 μ g. This resolution is

unreachable for our hardware as the data sheet specifies that the typical noise floor is $110 \mu\text{g}/\sqrt{\text{Hz}}$. Hence, the ± 5 range has been selected as the performance is not negatively affected compared to the ideal case of ± 1 and it has a key advantage, it allows to software filter the offset instead of adding an additional circuit.

Bandwidth selection and Noise filtering

A bandwidth of 50 Hz is enough for structural seismic and vibration monitoring (Lynch, 2003). To avoid aliasing problems the more we limit our bandwidth to this value the better. The DAQ includes a low pass filter of 700 kHz, which is evidently not enough for our purposes. Fortunately, the ADXL203 provides a band limiting function just adding capacitors to the X and Y outputs. These characteristic permits to avoid aliasing problems and easily filter the noise signals that can be encountered without adding an additional filter. According to the data sheet:

$$f_{3dB} = \frac{5 \mu \frac{F}{S}}{C} ; C = \frac{5 \mu \frac{F}{S}}{50 \text{ Hz}}$$

$$C = 100 \text{ nF}$$

Equation 3.3: Cut-off frequency and added capacitors relationship (Analog Devices, 2011)

Notice that the added capacitors purpose is to set the frequency response of the device but also determine the noise filtered, the noise is higher if the frequency response is increased. Therefore, a trade-off between bandwidth and noise should be reached. The intrinsic noise of the accelerometer, as specified by the manufacturer, will be white Gaussian noise affecting equally to all the frequencies the following way.

$$rmsNoise = (110 \mu\text{g}/\sqrt{\text{Hz}}) * (\sqrt{BW * 1.6})$$

Equation 3.4: Accelerometer noise

Hence, the bandwidth has been limited to 50 Hz, enough to the purposes and to limit the performance disturbing noise. The noise that will be suffered for the 50 Hz bandwidth that is going to be handled will be $rmsNoise = 1 \text{ mg}$, completely negligible as the acceleration levels are going to be classified in ranges of magnitude and destruction power being the lower range from 0 to 30mg.

Connection Schemes

The AI ground terminal- or terminals that are connected to the same electric point- will be used as reference. The 5 V supply provided by the DAQ is suitable and no external supplies are required. Thus, the most appropriate connection configuration for the accelerometer X and Y terminal will be a referenced single ended mode-RSE since the input signals are single ended and AI ground referenced.

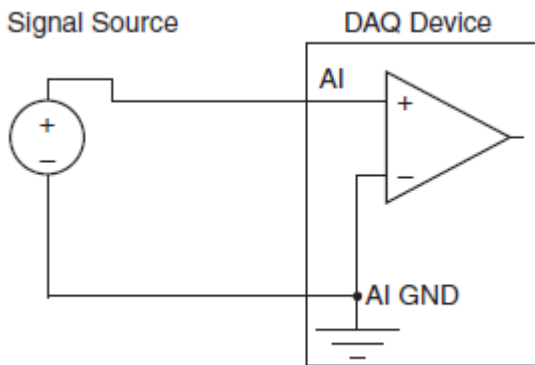


Figure 3.3: Connection scheme used

Nevertheless, the DAQ has been used through a BNC-2120 connector accessory which provides its own connection schemes. Since the acquisition card has been used as the supply and no other reference but AI GND was applied, the required AI input channels switch should be in FS mode. Despite the configuration name –floating source – the signal was already referenced to AI GND and the actual configuration is RSE as that is the type of signal the DAQ receives. The following diagrams illustrate the FS mode suitability. The FS mode is intended to floating signals; however, it is the optimal scheme if the signals are referenced to AI GND.

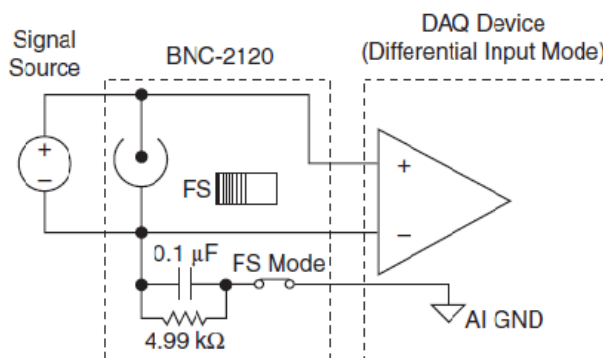


Figure 3.4: BNC 2120 GS input

3.1.5 ADXL203EB Evaluation board

Analog Devices commercialises an Evaluation Board with everything needed to perform tests and build a prototype with the ADXL203- ADXL203EB. It was decided to purchase this product in order to boost the project and focus earlier on the main topics. The board comes with different holes and pins to attach the accelerometer to the object on test.



Figure 3.5: ADXL Evaluation board

Notice that the evaluation board is intended to be used with SMD component only.

3.1.6 Enclosure and mounting

The system has obviously a dynamic purpose. Especially in this kind of devices is recommended to select a proper enclosure and mounting system. The enclosure protects the device from possible damage providing at the same time a better handling and a professional appearance and the mounting maximises the vibration transmissibility.

As stated in the accelerometer selection consideration, the accelerometer should weigh no more than the 10 % of the mounting device (the enclosure in this case) for more accuracy in its measurements, therefore, the use of a proper case that increases the weigh helps to accomplish this requisite.

It is clear then that a proper enclosure is needed, the selection criteria have been:

- **Preferable Plastic:** Because of its light weigh, besides, in a prototype like this, some cuts are needed so that we can have access from outside to the different connectors. Obviously, a malleable material like polymers makes this task much easier.
- **Simplicity and pragmatism:** As long as it carries out the tasks stated, the design and other issues are negligible.

- Measures:** It had to feature a minimum height of 16 mm as that is the Evaluation Board + header height. Regarding the depth and width, the smaller the better, taking into account that all the components had to fit. Although the components were not specifically ordered an approximation of their measurements was known. A security margin was applied for possible manufacture mismatches and predicting that the input and supply connectors may be bigger.
- Price:** Taking into account the budget, the cheapest enclosure that fitted the provisions was selected.

The enclosure chosen was a 1591XXMS model from Hammond Manufacturing™ .

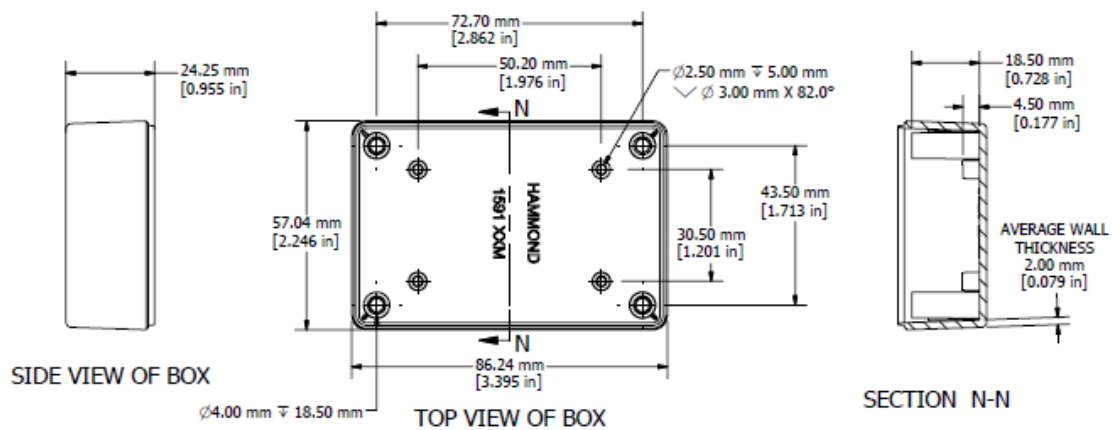


Figure 3.6:1591XXMS Dimensions

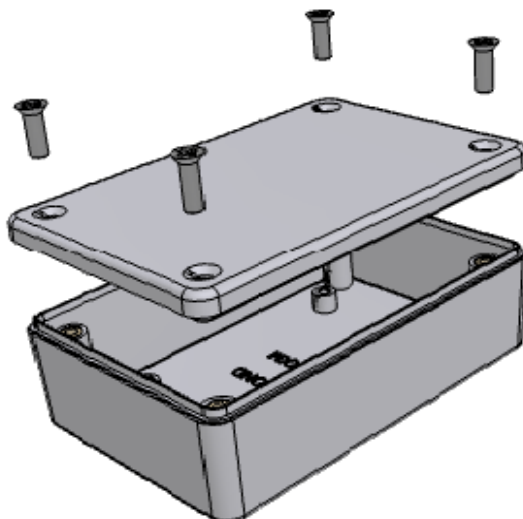


Figure 3.7:1591XXMS 3D model

In regard to the mounting system, a double-sided adhesive tape was selected. An adhesive mounting is often required, especially in small surfaces and PC board. In this case, the surface to attach the system is not fixed so an easily removable adhesive tape was suitable. The preferable adhesive is cyanoacrylate mainly because the reason specified above. Before attaching the tape, it is highly recommended to clean the surface with a hydrocarbon solvent. A thin tape is preferable as the adhesive thickness may play a critical role in the frequency response performance. (Endevco, 2006) (Lent, 2009)

3.1.8 PCB

The circuit to implement is simple so the possibility of using a simple veroboard has been weighted up. Nevertheless, the veroboard had to be adapted to the enclosure including borders and holes. In the end, the design of a Printed Circuit Board was resolved as there was a real risk that the time saved not doing the design would have been employed later on properly fit the veroboard. This test board borders are not designed to be easily shaped at will being impossible to accurately place the edges and pierce the holes.

The figure below shows the PCB design plan.

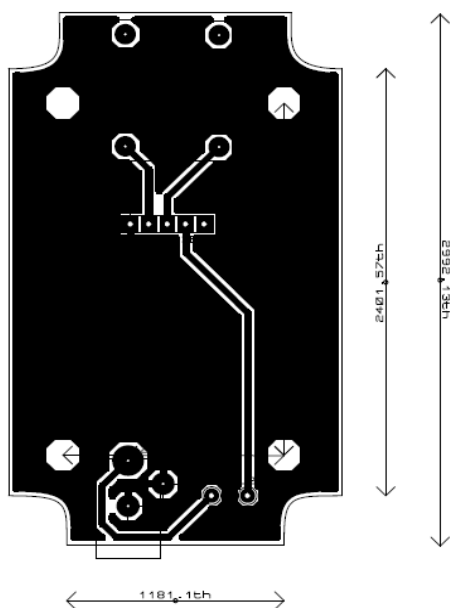


Figure 3.8:PCB artwork

Notes:

- Notice that some of the holes are positioned near the edges so that the input and output pins are accessible from the outside.
- Some of the holes have to lodge square or rectangular pins; the diameter of those holes is the diagonal of those pins.
- A power plane has been added to avoid EMI and noise problems.

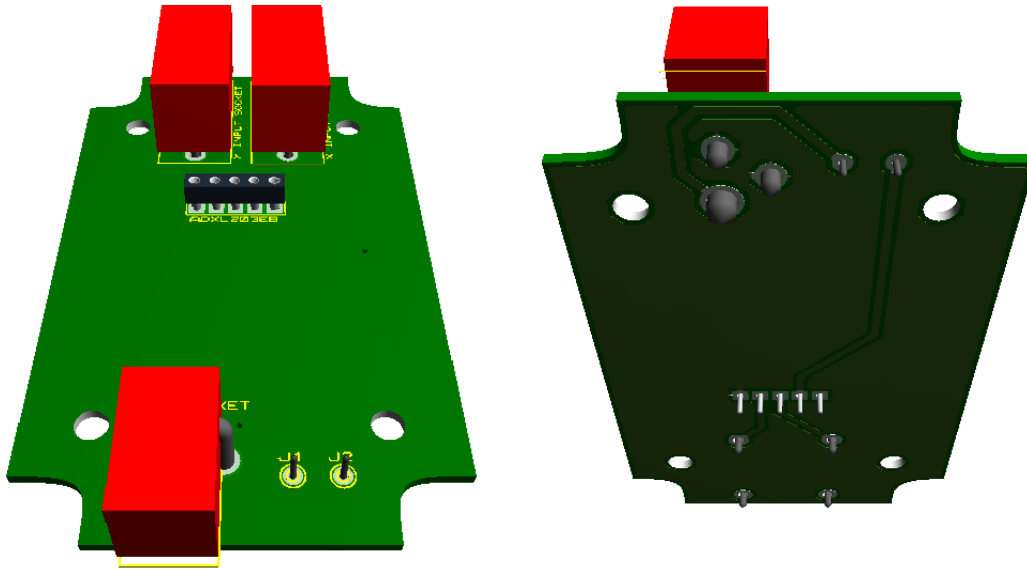


Figure 3.9: PCB 3D model

3.1.9 EMI/EMC considerations

National Instruments, as the accelerometer manufacturer, has to uphold the European regulations regarding EMI in order to commercialise the device. Hence, the possibility of the ADXL203 emitting disturbing electromagnetic signals is highly improbable. As no additional high frequency switching hardware has been inserted, the system it is going to follow the European normative in regard to emissions. (Barnes, 2011)

Although the system developed is not intended to work in an adverse EMI environment. Standard precautions have been taken for non-expected incoming EMI. BNC coaxial cables are going to be used to avoid the coupling effect between the noise and the signal. (Turkel, 2000)

Concerning the supply, a 0.1 μF capacitor has been placed in order to prevent noise or ripples in the supply that can affect to the output. This capacitor is usually enough but when the noise is present at 140 kHz or any harmonic thereof additional actions may be needed. For example, another parallel capacitor up to 2 μF or ferrite beads could be added. Moreover, 50 Hz low pass filters are allocated in each output. (Analog Devices, 2011)

3.2 Software

3.2.1 Global software framework

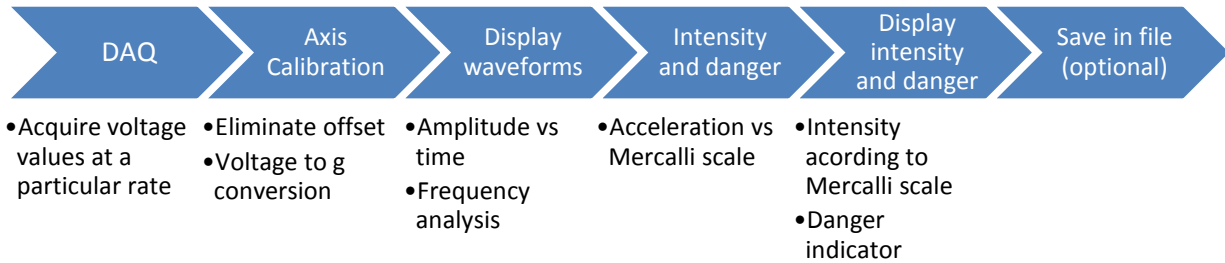


Figure 3.10: Vibration DAQ software framework

3.2.2 DAQ

The data acquisition rate is going to be controlled by the user so that the software can be adapted to different requirements and the processing power of different computers. However, it should be taken into account that in order to avoid aliasing problems, as stated before (3.1.2 DAQ selection):

$$f_s \geq 2 * f_{3dB} \rightarrow f_s \geq 100 \text{ samples/s}$$

Where f_s is the sampling frequency and f_{3dB} the upper corner frequency of the accelerometer outputs filters, that is, more less the maximum signal frequency (50 Hz in this case).

3.2.3 Axis calibration

The band pass filtering hardware was no implemented. A 2.5 volts offset is present in the input. This offset is going to be eliminated using software. A calibration subroutine will be developed. It will calculate the signals DC value and subtract it from them in real time. The signals without the offset will be output. The voltage values have a reasonable good coincidence with the g_s experienced ($\approx 1V/g$) so no conversion is needed.

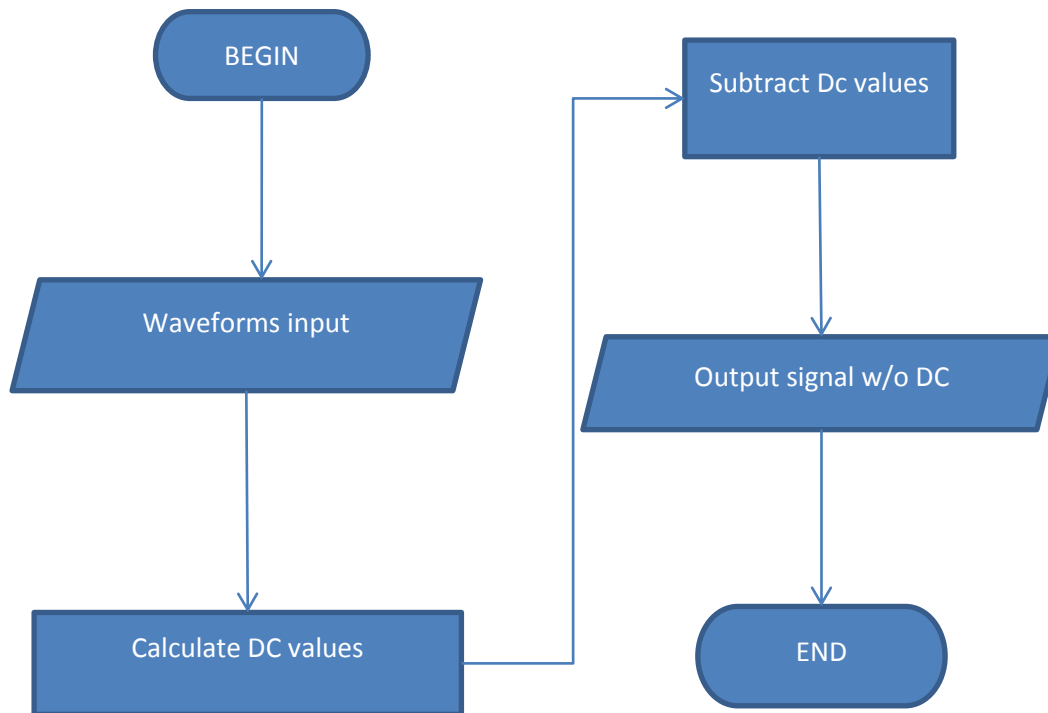


Figure 3.11: Calibration subroutine flowchart

3.2.4 Earthquake intensity and danger

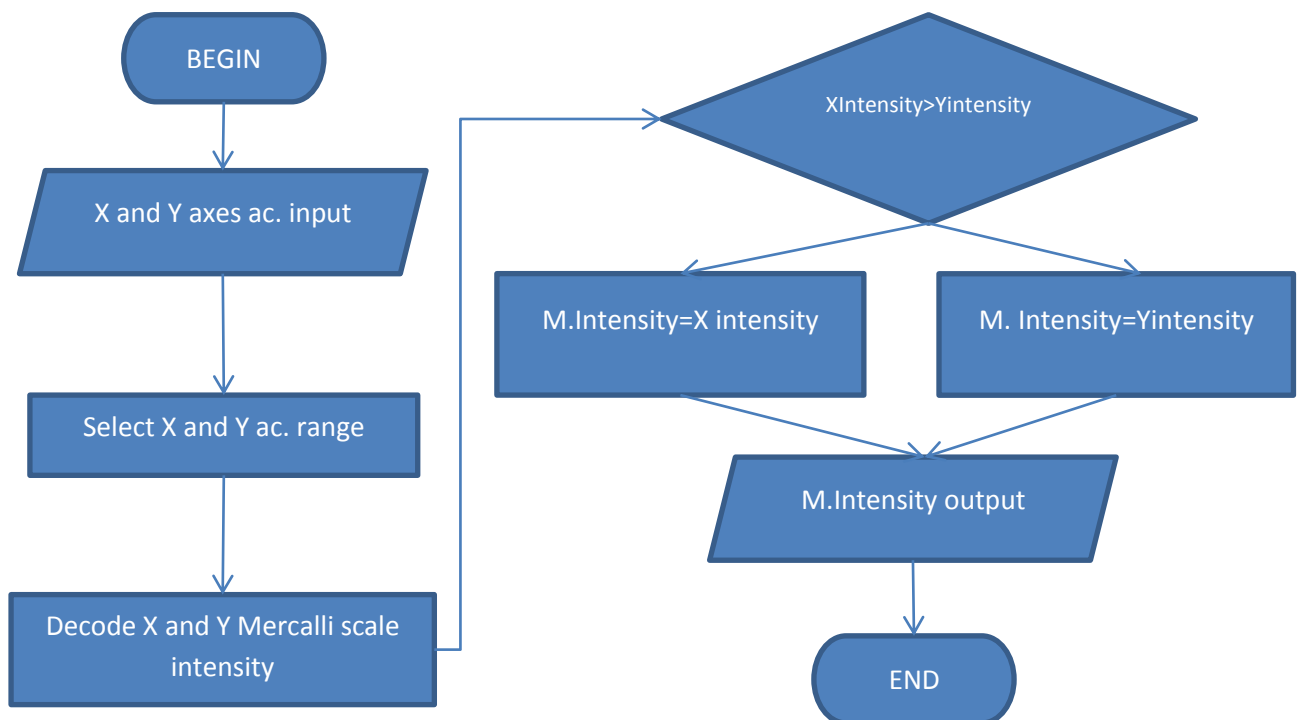


Figure 3.12: Magnitude and danger calculator subroutine

The PGA and the intensity are related (PREPA.R.E, 2008). The detailed relation can be seen in *2.1.5 Acceleration, intensity and damage*. The subroutine should recognise the acceleration range of each of the axes and identify the Mercalli intensity in real time. The axis with the higher intensity determines the final result.

3.2.5 Display characteristics and saving options

The display should have a proper zooming or autoscaling options to study the input signals in detail. Absolute time axis would be suitable. The danger indicator will indicate the Mercalli intensity scale danger in real time. For each execution another indicator should display what was the maximum intensity experienced during the current run. The user will select whether and when to capture the waveform data that is being displayed by clicking a saving button.

4. Seismological data analysis software design

4.1 Introduction and Specifications

The objective of this part of the project is to develop software that performs the tasks below.

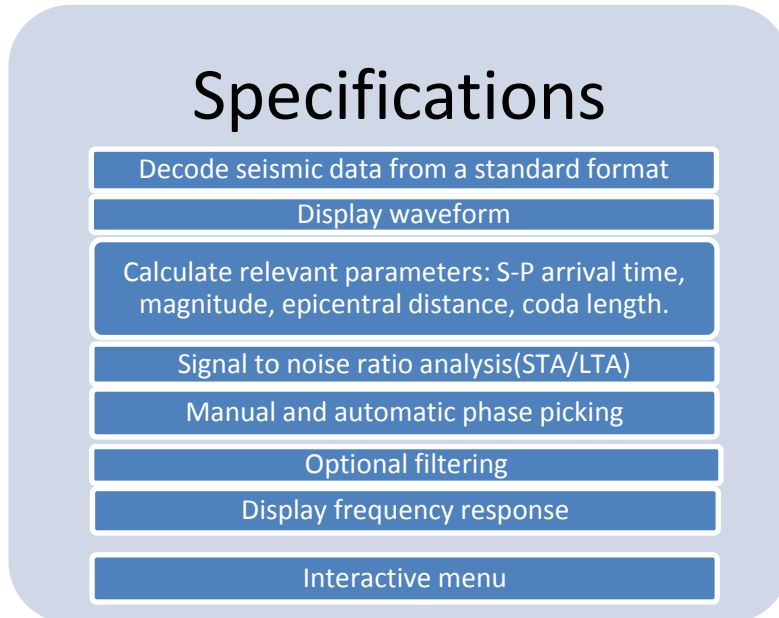


Figure 4.1 Seismic analysis software specifications

An important portion of this section consists of high-level flowcharts, as well as notes if necessary. LabVIEW is a really high-level programming language as so they are the flowcharts. There is no need to enter into low-level programming when the software has those processes automatized. This section aim is to briefly describe and justify the design options adopted.

4.2 Data format selection

When analysing the project requisites, the first problem that was encountered was what seismic data format to use and whether it was freely distributed or needed to be requested to the proper institutions. An important research work needed to be made in order to gather information about seismic data and sources. A good amount of this information is available in the seismic background section.

Although the SEED and miniSEED data formats are probably the most popular types, the SEED format is an exchange format, what is to say, it stores absolutely all the data of the event (Havskov & Ottemöller, 2010). According to the purposes and scope of the project, a waveform (or processing) data type is more than enough; it was not recommendable to add complications until the basic requirements were completed. In any case, although miniSEED

is part of that group, National Instruments does not provide a plug-in in their support website. National instruments do provide numerous strong motion data plug-ins, including another standard for a processing format; the SAC data format (National Instruments, 2011). Hence, SAC format was used to process the data in this project as it is possible to obtain this type directly and very easily from the biggest database found, IRIS. Not only that, the British Geological Survey offers its earthquake data in this format too. This is particularly useful because it allows the retrieval of local data. (British Geological Survey, 2012)

4.3 Global software framework

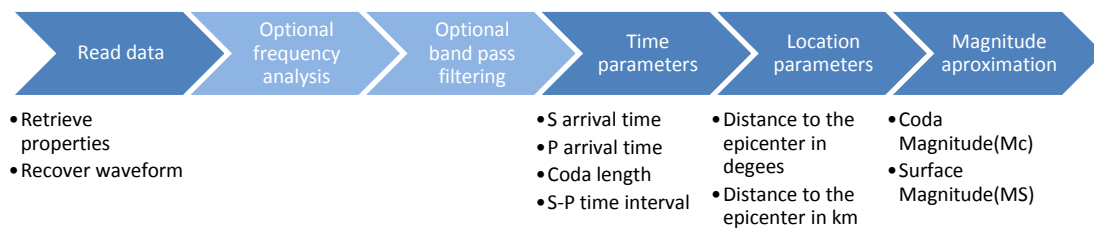


Figure 4.2: Global computation framework (Attri R. K., 2005)

The figure above represents the software structure. The process is controlled by the user, deciding in which step should be picked up. Some phases need data from previous processes so the user should be careful and know what it is being done. In any case, indications will be included to help users not familiarized with seismic analysis. As we are using recorded digital data, obviously a triggering process is not necessary.

4.4 Reading SAC files

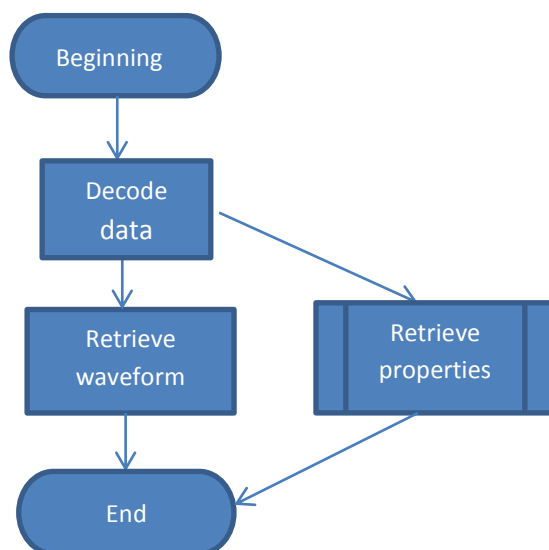


Figure 4.3: Read data flowchart

The plug-in has to carry out the decoding. The SAC files, as explained in the background, include a waveform and headers with properties as the event date or the name of the seismic station. Those also need to be retrieved to be displayed.

4.5 Frequency analysis and optional filtering

Sometimes it may be necessary to filter the seismograms, for example for a better phase arrival timing (Havskov & Ottemöller, 2010). The software should include an option to filter the waveform. Havskov et al (2010) recommends 4 order Butterworth filters. In order to properly select the cut-off frequencies a tool to display the spectra would be really useful. The seismic events have a typical low frequency so in this case a logarithm frequency scale is not necessary.

4.6 Arrival times

4.6.1 Introduction

A system to automatically detect the wave arrivals is going to be developed due to the importance of these parameters – described in seismic background (2.3.6.1 P and S arrival times). One of the algorithms available to perform this task need to be applied but also a manual picking tool is necessary.

4.6.2 Automatic picking

4.6.2.1 Algorithm selection

Among the available algorithms, the time domain energy based algorithms appeared to simplify the tasks, featuring an acceptable accuracy. The STA/ LTA ratio method was selected because of its simplicity and popularity (Han, 2010). Refer to STA/LTA ratio description in the seismic background to see the algorithm detailed description.

$$STA = \frac{\sum_{j=1}^{i-l_1} grm(i)^2}{l_1} \quad \text{Short-term average}$$

$$LTA = \frac{\sum_{j=1}^{i-l_2} grm(i)^2}{l_2} \quad \text{Long term average}$$

$$STA \text{ LTA ratio} = STA/LTA$$

Equation 4.1: STA/LTA ratio equations

As it is explained in the background there are different expressions for this method. The expressions above present these advantages:

- 1) They can be calculated using data from one station only. Recall that a SAC data file only includes one waveform.
- 2) The expressions do not include square-roots as other do. The calculations have to be performed, sometimes, in thousands of points. Eliminating one of the operations can result in a significant improvement on performance.

In contrast, it does not have the precision of other algorithms (Han, 2010). Nevertheless, considering the scope of the project it is far enough.

4.5.2.2 Flowcharts

If there is a proper preprogrammed VI in among the available in LabVIEW to perform the calculation it will be used, in any case the following diagram represents the programming structure designed for its later LabVIEW implementation.

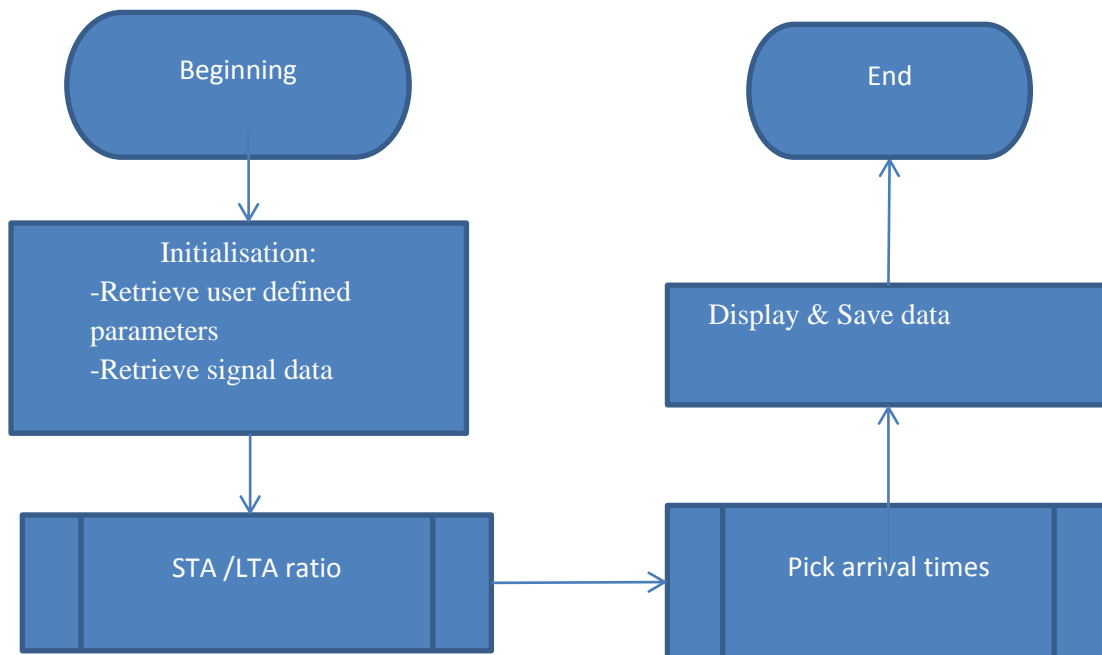


Figure 4.4: Automatic Arrival time picking global flowchart

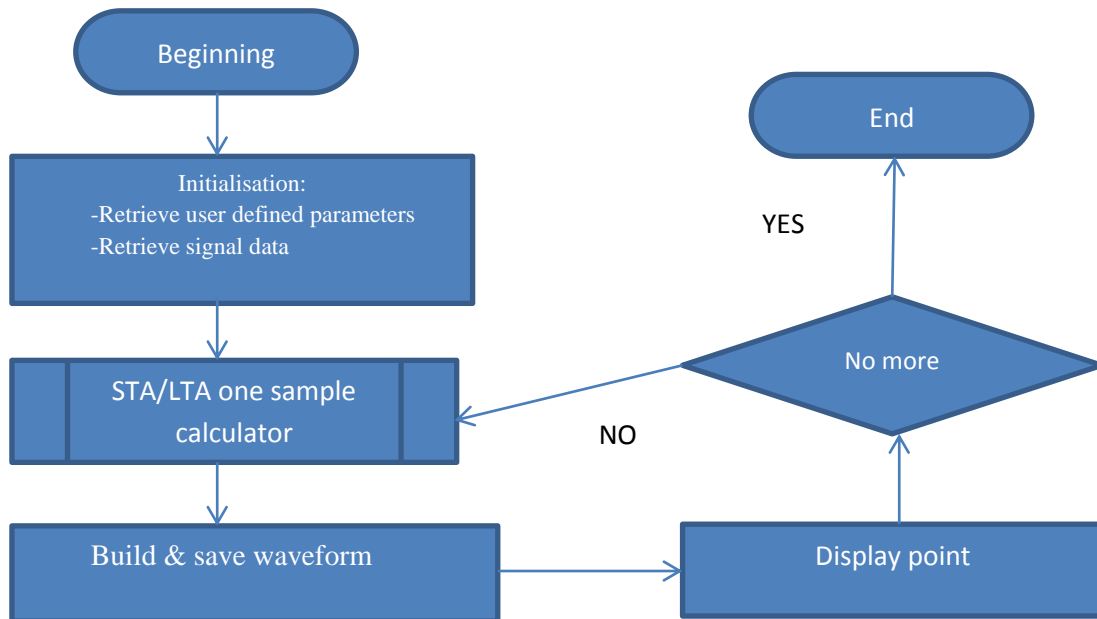


Figure 4.5: STA/LTA ratio implementation subroutine flowchart

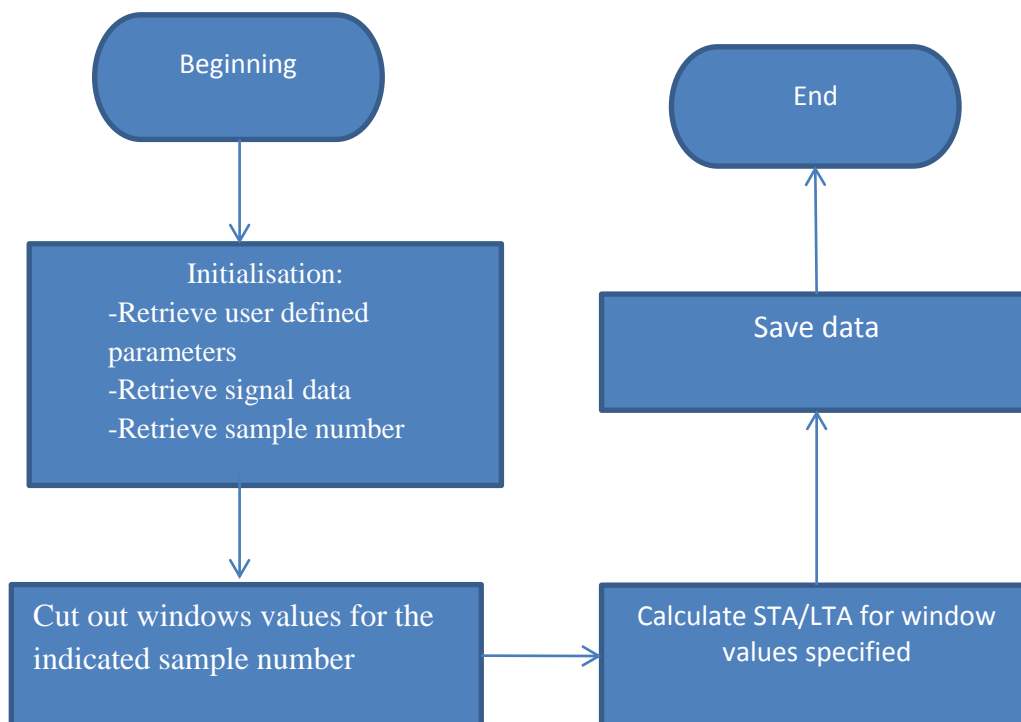


Figure 4.6: STA/LTA one sample subroutine flowchart

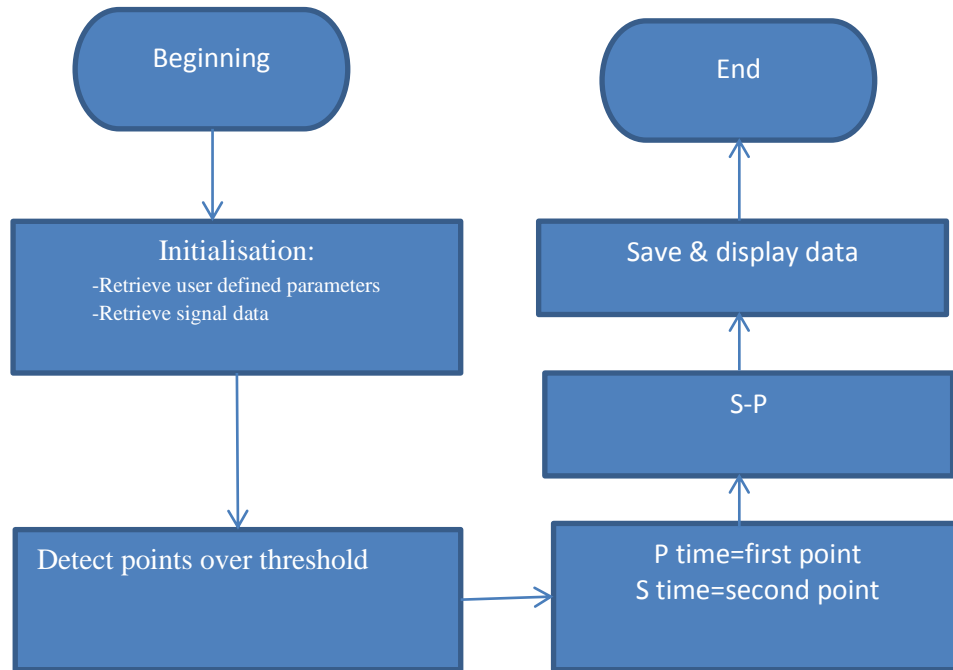


Figure 4.7: Pick arrival times subroutine

4.6.3 Manual picking

It was stated in the STA/LTA ratio description that the automatic picking has a great dependence on the station and type of event sensed. If there is not data available or there is not enough time to proceed with that calibration, the automatic picking is useless. Sometimes, the seismograms available contain too much noise in the same bandwidth than the signal, making difficult the correct functionality of modest automatic picking software like in this case. These problems are common even in advanced professional software and sometimes are compensated averaging the timing information of several channels available in the same station (Munro K. A., 2005). However, in this project only one waveform is available. The distance and magnitude calculations depend on the timing parameters so an alternative method is required so that the analysis does not reach a dead-end. The software should allow easy manual pickings using a cursor or similar techniques.

4.7 Coda length

This parameter has significance enough to develop a subroutine that performs the task. The method followed to design that subroutine is showed in the next page.

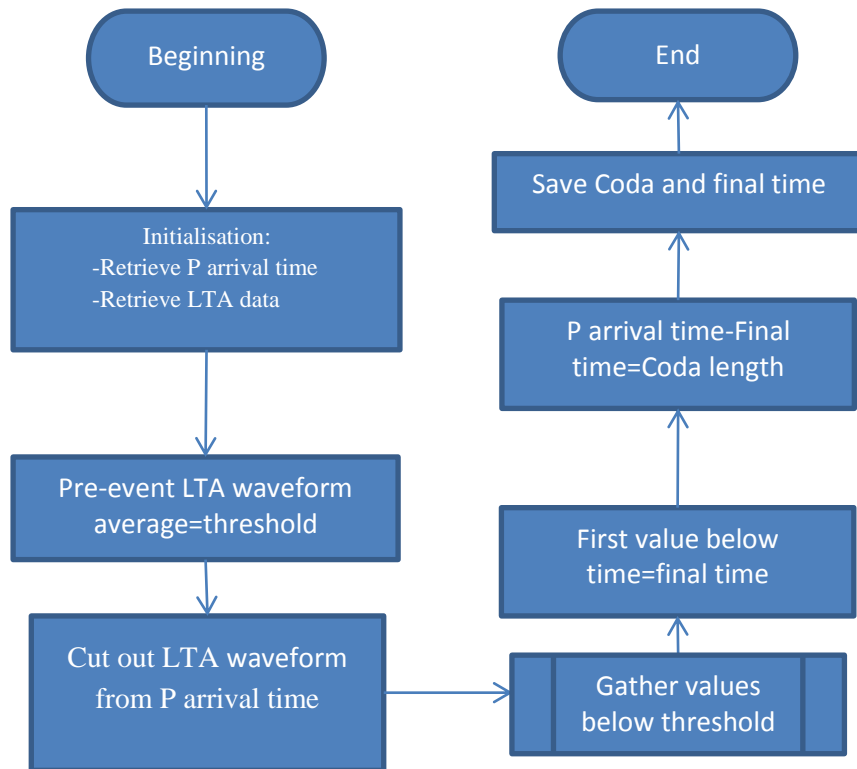


Figure 4.8: Coda lengthy subroutine flowchart

The P arrival time indicates the earthquake start. The software has to determine when the event is finished, when the earth has calmed down (Attri R. K., 2005). It is known that LTA values characterise a measurement of the noise level (Munro K. A., 2005). Therefore, it can be used to determine an event conclusion. This happens when the current LTA levels are compared with an average value before an event was triggered. If $\text{current LTA} \leq \text{LTA (averaged before P)}$, the noise level is back to what it was before there was an earthquake. The duration or coda length can be calculated with a simple subtraction.

$$\text{Coda length} = P \text{ arrival time} - \text{Event conclusion time}$$

Equation 4.2:Coda length

4.8 Distance to the epicentre

The habitual computational location methods used in professional stations around the world - iterative approaches - are far over the scope of this project, not only because of the difficulty of the implementation but because data from more than one station is required. Recall that this project aim is to retrieve information from one seismogram at a time only. Moreover, the task is to calculate the distance from the epicentre not locate the exact coordinates in 3D as the mentioned approaches are able to do. (Havskov & Ottemöller, 2010).

In order to calculate this distance with a single seismogram there are two options. Using lookup tables or approximation algorithms. (Attri R. K., 2005) A priori the incorporation of these tables in the software looks like the most precise way to realise the software. However, the integration of these tables in the software could represent an important amount of time and even more if depth wants to be taken into account in order to make the most of this procedure. Prior the programming of these tables the approximation equations have been tested manually resulting in an error range of less than 1 ° in most of the cases up to a distance of 100 °. For events in a 2000 km range the inaccuracy was often around 0.1°. The precision has been considered acceptable for the objectives of the project. This approach saves lots of hours of programming and table lookups in the internet.

Recall that the equations implemented, depending on the distance, are

$$1) \text{ From 0 to 250 km } \Delta(km) = (t_p^{arr} - t_s^{arr}) \frac{v_p v_s}{v_p - v_s}$$

$$v_s = \frac{v_p}{\sqrt{3}}$$

$$v_p = 5.9 \frac{km}{s}; v_s = 3.4 \frac{km}{s}; \text{ for normal crust}$$

$$2) \text{ From 250 km to 2222 km (20°) } \Delta(km) = (t_p^{arr} - t_s^{arr}) * 10$$

$$3) \text{ From 20° } \Delta(^{\circ}) = [(t_p^{arr} - t_s^{arr})min - 2] * 10; [t] = \text{minutes}$$

Where t_p^{arr} and t_s^{arr} are P and S first arrivals respectively and Δ is the distance to the epicentre.

Notice that from 9° to 20° and over 100° theoretically the algorithm is not valid. In the evaluation section the magnitude of the probable inaccuracies will be tested. (Havskov & Ottemöller, 2010)

The software will be based on the following structure:

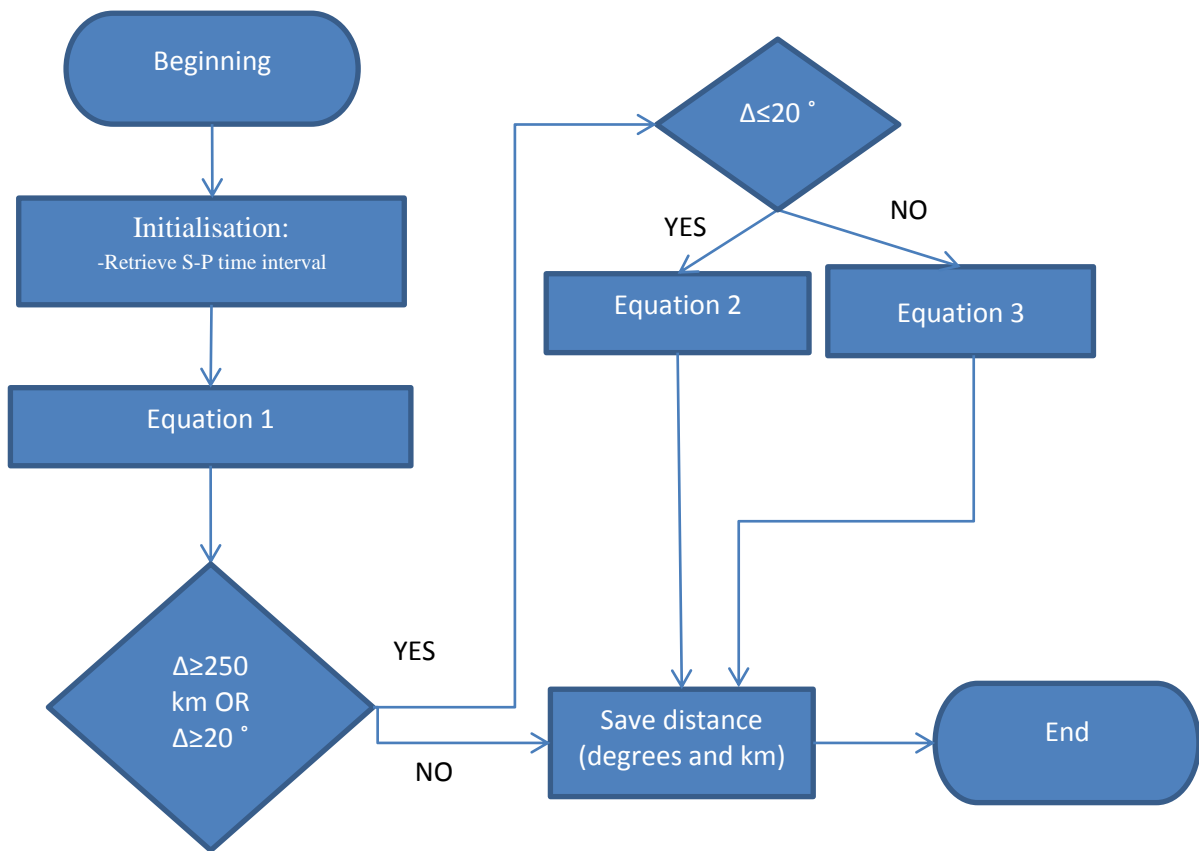


Figure 4.9: Epicentre distance subroutine flowchart

4.9 Magnitude

Among the several magnitude scales it was decided to use M_c and M_s . M_c is an approximation of M_L (known as Richter scale) but the application is much simpler. Both M_c and M_L are local Magnitude scales so the programming of another magnitude that extends the application range it is appropriate. Although, only for swallow events, M_s expands this range up to 160° for magnitudes from 2 to 9 (Havskov & Ottemöller, 2010). Its application in LabVIEW looks a priori simple because it only requires a filter and a peak detector, it has one of the highest application ranges among the scales available and, moreover, it is recommended by the BGS (British Geological Survey, 2011). For detailed Magnitude scale range limitations see background.

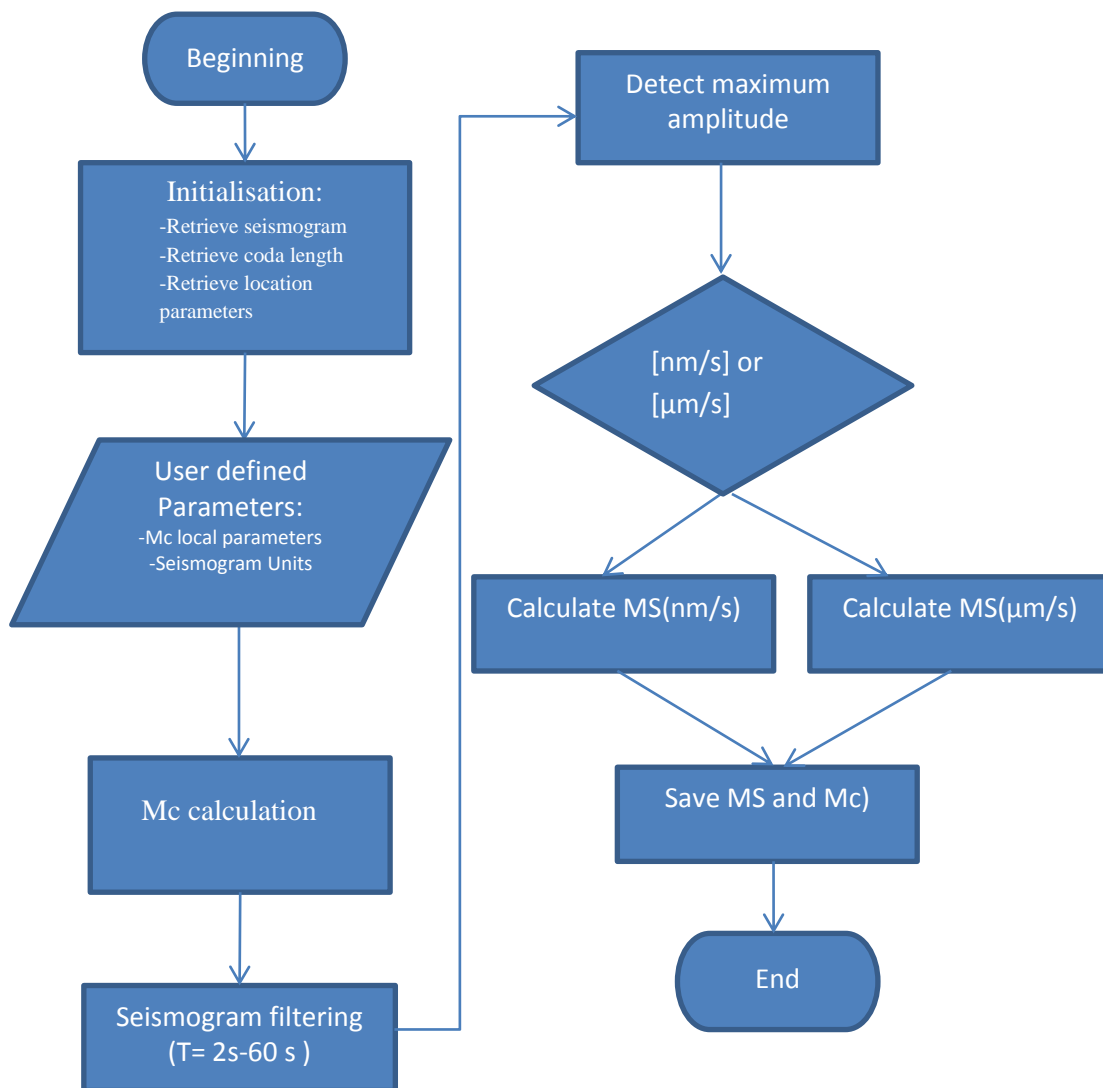


Figure 4.10: Magnitude calculations flowchart

5. Analogue output design

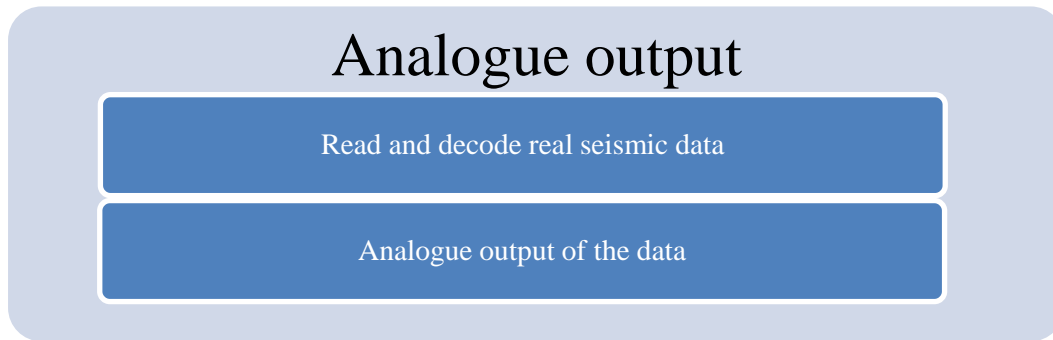


Figure 5.1: Analogue output specifications

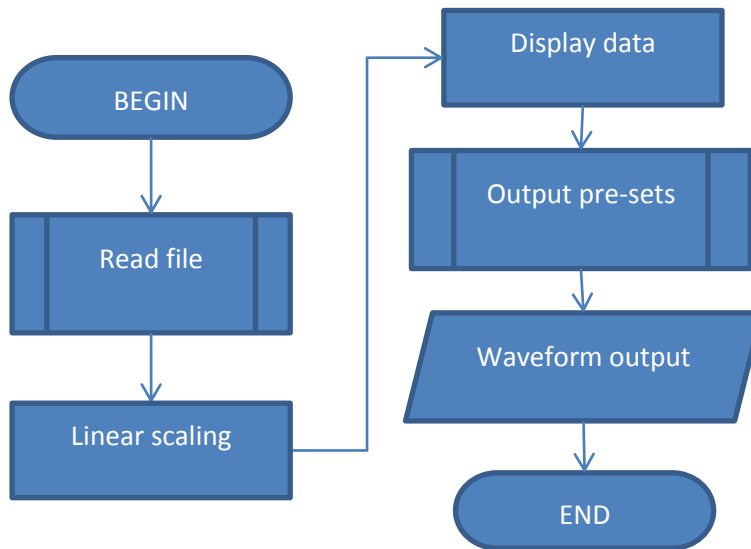


Figure 5.2: Analogue output flowchart

A subroutine to read the data will be developed; the one created for the seismic analysis may be reusable. A user controlled linear scaling is going to be included. The fact that is controlled by the user implies that the operator should be aware of the output voltage limitations but, on the other hand, the real amplitude is always known, something that doesn't happen if the system automatically scales to the maximum values. This program is meant to display both acceleration and velocity waveforms so the operator should indicate what unit is using. The output should be able to be paused and restarted at any time. *Output pre-sets* subroutine has to retrieve critical parameters for the signal output as the output rate, buffer or maximum and minimum voltage values.

6. Vibration monitoring system construction and implementation

6.1 Hardware

Preliminary tests have been performed using the ADXL203 evaluation board and oscilloscopes. Once the PCB was manufactured, the different connectors, a header and a switch have been manually soldered. When the tracks connections were tested the accelerometer was included

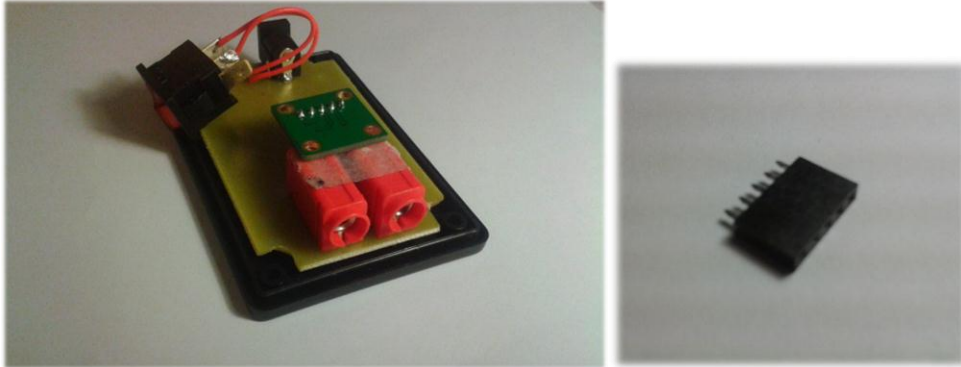


Figure 6.1 Vibration sensor device without the lid and header on which the evaluation board is mounted

The header inclusion possibilities the accelerometer substitution in case of failure. The header connections were confirmed to be loose, slightly moving when the device is shaken, this involves performance problems because the system is meant to be a high sensitive vibration system. Hence, the accelerometer was placed and attached on the 4mm banana sockets using easily removable adhesive in order to provide stability.

The PCB is fastened to the enclosure with instant adhesive to guarantee a satisfactory vibration wave transmission. Holes have been cut out from the enclosure so that the supply and input signal jacks can be connected. The already mentioned double-sided tape has been applied.



Figure 6.2: Complete vibration sensor module.

6.2 Software

The user should select the data acquisition sample rate and buffer size, the data acquisition is made by the DAQ assistant in order to save time as long as its limitations doesn't bound the design requisites. *Acquire* and *pause* buttons control the running. Big differences between the sample rate and buffer size may cause issues so the operator should be careful. Too big buffers can provoke excessive memory usage and crash. Do not exceed DAQ card sample rate capabilities. The *axes calibration* VI filters the axes offset values, it requires separate axes input so the DAQ dynamic data should be previously unbundled.

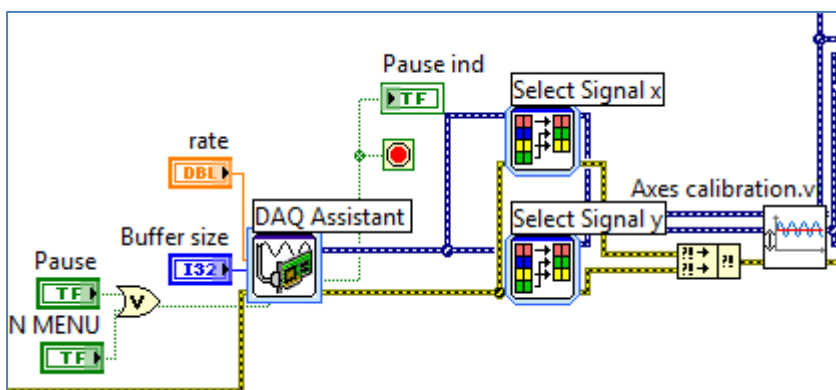


Figure 6.3 code section comprising DAQ assistant and calibration VI

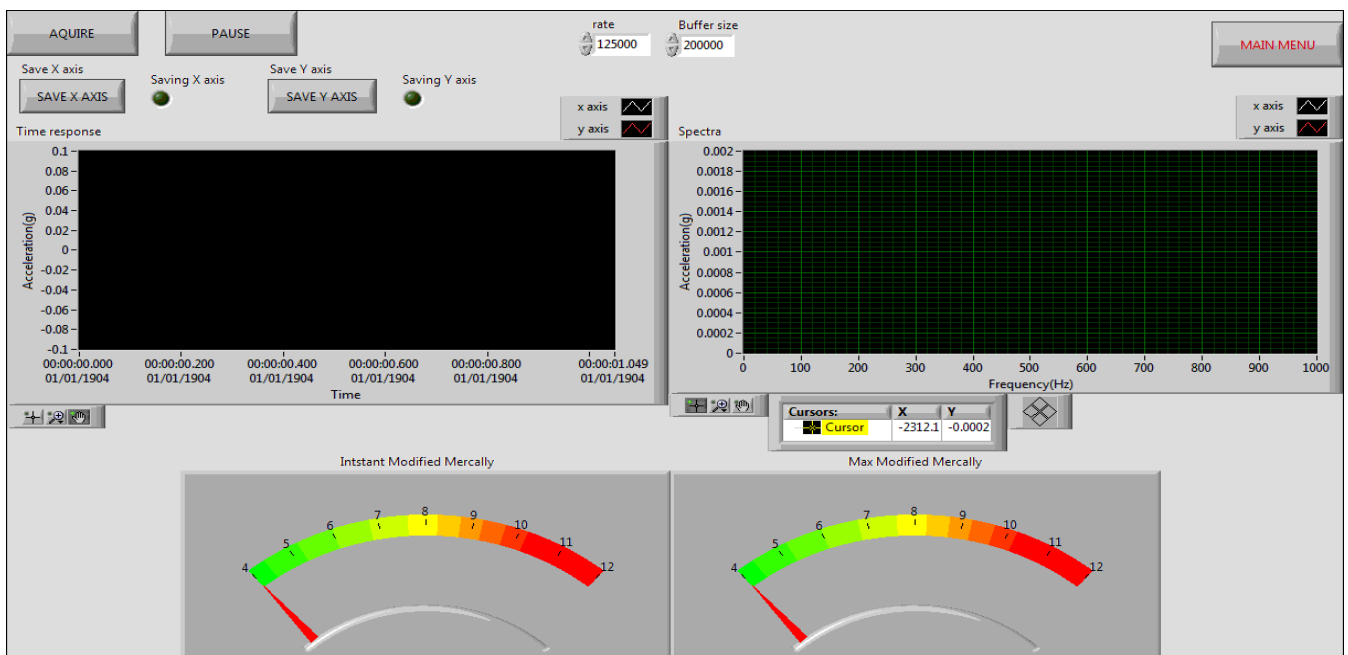


Figure 6.4: Vibration DAQ front panel

Spectra and acceleration time response are displayed in real-time for each of the axes. A chart instead of a graph was believed to be more suitable for the time response. The VI displays the instant and maximum Modified Mercalli intensity scale. The maximum intensity is saved during execution but it initialises to 4 in each run. When considered appropriate, the operator can decide whether to save the axes acceleration vs. time. The data format will be LVM and the file is overwritten if there is previous data. LabVIEW graphs allow taking function snapshots when running.

The *Intensity and danger Display* VI uses the axes absolute acceleration values and determines to what intensity range the acceleration corresponds. The axis with the maximum intensity determines the earthquake intensity final value.

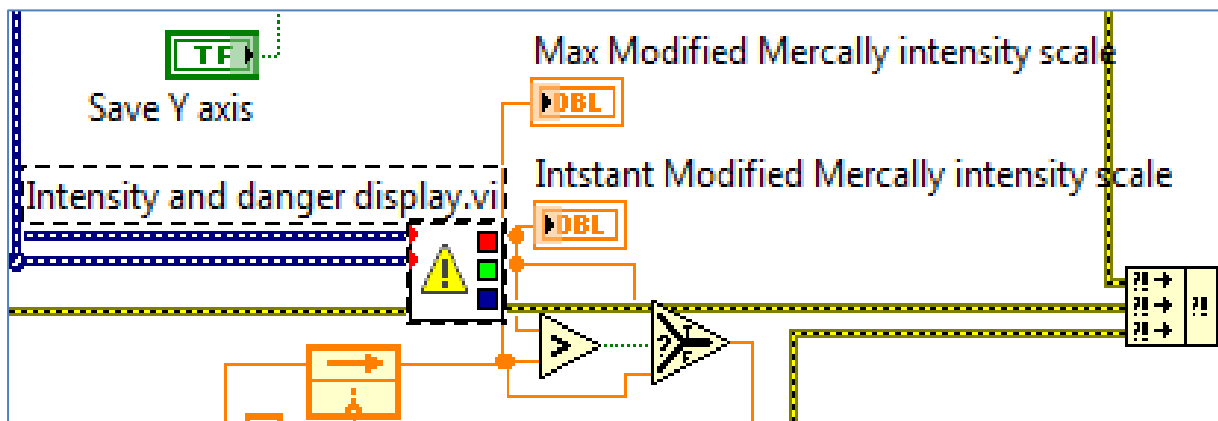


Figure 6.5: "Intensity and danger Display" VI in the vibration DAQ main code

For more information, the complete code can be found in Appendix B.

7. Seismological data analysis software implementation

In this section general comments about the main LabVIEW structures used are going to be made. The Appendix A contains the whole code with more detailed explanations.

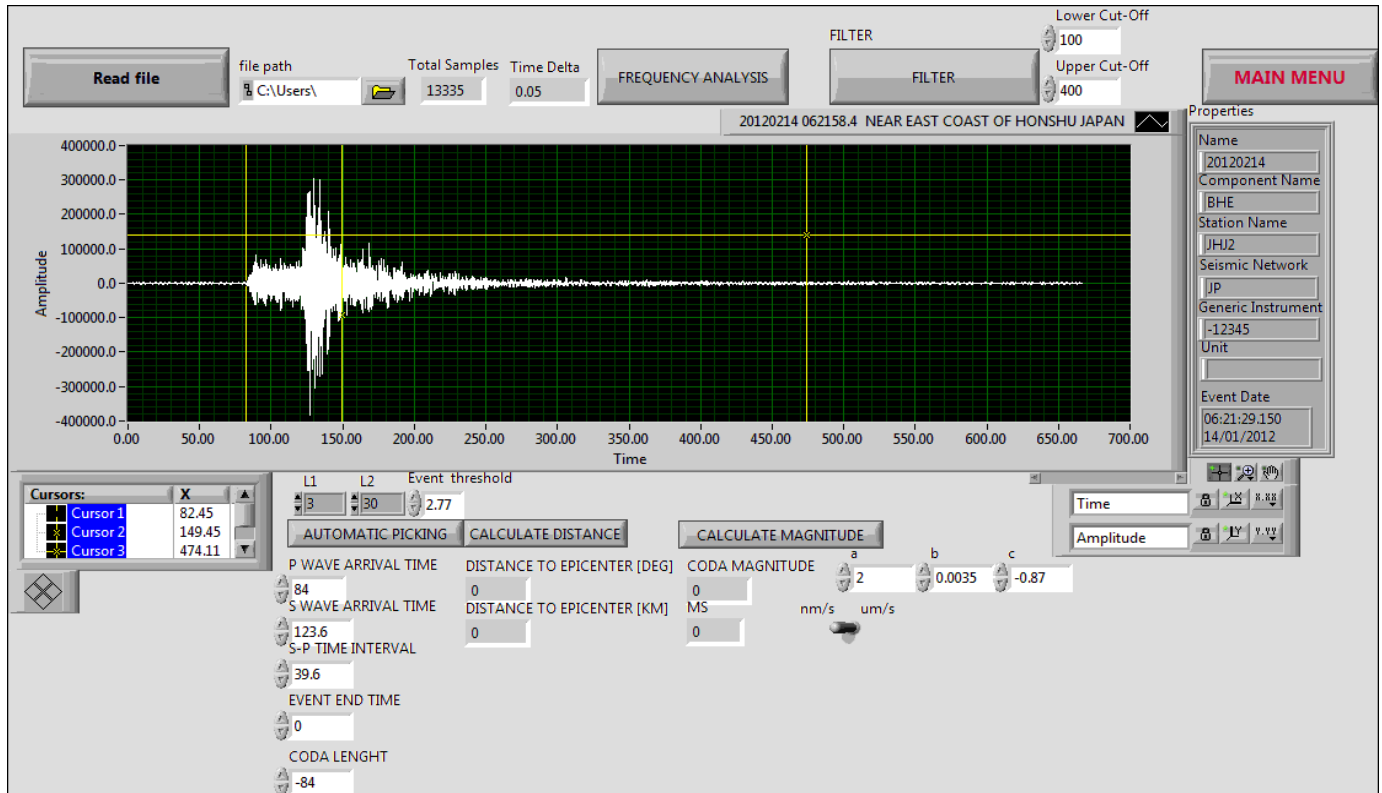


Figure 7.1 Seismic analysis VI front panel

In order to read and decode the data files, a subVI called *ReadSAC* has been developed. It retrieves the SAC file waveform and properties. The *Open Data Storage* express VI allows opening external types of files when the data plug-in is available, once it is installed, it can be selected in its dialog box. After the decoding, the file can be read with *Read Data* in channel mode returning the seismogram waveform as dynamic data. To obtain the properties was more problematic and it required the creation of another SubVI called *RetrieveProperties*. It is based on the *Get properties* VI example available in the Labview 2010 data base (National Instruments, 2010) and it uses For loops and the *Get Properties* VI to obtain metadata from the file, channel groups and groups. Waveform and data are displayed in the seismic analysis front panel. Notice that most of the data obtained does not inform in the properties about the amplitude units so it is impossible to programmatically display them. The unit information depends on the source and, therefore, a selector has been built-in so that the operator selects the units of the waveform that has read. It is usually nm/s or $\mu\text{m/s}$ (IRIS, 2011) (British Geological Survey, 2012). With respect to the calculations this selections only affects to M_S .

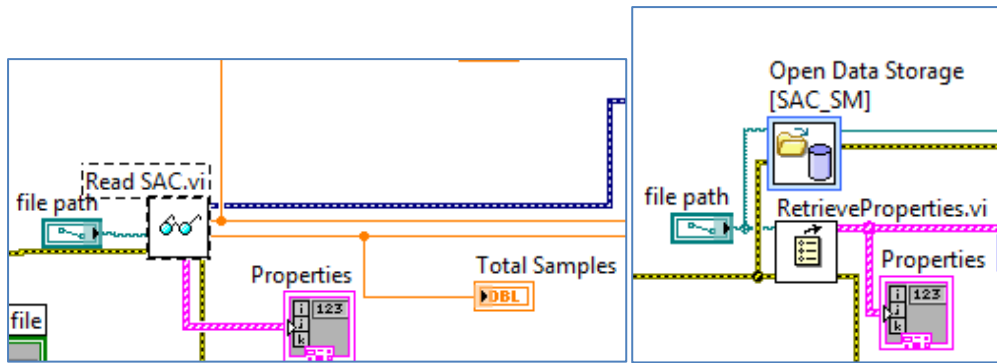


Figure 7.2 Code sections where the mentioned SubVIs are used

A subVI was created to calculate and show the seismogram vs. spectra. A dialog box opens showing both graphs in a window separated from the seismic main controls and indicators. Spectra magnitude is linear so that it can be compared in a better way with the seismogram, the usually low bandwidth of typical earthquakes advises a linear frequency axis scale.

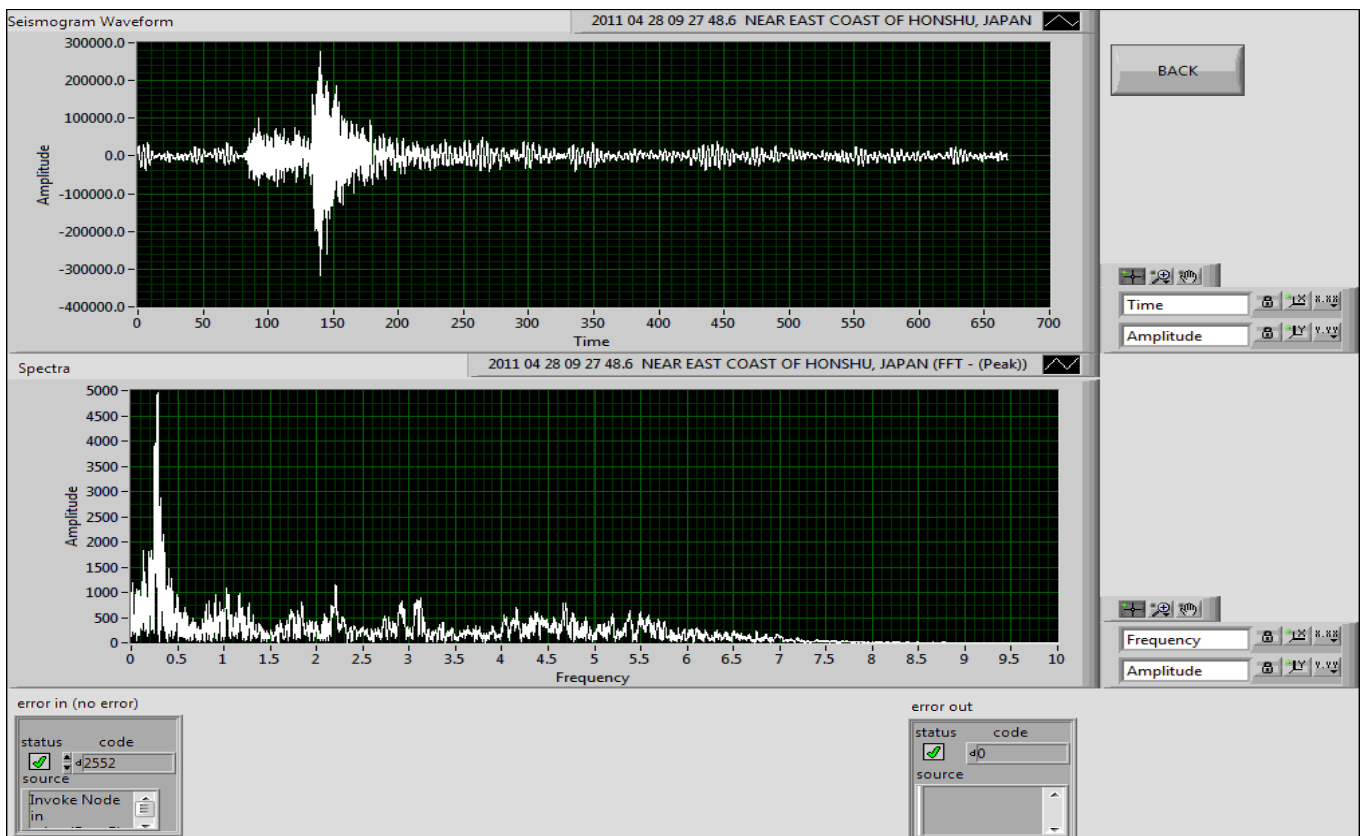


Figure 7.3 Seismogram and its spectra

The operator can define the low and upper cut-off frequencies of a band-pass filter. The resulting filtered waveform is saved in a shift register so all the analysis operations can be performed to the filtered signal. The LabVIEW *filter* VI can be set to use a 4 order

Butterworth as recommended by Havskov et al. (Havskov & Ottemöller, 2010). Notice that if the cut-ff frequencies do not fulfil the Nyquist criterion the software will return an error.

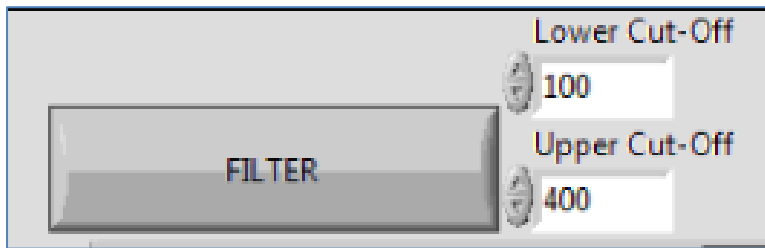


Figure 7.4 Filtering options in the seismic analysis front panel

In order to calculate the STA/LTA ratio, a proper pre-programmed VI was searched among the VI's available in LabVIEW. However, it was not possible to implement it in a satisfactory way. It was considered that the development of an own subVI could save time and effort. The subVI *STA LTA wave* (SNR) provides the STA/LTA ratio using window lengths selected by the operator while *Pick arrival times* VI uses this ratio along with a user defined threshold to automatically pick the P and S arrival timing.

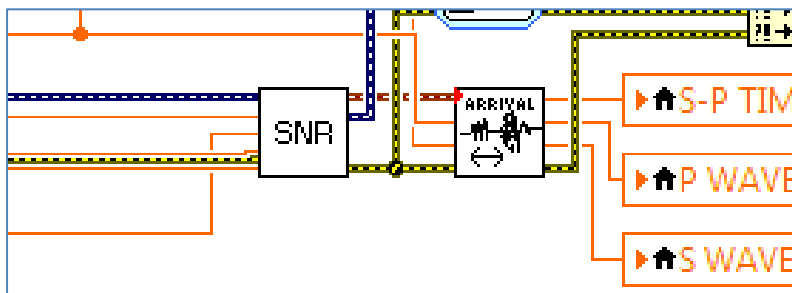


Figure 7.5 : STA LTA ratio and Pick arrival times VIs in the main seismic code

The *STA/LTA wave* SubVI is set up in dialog mode so that a new window with its front panel pops up when the *automatic picking* control is pressed. The use of different windows was considered an appropriate way to expand the information showed in screen and to show the user the state of the SNR calculations, as it take some seconds until it is completed.

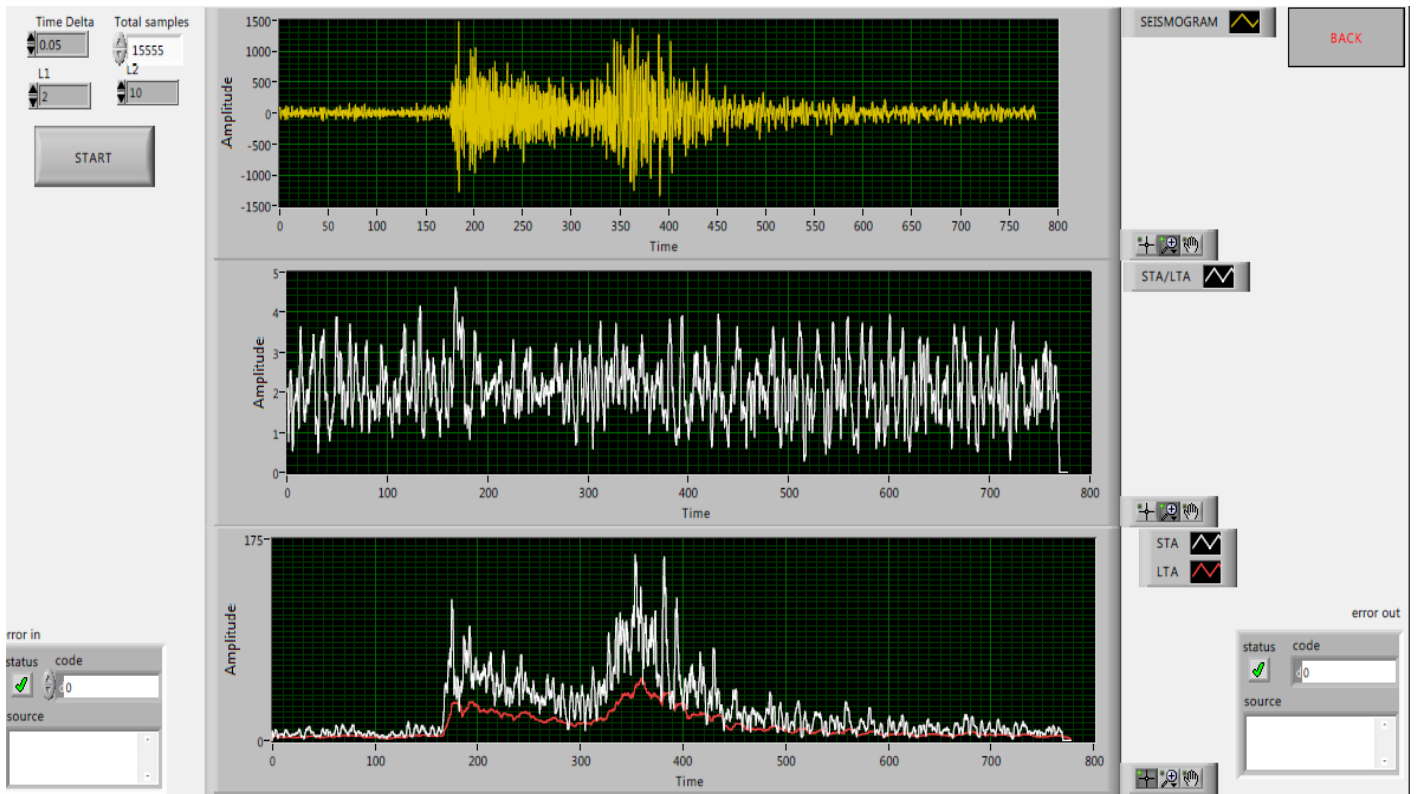


Figure 7.6 STA/LTA ratio VI front panel. The figure shows an earthquake seismogram, the STA/LTA ratio and the STA and LTA waves for specific L1 and L2 window lengths

The SNR calculations are performed sample by sample by a VI called *STA LTA one sample*. Basically, the *STA LTA ratio* VI function is to control the running of that other subVI, window lengths and to put together the waveform. The *Pick arrival times* VI takes advantage of the fact that the first two values that surpass the threshold value are, respectively, the P and S arrival times. Arrival time values are actualised when *STA LTA ratio* dialog box is closed. Detailed comments are written in Appendix A.

The manual picking has been carried out using three vertical cursors which display the time axis values. To use this tool the user should manually identify and introduce the correct P and S arrival time values as well as the end of the event time in the proper controls before proceeding with further automatic calculations. The subtractions required to determine S-P time and coda length are automatically performed.

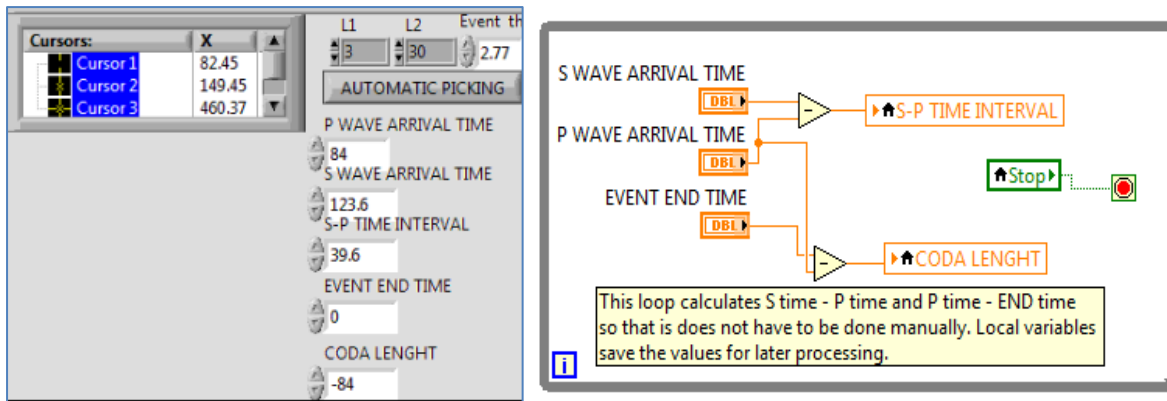


Figure 7.7 Cursors and controls for manual picking in the seismic analysis VI front panel(left) and the loop that actualises coda length and S-P when the use modifies arrival times.

A *coda length meter* VI was developed in order to retrieve this magnitude. It performs the actions described in the design section. It uses the LTA waveform and the P wave arrival time to obtain the coda length and the event end time. In this case only the event end time is retrieved as the final subtraction to calculate the coda (P arrival time – event end time) is performed in the main *seismic analysis* VI in order to allow the user to manually change the event end time at any time (manual picking). The automatic coda results are actualised at the same time that the arrival times. A subVI called *Gathering Signal Values below a Threshold value* is used. This design is a modification of *Gathering Signal Values passed Threshold value* VI developed by one of the NI Instructors in the NI developer zone. It is available to public (NI Instructors, 2011). Detailed description in appendix A.

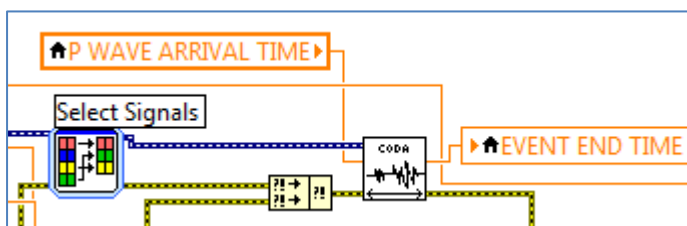


Figure 7.8 "Coda length" VI in the main seismic code

The *Distance to the epicentre* VI uses the P and S arrival times – previously calculated or manually typed - and the already known P and S wave speed - in a normal crust – to determine the station distance to the epicentre in km and degrees. Empirical formulas are used. Notice that the algorithm should change depending on the event distance; this is achieved with a case structure. Values are returned and displayed in the main seismic menu; no dialog box is opened when running.

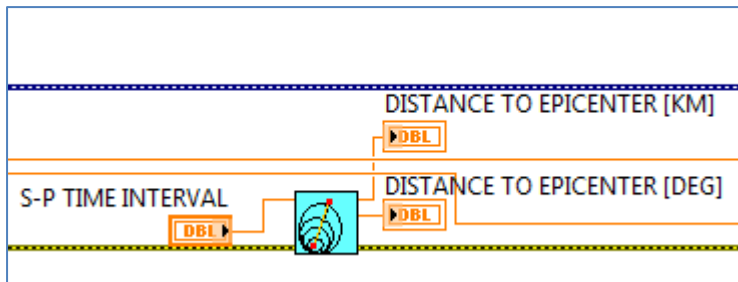


Figure 7.9: Distance to the epicentre subVI placed in the seismic analysis code.

When *Calculate magnitude* button is pressed in the front panel, the system processes the seismogram, coda length and distance to the epicentre parameters – that should be previously settled – to calculate the M_S and M_c magnitude. To calculate M_c , a, b and c parameters should be input by the user and a coda length value has to be available. M_S requires previous bandpass filtering (2 to 60s) as indicated in the background. The maximum value of the filtered signal, as well as the epicentral distance in deg, is used to compute this magnitude scale. The user can select the signal units so that the formula rearranges for correct calculation. The block diagram can be seen in the Appendix A.

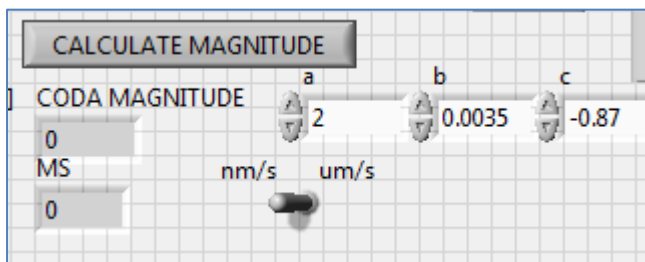


Figure 7.10: Magnitude controls and indicators in the front panel

8. Analogue output software implementation

An *analogue output* VI has been developed. The software is able to read LVM files, containing acceleration time response, and SAC files, it auto detects the input format. There is a user controlled linear scaling. The output start and pause is user managed. When scaling, the output must be within the configured max and min voltage. In this case ± 10 V. As different type of data may be read, the user should manually indicate the amplitude units. The DAQmx auto start function should be on to avoid overwriting errors (-200279) when starting the output after stopped (National Instruments, 2012). *Output presets* VI defines the output task characteristics, in this case, outputs the signal at 50 kHz using a 10 samples buffer. High buffers may cause errors.

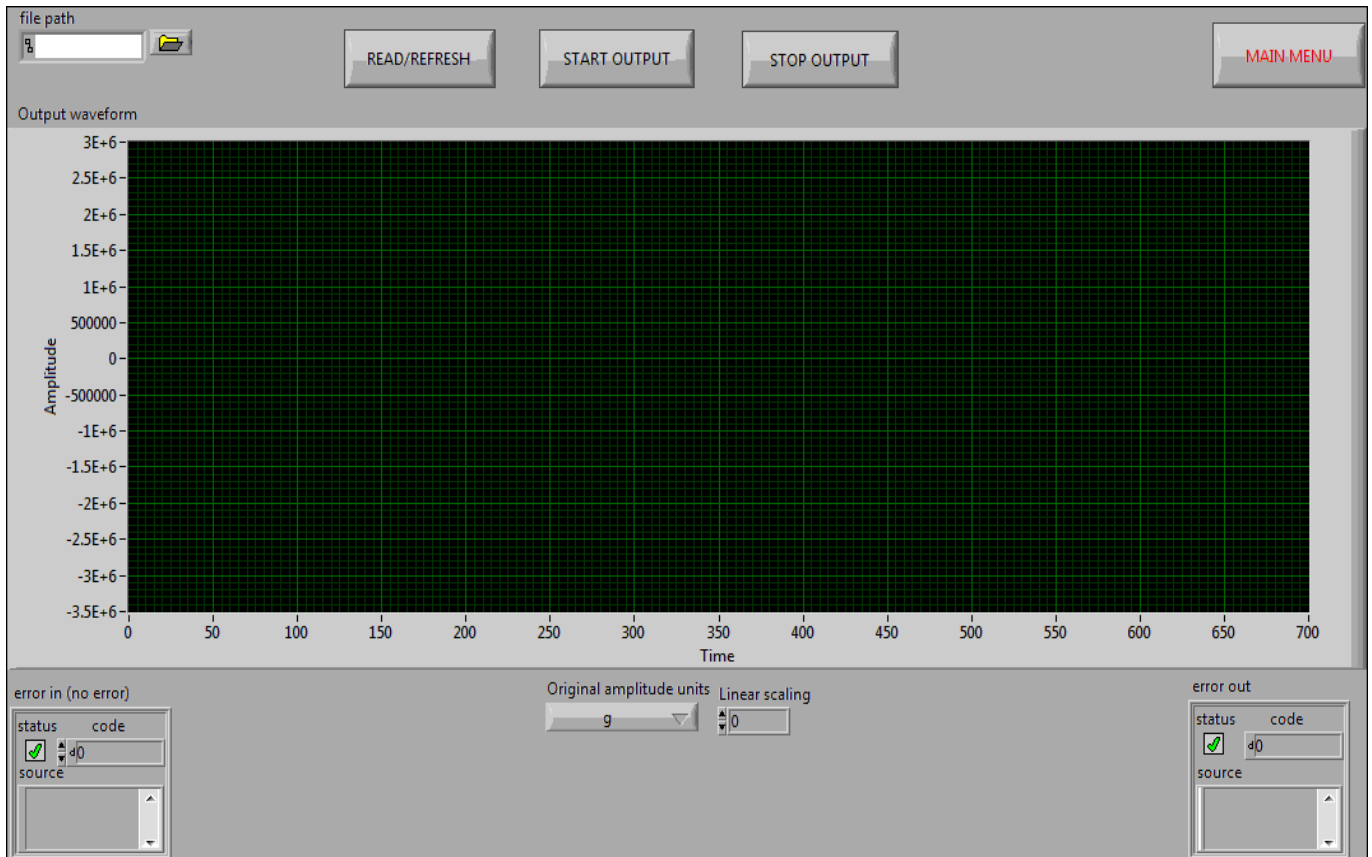


Figure 8.1: Analogue output VI front panel

9. Dataflow and Interface

The interface and data flow has been managed using mainly the event structure. The events are usually buttons pressed. When that happens the program jumps to different running points. Shift registers save event common data while the VIs is running, like the seismogram or errors. Although they are a resource many times avoided, local variable have been required so that controls can be changed both automatically and manually by the user, for example, the P arrival time control can be set by the user but when it is calculated automatically the new value actualises the control through a local variable. SubVIs have been created to perform tasks in a more organized way. Generally, SubVIs were created after processes that were considered important and independent enough to be called subroutines in the design chapter.

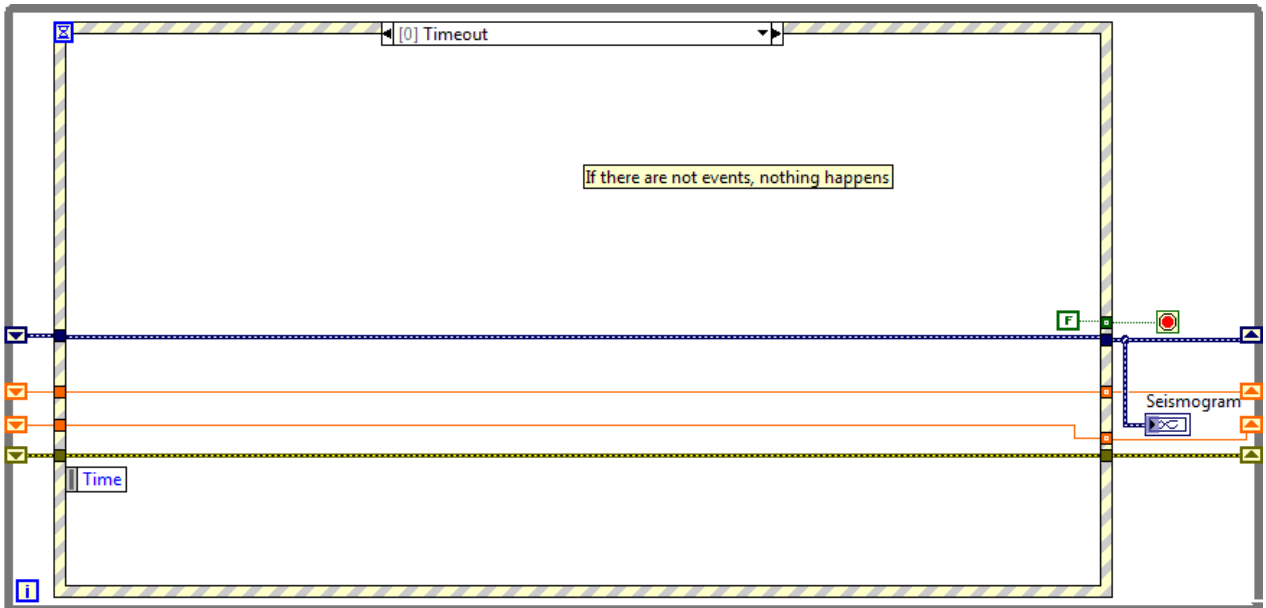


Figure 9.1: Example of the event structure continuously used in the software. The External loop keeps it running. The shift registers and local variables can be seen.

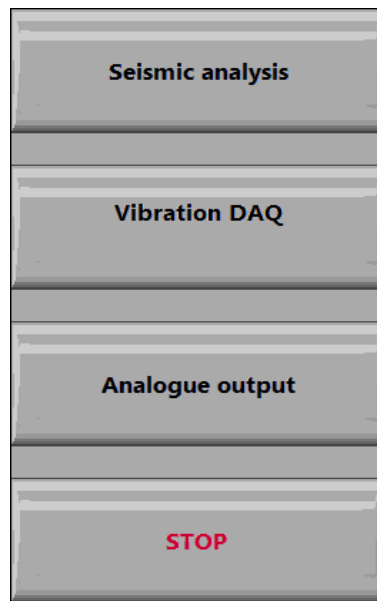


Figure 9.2: Main menu interface

All the front panels used as interface front panels are included in the Appendixes along with the VIs block diagrams. The Appendix D comprises some usage instructions.

10. System evaluation and results

10.1 Vibration DAQ evaluation

The figure below shows the hardware configuration in the tests performed. Note the BNC input connected to the vibration module and the analogue output connected to the oscilloscope through a BNC coaxial wire.

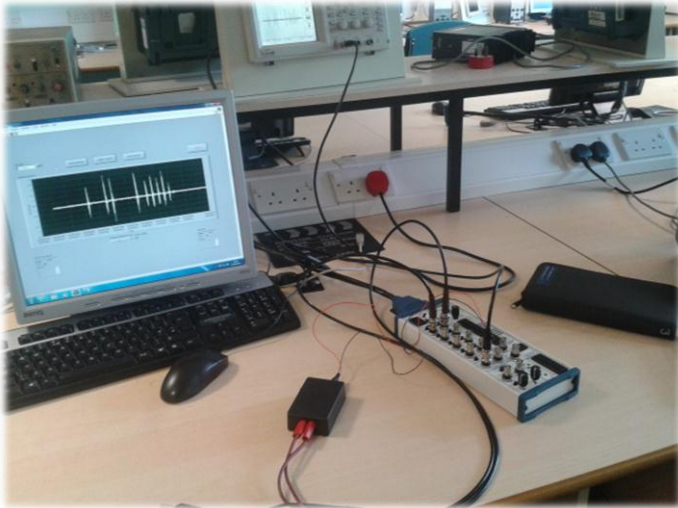


Figure 10.1: Hardware system distribution for vibration DAQ and output testing

Prior to the insertion of the accelerometer analogue outputs into the NI2120 they were tested in an oscilloscope to ensure that the device is not defective.

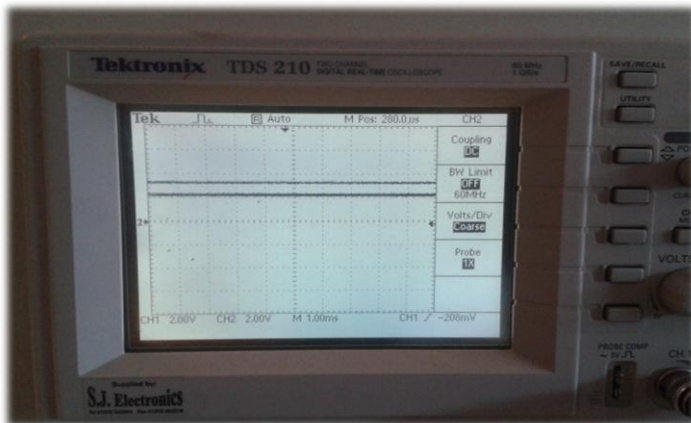


Figure 10.2: Accelerometer voltage outputs when tilted so that the two axes support different accelerations

The vibration DAQ has been tried for different vibration conditions using a 12 kS/s sample rate and a 1000 samples buffer size. Previously, the intensity indicator was tried out with simulated signals to assure that it indicates the correct level. The tests were carried out

attaching the vibration module to a table and applying different magnitude vibrations, hits, and shakings.

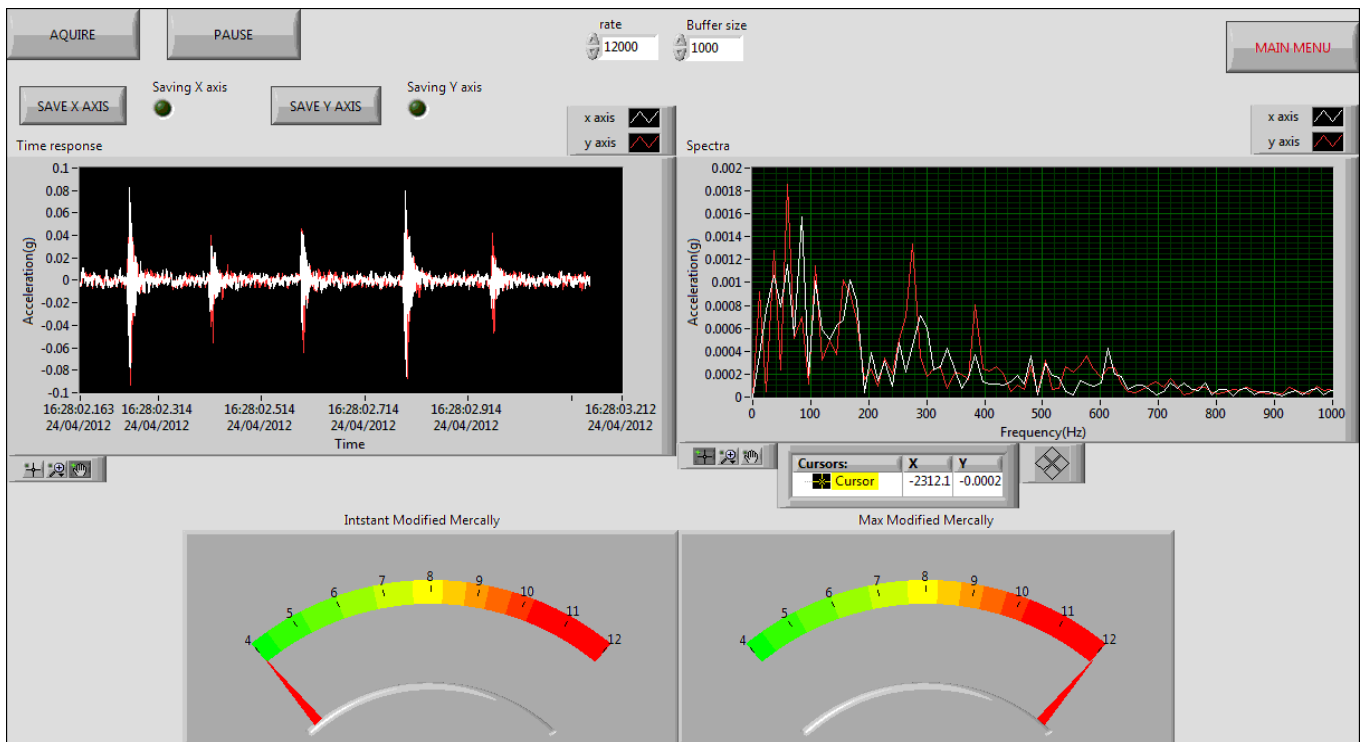


Figure 10.3: DAQ front panel when running

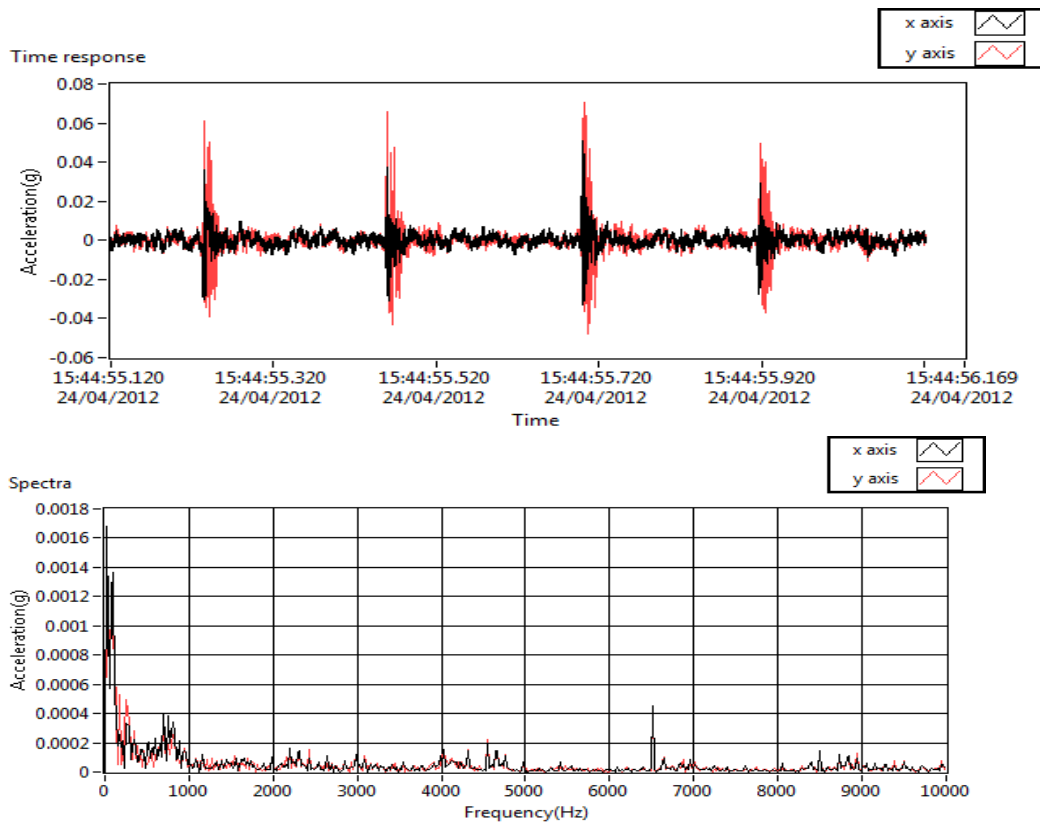


Figure 10.4: Light table hitting (Y axis) time and frequency responses

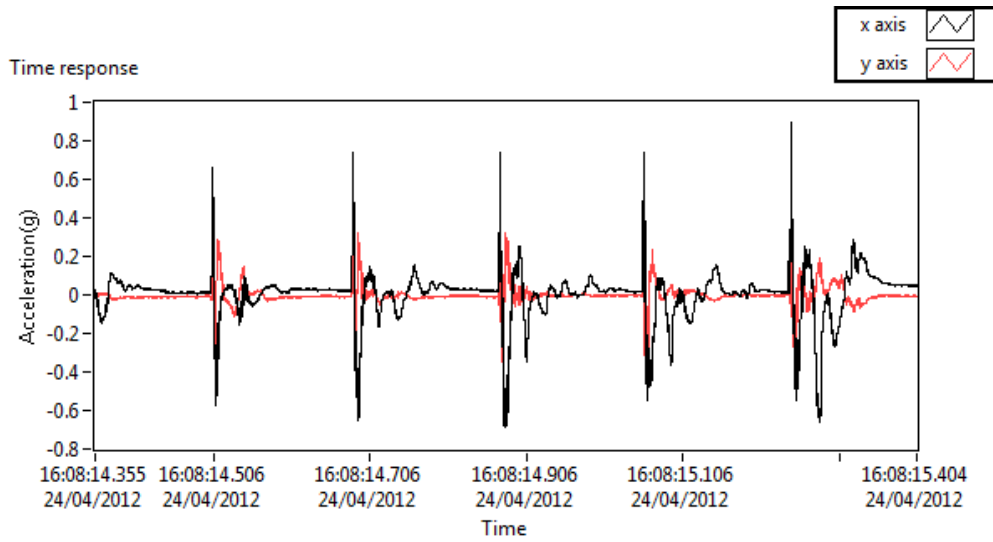


Figure 10.5: Strong enclosure hitting (X axis) time responses

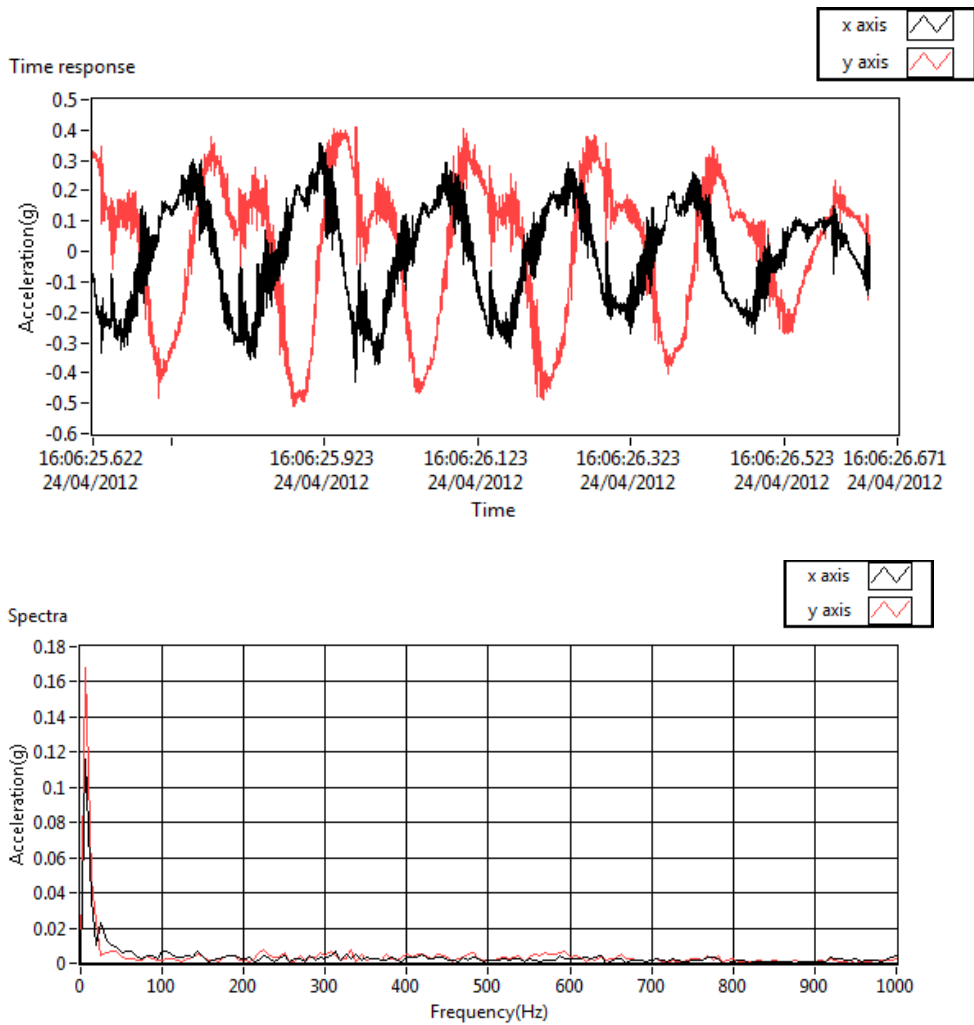


Figure 10.6: Strong shaking time and frequency responses

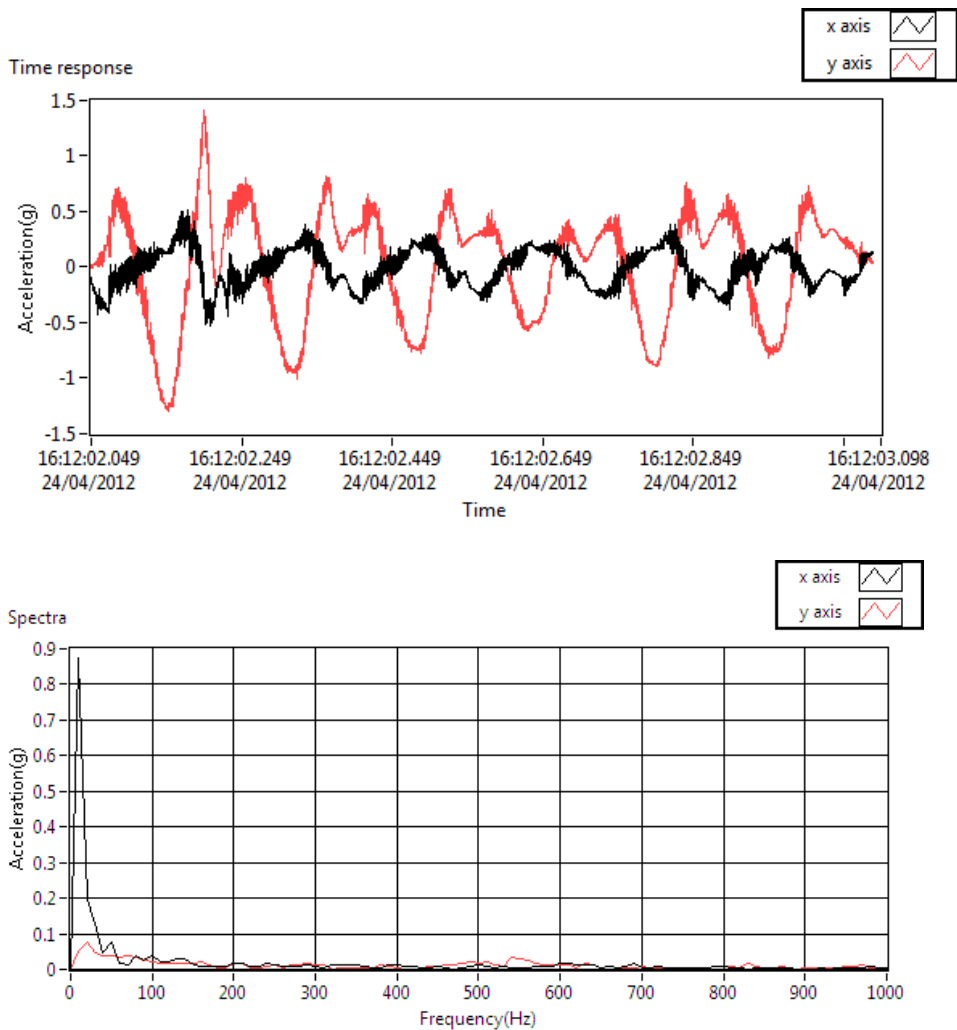


Figure 10.7: Heavy shaking time and frequency responses

The saved files were successfully opened using the *analogue output* VI that is going to be later analysed.

It appears that the system is working well showing coherent responses to the different excitations. It proved to be really sensitive, responding to really light finger tapings. More exhaustive analysis may be needed in the future.

10.2 Seismic analysis evaluation

The software successfully decodes and reads SAC data. The seismogram waveform was displayed successfully in a 100% of the tried data. The property reading varies depending of the data source; some sources provide parameters that other don't. A failure in National Instrument's plug-in has been detected as some of the dates are not displayed correctly. The software successfully reads the metadata that has been considered appropriate and that is commonly present in main providers' files (see Seismic analysis implementation). Critical

parameters for the software development like the time delta or total samples are not always included in the metadata, therefore, the program obtains them analysing the characteristics of the incoming data. The station coordinates are either not included or the plug-in is unable to acquire them, this represent a major inconvenience because it limits the possibility of calculating and plotting the earthquake epicentre coordinates if seismograms from 3 different stations were available (Attri R. K., 2005).

As it can be appreciated, the data properties displayed in my software match the ones in the *data file viewer* VI provided by LabVIEW.

Property name	Property value
name	Velocity
description	
group	
unit_string	nm/sec
datatype	DT_FLOAT
minimum	0.000000
maximum	0.000000
wf_samples	1
wf_xname	time
wf_xunit_string	s
wf_start_time	18/12/2012 18:31:00
wf_start_offset	0.000000
wf_increment	0.049994
wf_time_pref	relative

Figure 10.8: Properties in Data file viewer

Property name	Property value
name	English Channel 1
description	
root	
channels	
ComponentName	E
EventDate	18/12/2012 18:31:00
FileVersion	6
GenericInstrument	-12345
SeismicNetwork	-12345
StationName	WORDW

Properties	
Name	English Channel
Component Name	E
Station Name	WORDW
Seismic Network	-12345
Generic Instrument	-12345
Unit	nm/sec
Event Date	18:31:00.589 18/12/2012

Figure 10.9: Data properties in seismic software

The epicentre distance algorithm has been tested using the travel time tables provided by the US geological survey. These tables, often presented as graphs, relate the S-P time interval to the distance of the event in degrees or km. The figure below compares the distance calculated for an established S-P time interval with the distance in the chart for the same time interval. Recall that the relation between S-P time and distance depends on the depth. The table study 33 km depth events and, although the software implemented is a good approximation, supposes surface events, consequently, the shallower the earthquake the more precision it provides.

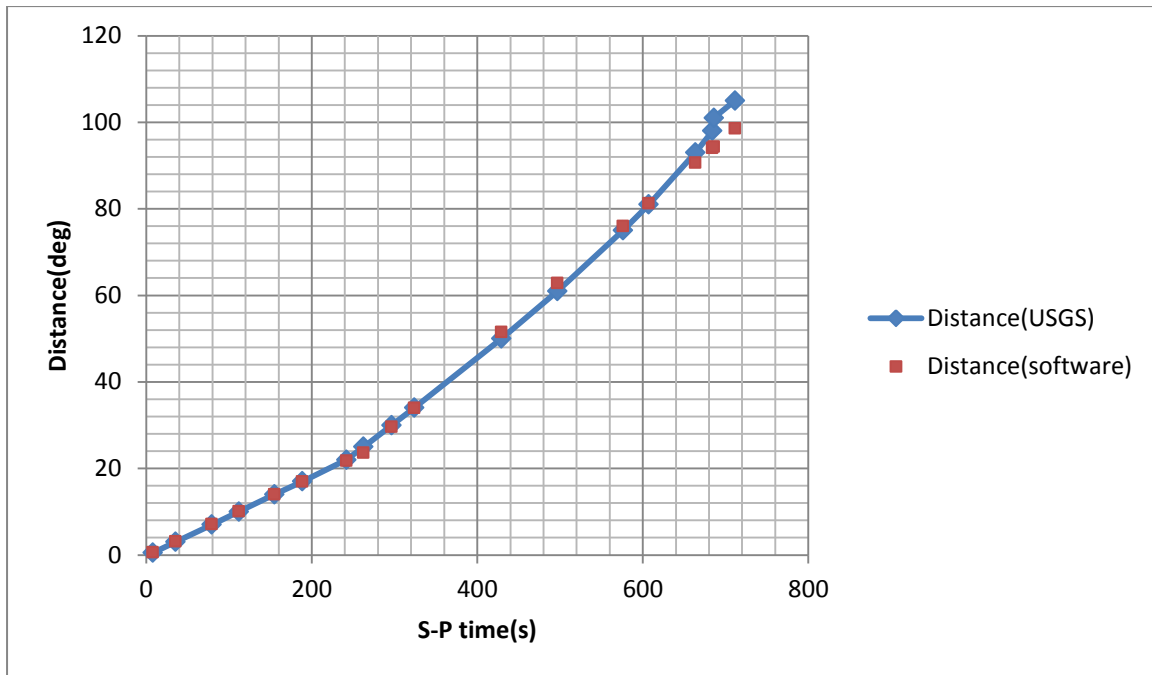


Figure 10.8 Software distance calculations compared to USGS Distance vs S-P time table

The results surpass the theoretical strength of the algorithm used. Notice that, between 1000 km (9°) and 20° , there was a gap where there was not a proper algorithm available. In view of the situation, the equation used from 250 km to 1000 km was extended to that breach with satisfactory results. As expected, over 100° there is a worse performance. However; in most of the cases below that distance the divergence rarely exceeds 3° .

To test the software magnitude calculations, the results have been compared with the ones provided by IRIS (IRIS, 2011). They are represented in the figure below along with some other values related to the software limitations. There was a preference for local data, however, most of the data from the British Geological Survey page comes from non-professional networks and it was difficult to find clean seismograms with an acceptable SNR in the professional networks available (British Geological Survey, 2012). Therefore, the alternative chosen has been the Japan Meteorological Agency Seismic Network because it provides extensive and varied earthquake data due to the region activity. Besides, the signal's SNR is usually high allowing an ideal study of the signals. Its data is available from IRIS using the WILBER II tool for seismic data downloading.

Event	Depth(km)	Distance(°)	Magnitude(IRIS)	Mc	MS
2011/09/15 08:00:07.1 NEAR EAST COAST OF HONSHU, JAPAN(JHJ2)	10	3.4	6.3	5.65	5.63
2012/03/14 09:08:37.5 OFF EAST COAST OF HONSHU, JAPAN(JHJ2)	26.60	8.56	6.8	8.4	6.9
2011/10/21 08:02:38.1 HOKKAIDO, JAPAN REGION(JHJ2)	188.20	10.35	5.8	7.7	5.7
2011/06/26 09:19:48.2 MARIANA ISLANDS (CBIJ)	99.90	8.38	5.7	7.07	5.07
2011/08/20 18:19:21.0 VANUATU ISLANDS(YOJ)	2	65.5	7	30.59	7.06
2012/01/10 18:37:01.2 OFF W COAST OF NORTHERN SUMATERA	29.10	38	7.3	20.4	6.96
2011/09/18 12:40:48.1 SIKKIM, INDIA	20.7	46.09	6.8	23.59	6.86
2007/08/15 23:40:56.8 NEAR COAST OF PERU	30.20	207.32	8	86.28	8.22

Table 10.1 Software magnitude calculations evaluation. Comparison with magnitude of different data retrieved from ISIS.

The manual picking function has been used to determine the arrivals. The equation parameters selected for the Coda Magnitude determination are the ones determined by the US Geological Survey in 1972 (W.H.K Lee et al, 1972). It was not possible to find these

particular parameters for the Japan region. Nevertheless, some references indicated that the parameters are still used nowadays for the detection of earthquakes in places where there are not coda magnitude studies or they cannot be found (Havskov & Ottemöller, 2010) (Kayal, 2008).

From these results it can be stated that:

- M_S is a good approximation for relatively shallow earthquakes
- In really short and long distance events generally M_S lacks accuracy
- Really deep events also reduce M_S accuracy.
- It shows why the coda magnitude is discredited (Havskov & Ottemöller, 2010), it is an approximation to Richter magnitude in local events but as it can be seen, it is not working properly. For long distance earthquakes it is not even close.

The results match with the theoretical specification that was known when implemented. M_S works well with events in a distance range from 2° to 160° and less than 60 km depth. M_c is an approximation for local events but it didn't work well in this case. It is not a good method when using manual picking because of its critical dependence on coda length. Also, the generic expression by Lee et al has been used because a particularization for the expression has not been found for Japan, probably that contributed to its bad performance in the studied cases.

In order to confirm this aspect a test has been performed using data from the Oregon University Network and Coda Magnitude parameters for the adjacent California.

Event	Depth(km)	Distance($^\circ$)	Magnitude(IRIS)	M_c
2011/09/09 19:41:35.0 VANCOUVER ISLAND REGION	25.90	5.8	6.7	6.9

Table 10.2 Coda magnitude characteristics verification

The result corroborates a great improvement compared to the previous coda Magnitude values.

The system successfully displays the LTA, STA and its ratio, therefore, a SNR measurement is available for its study. The graphs built show a ratio growth when there is an incoming signal - P and S wave respectively. Occasionally there may be other peaks due to the

incoming surface waves or particularly intense noise. Notice that this happens often in far events due to the wave speed difference which tend to separate surface waves from S signals.

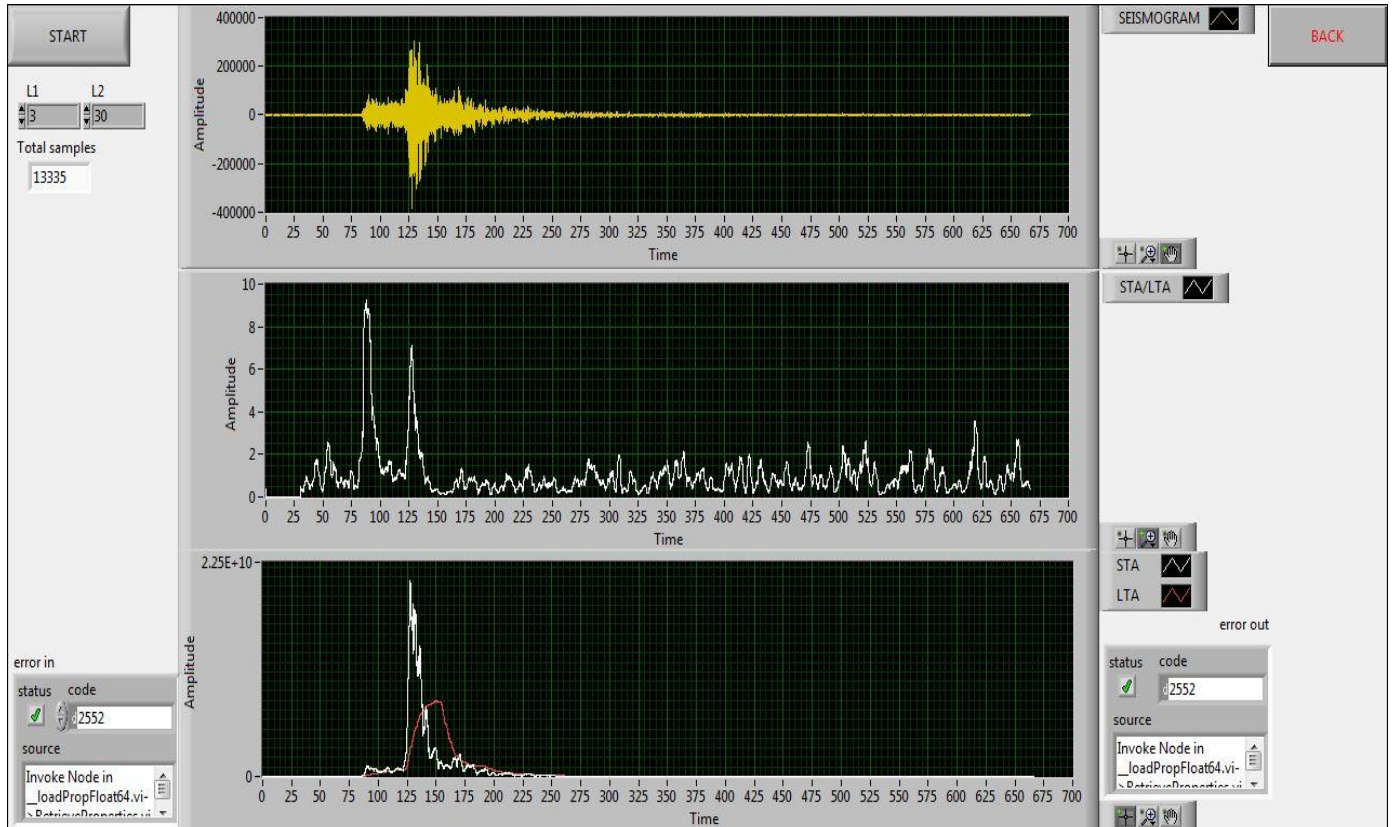


Figure 10.9: STA/LTA ratio VI front panel

The software was intended to use this information to automatically calculate the P and S waves arrival times – in this text sometimes denoted as automatic phase picking. Before the performance of this part can be evaluated, a process of calibration must be performed. The threshold that determines the wave arrival has to be defined depending on the station that makes the measurements. These calibration processes are made taking into account the station history (Attri R. K., 2005), however, for obvious reasons the one that is included in this report doesn't cover that extension. The threshold values have been calculated averaging 16 different thresholds from 8 different events.

The process followed comprised these steps for each of the events:

- 1) Manual picking
- 2) Selecting L1 and L2 windows depending on the signal frequency response.
 $L1 = 3 \times \text{expected signal period}$; $L2 = 10 \times L1$. Frequency analysis performed with the previously developed software function.
- 3) SNR study, pick the threshold value that provides an arrival time that matches with the manual picking. For both P and S waves.

A history chart was made and averaged to obtain a proper threshold value.

Probably, trimming could be performed by statistically adjusting L1 and L2 for each event based on the manual pickings (Munro K. , 2004) but is out of reach with the available time. The calibration has been made for the station JHJ2 based in Hachijojima Island belonging to the Japan Meteorological Agency Seismic Network. Again, the reason is the amount of events to choose from after the March 11 earthquake and the clarity of the seismograms available.

EVENT	MAN(P)[s]	MAN(S)[s]	L1	L2	Tp	Ts
1) 2012 02 14 NEAR EAST COAST OF HONSHU JAPAN	84.54	123.98	3	30	3.1	3.1
2) 2011 10 21 HOKKAIDO, JAPAN REGION	96	209.35	3.75	37.5	2.6	2.4
3) 2011 12 09 SEA OF OKHOTSK	89.12	245.58	3	30	2.9	3.7
4) 2011 08 01 NEAR S. COAST OF HONSHU, JAPAN	84.54	109.59	6	60	2.9	5.5
5) 2011 07 23 NEAR EAST COAST OF HONSHU, JAPAN	84.55	143.8	7	70	2.7	2.1
6) 2011 04 01 EASTERN HONSHU, JAPAN	86.46	151	6	60	3.2	2.2
7) 2011 04 07 NEAR EAST COAST OF HONSHU, JAPAN	90.56	149.56	7.5	75	3.2	1.8
8) 2011 04 28 NEAR EAST COAST OF HONSHU, JAPAN	85.73	134.33	7.5	75	1	1.7

Table 10.3 Threshold determination for different earthquakes

The following chart displays different threshold values and averages them.

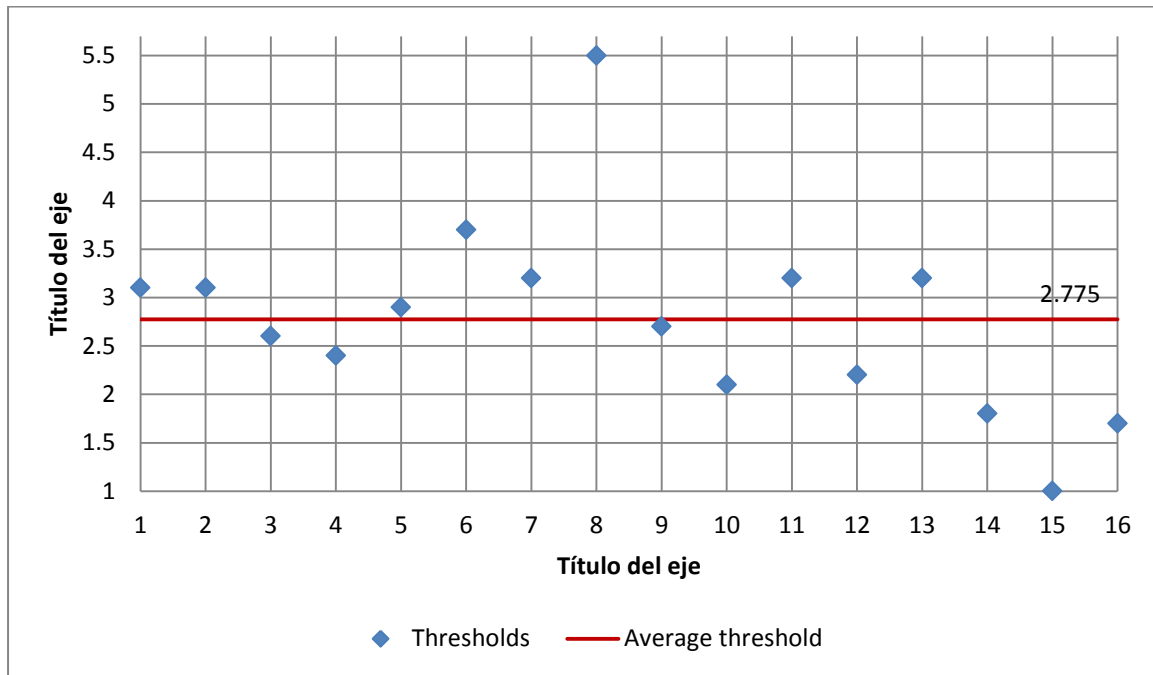


Figure 10.10: Averaged threshold

The average value $T=2.775$ was used to test the automatic phase picking software. The automatic arrival values are compared with the manual picking ones. L1 and L2 are the same indicated in the previous table.

EVENT	MAN(P)[s]	AUT(P)[s]	MAN(S)[s]	AUT(S)[s]
1) 2012 02 14 NEAR EAST COAST OF HONSHU JAPAN	84.54	84.1	123.98	123.6
2) 2011 10 21 HOKKAIDO, JAPAN REGION	96	96.05	209.35	209.65
3) 2011 12 09 SEA OF OKHOTSK	89.12	89	245.58	245.35
4) 2011 08 01 NEAR S. COAST OF HONSHU, JAPAN	84.54	84.5	109.59	-
5) 2011 07 23 NEAR EAST COAST OF HONSHU, JAPAN	84.55	84.65	143.8	144.55
6) 2011 04 01 EASTERN HONSHU, JAPAN	86.46	85.6	151	151.7
7) 2011 04 07 NEAR EAST COAST OF HONSHU, JAPAN	90.56	90.55	149.56	151.35
8) 2011 04 28 NEAR EAST COAST OF HONSHU, JAPAN	85.73	7.5	134.33	136.5

Table 10.4: Automatic and manual picking comparison

The results are mostly satisfactory for the number of arrival threshold that have been averaged, the error rarely exceed 0.5 seconds. Number 7 and 8 S wave arrival appears to be problematic probably due to the number of averaged sampled. However, number 8 is a really noisy seismogram, there is apparently a bad influence of background noise in picking that this algorithm is not able to solve. The generalized threshold – for both P and S picking – appear to have also a negative effect compared to other studies found (Munro K. , 2004) reducing the precision that could have been reached if using different values. In events with P and S waves arrivals really close in time doesn't work properly – earthquake 4.

This algorithm seem to be a good qualitative method to calculate approximated arrival times with a precision of around 0.5 seconds –probably much less with the appropriate history study. Nevertheless, fails to be the ultimate method to provide timings precisely with real data. Kim Munro concludes the same in her study *Automatic event detection and picking of P-wave arrivals* (Munro K. , 2004). An algorithm modification for improvement was presented in her later Thesis *Analysis of microseismic event picking with applications to landslide and oil-field monitoring settings* (Munro K. A., 2005).

The first STA/LTA software programmed had serious performance problems as the processing of data comprising around 15'000 samples took between 40 and 50 seconds (Intel Core i5 processor 2.3 GHz). By substituting express VIs and modifying the algorithm, that time has been reduced to half. It is not a brilliant performance though. Performing the window calculations point by point to such amount of data requires processing power. However, it is considered that in the future a reduction in processing time is still possible with the current implementation, especially regarding the resetting. In the current state it is not recommendable to use the automatic picking with data over the samples indicated above. The SNR ratio front panel pops up when using the automatic picking allowing the user to see the calculation progress.

The coda length calculator present problems related to the algorithm, from the several test performed only few gave satisfactory results. It is important to notice that the evaluation of this piece of software was extremely difficult due to the subjectivity of the magnitude to measure (Havskov & Ottemöller, 2010). The automatic detector is far more sensible than the manual picking so it is was sometimes difficult to say if the problem was the user ability to choose a proper coda or the software performance. However, the poor execution was evident

with a naked eye due to some impossible results. The problem was identified and described below.

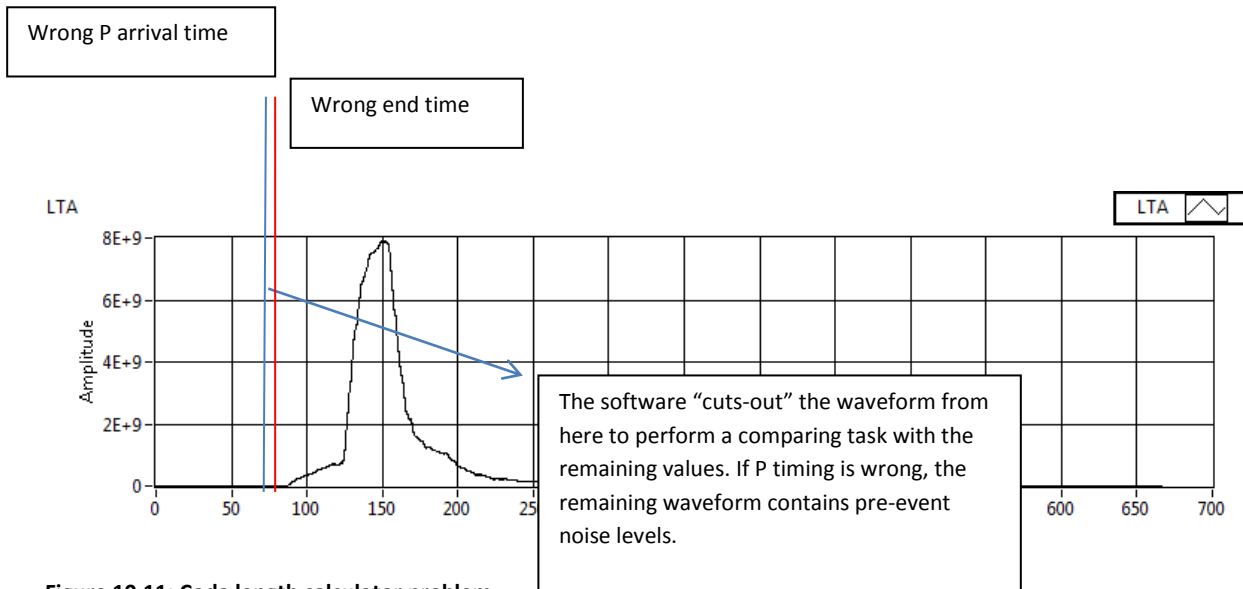


Figure 10.11: Coda length calculator problem

The detection extremely depends on the correct P wave time arrival detection. The figure above represents the LTA wave, the background noise. If the P wave timing is slightly imprecise the VI “cuts out” the waveform before it was supposed. The remaining waveforms values are later compared with a typical noise value before the earthquake arrival, notice that if the remaining values contain pre-event noise levels the event end time picked is going to be incorrect, far before than when it was supposed. As explained above, it is impossible to assure a perfect automatic P or S arrival picking with the available resources, and the precision required for the algorithm above may be tens of milliseconds- few samples make the difference. This issue improvement will be one of the future works suggested. It is also important to highlight that the data analysed has to include the samples where the earth is settled down. This is not trivial, good amount of data samples available in the internet do not include this information, they are cut out before, the waveform never returns to the pre-event levels and, hence, the analysis always returns wrong values.

Other additional functions as the frequency analysis or the band pass filtering are working correctly. The following charts correspond to a 2012 event near the east coast of Honshu.

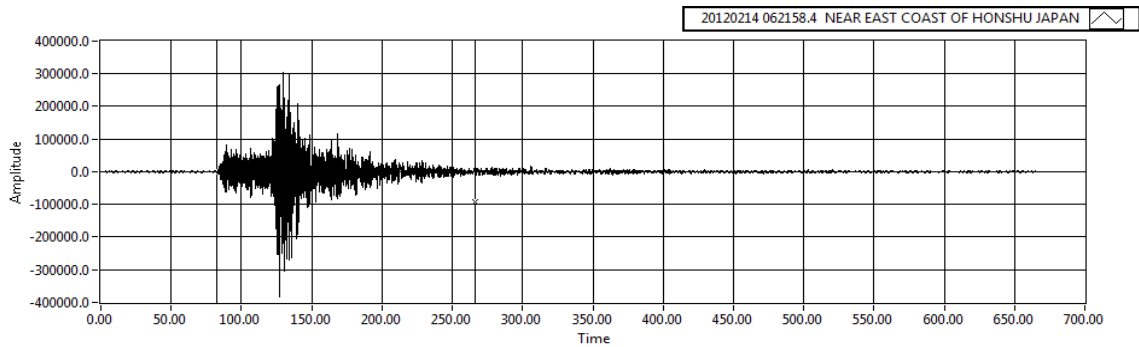


Figure 10.12: Non- filtered seismogram

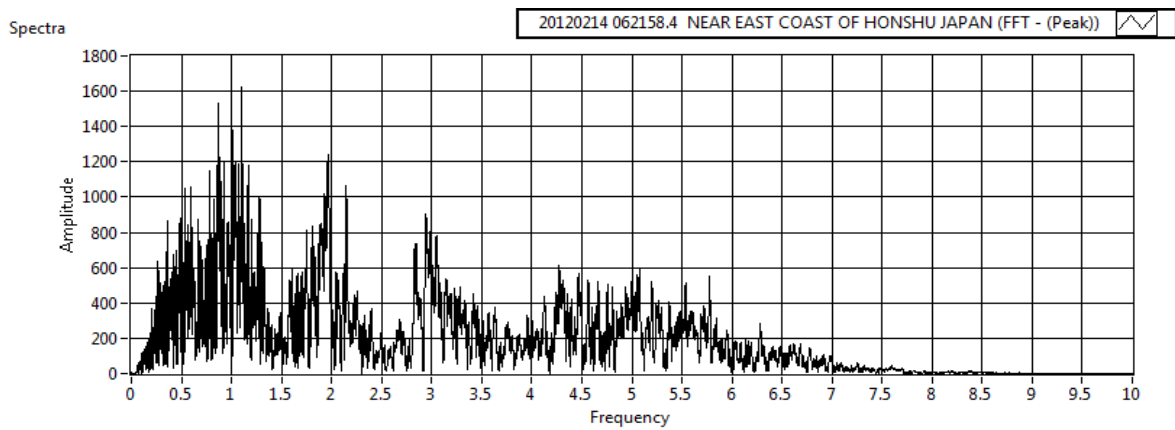


Figure 10.13: Seismogram spectra

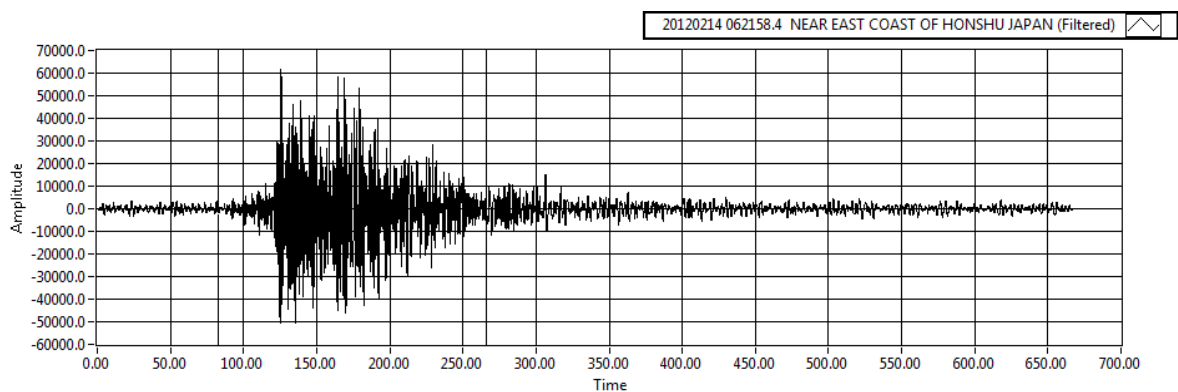


Figure 10.14: Filtered seismogram. Low cut-off = 0. 01 Hz. High cut-off =1 Hz

By the time this report is being typed, some user interface issues are not still polished causing occasional crashes but allowing the evaluation of the different VI's developed. It is expected that this issues are solved before the demonstration.

10.3 Analogue output evaluation

The analogue output software successfully reads and outputs LVM files containing X or Y axes acceleration recorded with *Vibration DAQ VI* and the designed hardware module. It also works well with the SAC files (velocity) downloaded from the IRIS database. The stop, refresh and scaling options don't show problems if the operator works within the restrictions stated in the implementation section.

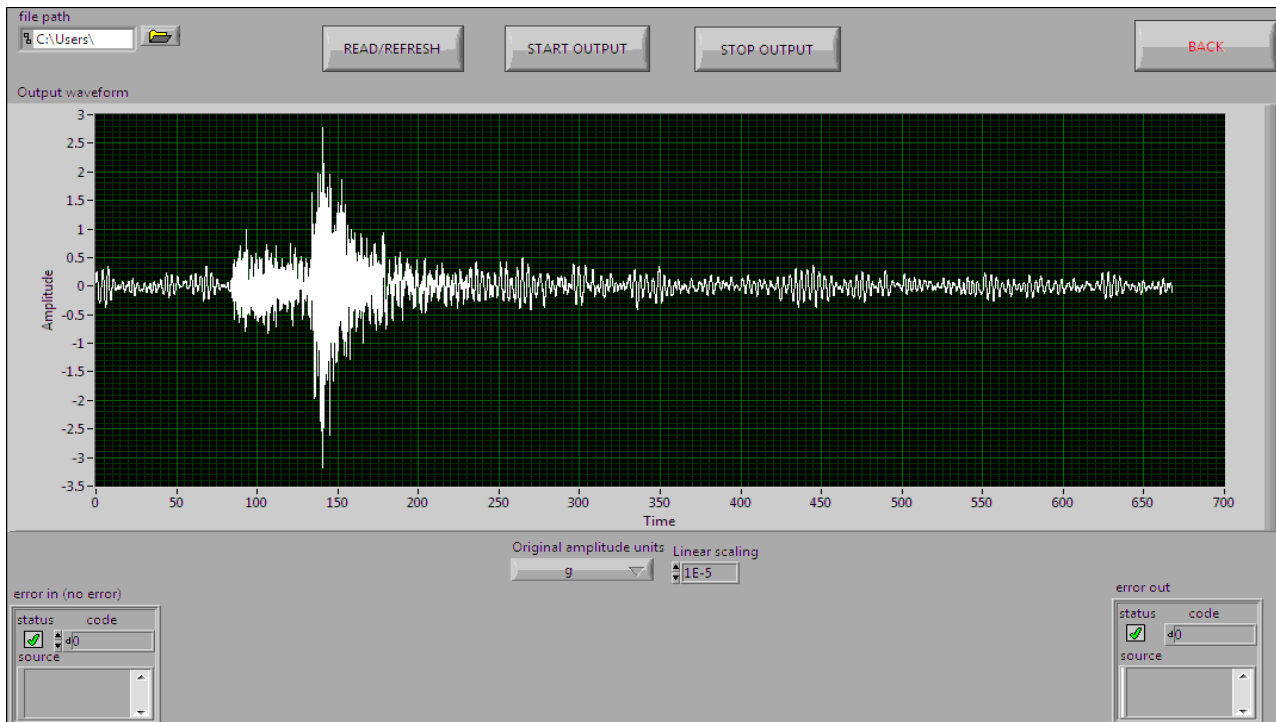


Figure 10.15: Analogue output front panel running and reading a SAC file.

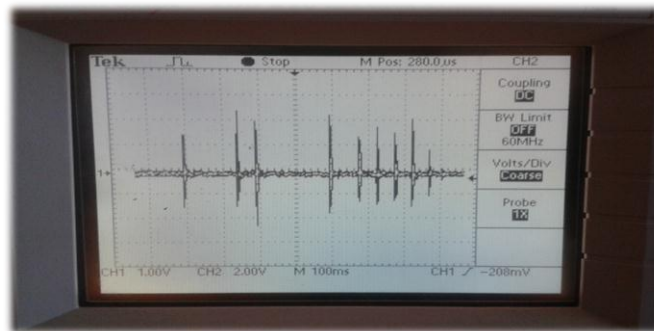
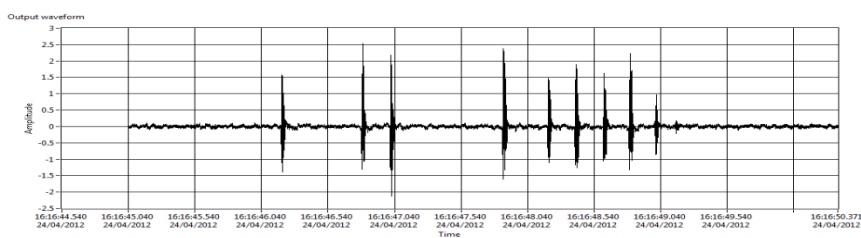


Figure 10.16: LVM vibration file reading and analogue output

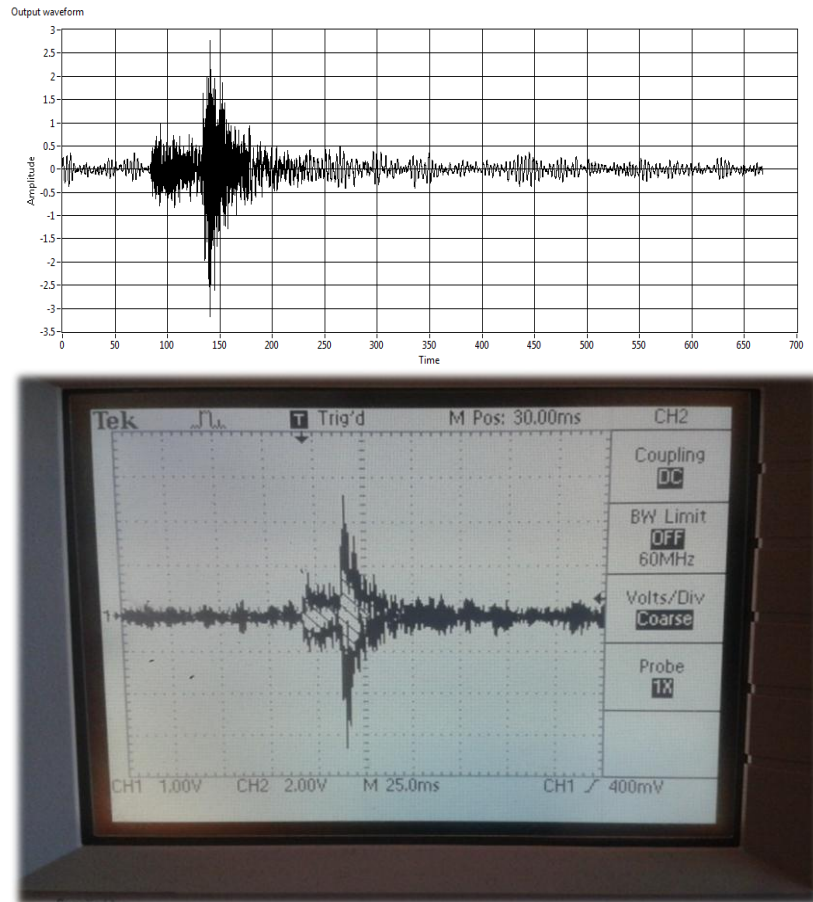


Figure 10.17: SAC file reading and analogue output

11. Future work: Potential improvements and modifications

The project accomplishes most of the objectives that were set. However, when designing and implementing the work, alternative development procedures and improvement ideas came up. Unfortunately, as always, time and resources were limited and they had to be abandoned or at least postponed in order to deal with the main objectives. Some of them are going to be proposed in this section:

- In order to monitor ambient noise in some structures as bridges a μg resolution is required (Wenzel & Pichler, 2005). The addition of a second accelerometer that measures acceleration in another axis may be a useful approach to improve the hardware module so that can be used for that purpose.
- An aisled vibration DAQ module has been developed. In order to study the large structures vibration behaviour a good amount of them, distributed in strategic locations, are needed (Wenzel & Pichler, 2005). The development of a decentralised

networking system that uses, for example, microcontrollers would be suitable to perform this task.

- The *seismic analysis* VI analyses one seismogram at a time and the location parameter that returns is the distance to the epicentre. It is possible to plot the location when the distance from at least three different seismic stations is known. A logical work continuation is the development of software that processes that distance values and uses a graphic interface to plot the location on a world map.
- The use of tables instead of formulas to calculate the distance to the epicentre would improve that parameter precision.
- The calculation of the magnitude using more scales would save the user time as there would be no need to use conversion graphs (Havskov & Ottemöller, 2010).
- Better algorithms for arrival time detection using wavelet transform or frequency analysis among others could be integrated in the software (Han, 2010).
- Coda length algorithm improvement to avoid the errors detected in its evaluation
- STA/LTA average performance optimization. Another approach for its development or an improvement of the existing one (the *collector* VI appears to be the cause of a lot of this issue) is required.
- In order to gather samples to shape a waveform only the *collector* VI has found among the LabVIEW library. That VI is not only slow but also has the collected samples limited. The development of a fast sample collecting VI without pre-established sample number limitation would boost the improvement of the STA/LTA average calculation performance.
- Because of the time limitations, the main menu (event structure) that should have joint the access to the three main software functions (DAQ, seismic analysis and output) in a common interface could not be completed. Also, some bugs in the seismic interface as occasional crashes without apparent reason were noticed. It is expected that this issues are solved by the time of the demonstration.

12. Conclusion

Monitoring and analysis of seismic signals have become a fundamental discipline when trying to minimize the human and economic loss that earthquakes cause every year. To deal with this menace, geologists need to be supplied with analytical tools that help with the arduous work of determining the seismic event characteristics in order to take preventing actions, establish patterns or study the earth structure. Preventing work has to be made in building structures as well, cheap maintenance and failure detecting systems are highly on demand and it is there where MEMS accelerometers play a fundamental role.

The seismic analysis software developed manages to successfully retrieve timing, location and magnitude parameters with an acceptable precision according to the scope of the project. The precision achieved is probably not suitable for the accurate calculations of professional seismic stations. However, taking into account the resources and time available and that the geo-instrumentation and LabVIEW knowledge was acquired as part of the project, it represents a good approach and prototype from which build up a more complex software using this popular graphic programming language. It is important to highlight that the software has performance issues when computing SNR analysis and automatic timing parameters detection and that improve this in the future is essential. The coda length software needs also polishing or algorithm reconsideration to avoid some calculations errors. The event date that can be retrieved from the SAC_SM plugging does not match with the source date too often; this might point out a problem with either the plug-in or the seismic data source.

The vibration DAQ effectively performs acceleration versus time and spectra measuring and monitoring. It manages to translate the incoming acceleration into earthquake intensity rank in accordance with the Modified Mercalli scale. Saving and zooming options are properly working and the enclosure and double sided tape using for attachment fits very well the specifications marked at the beginning of the development. Nevertheless, the user should be careful with the sample rate and buffer selection as a wrong selection may cause conflicts with the hardware. The system is a good starting point to develop a networked system for structural monitoring.

The software manages to output vibration and seismic signals based on real data without problems. This analogue output may be used to be read in an oscilloscope or to excite a shaking table in order to simulate history-based earthquakes.

Although an initial objective, the usefulness and practical applications of an analogue input that acquires the analogue output commented above has been questioned. Especially when digital data can be easily found in the internet and vibrations were already acquired with the vibration DAQ. It could be interesting to simulate the real acquisition process that occurs in professional seismic stations but, taking into account that the project is already branched in different areas and the lack of time available it was decided to focus in the ones that looked more valuable.

As a whole, the project reasonably accomplishes the objectives initially set, but it is evident that the fields studied have a lot of potential and room for improvement. Complex and valuable applications can be developed taking this work as a starting point.

Appendix A: Detailed Seismic analysis software

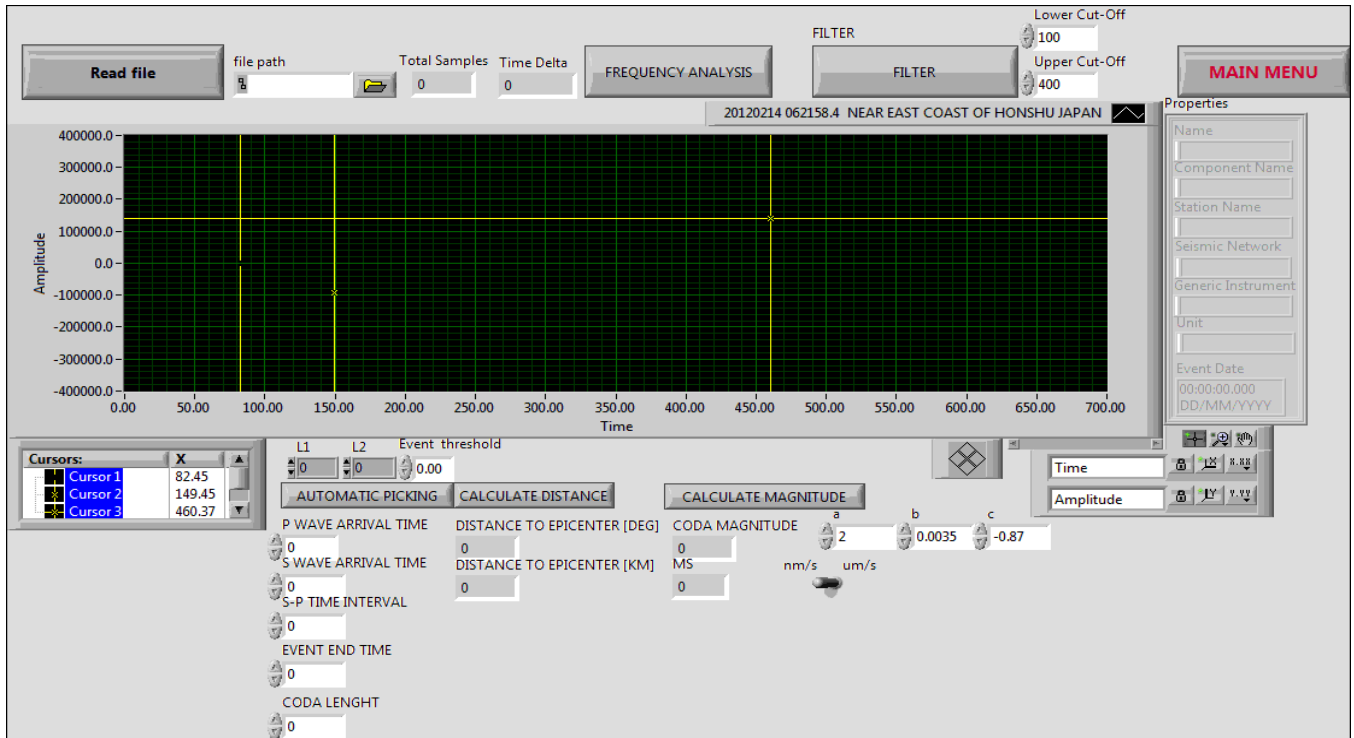


Figure A. 1: Seismic analysis VI front panel

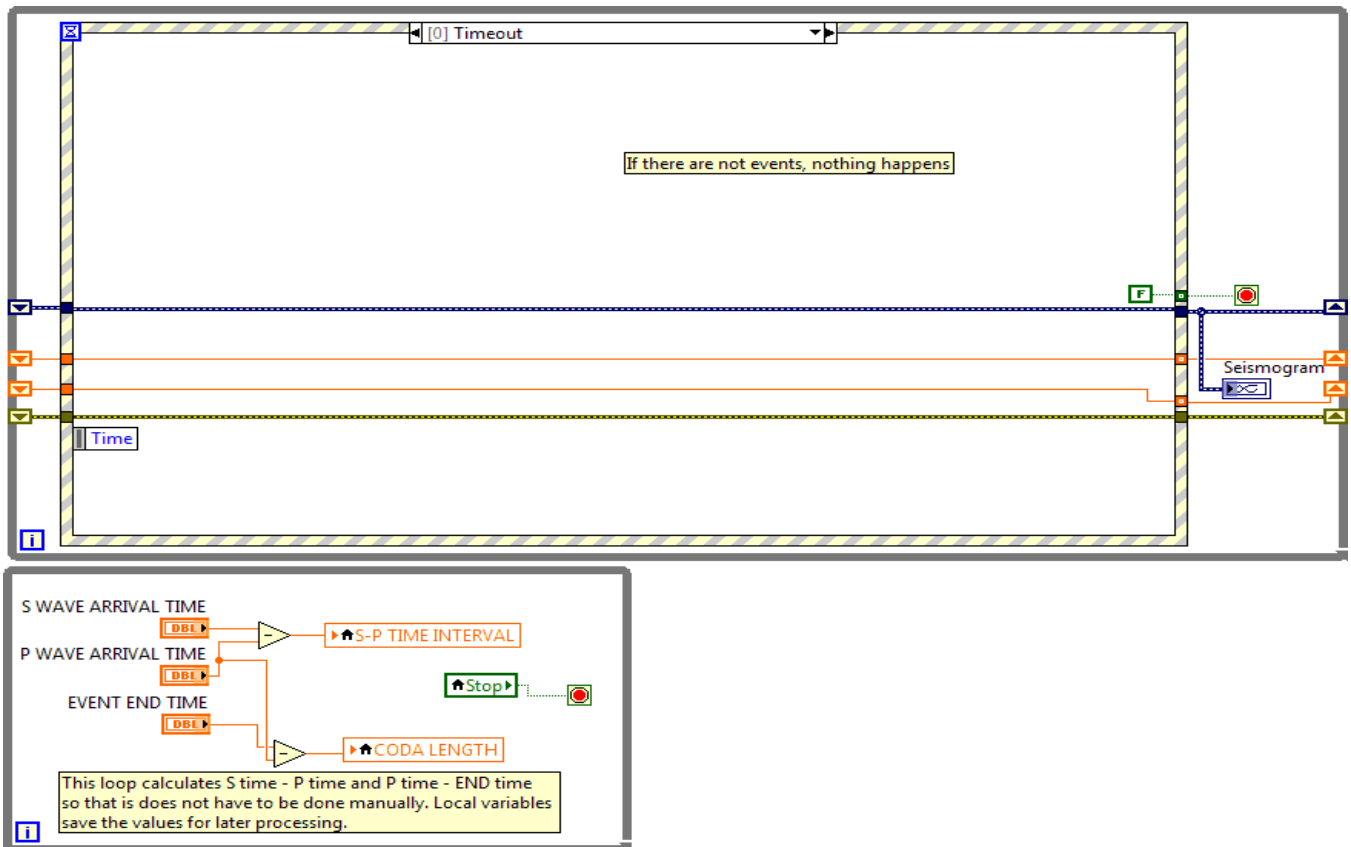


Figure A. 2: Seismic analysis VI global structure. Timeout event.

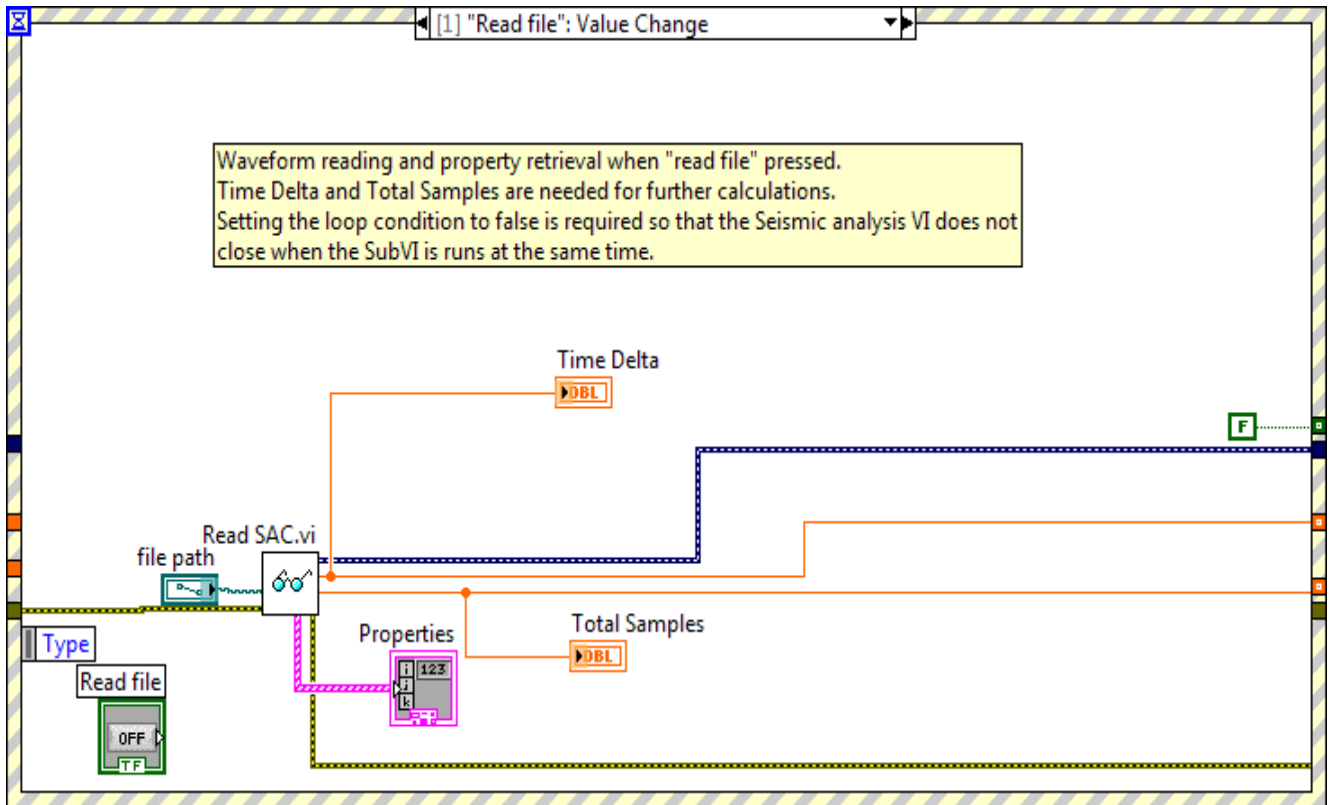


Figure A. 3: Seismic analysis VI. Read file event

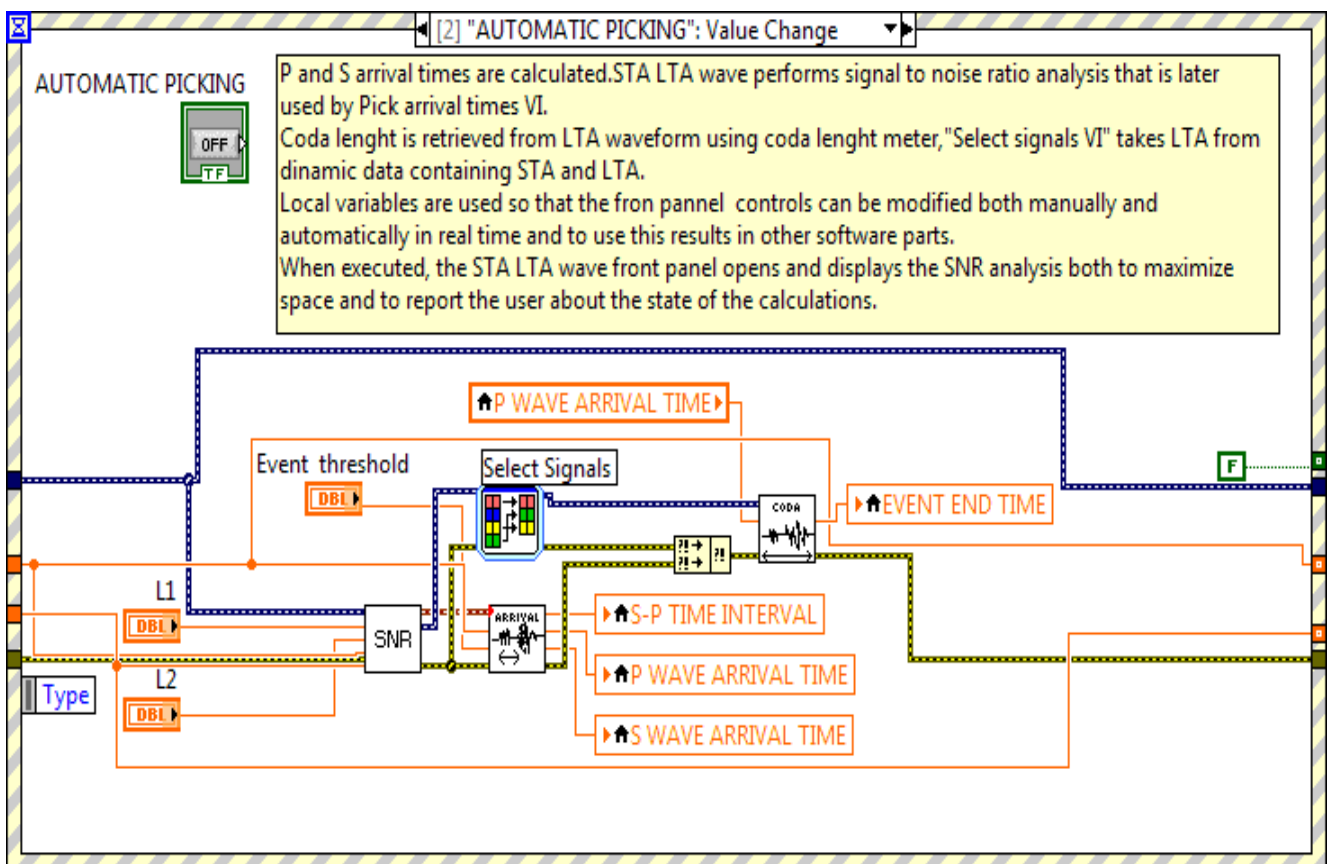


Figure A.4 Seismic analysis VI. Automatic picking event

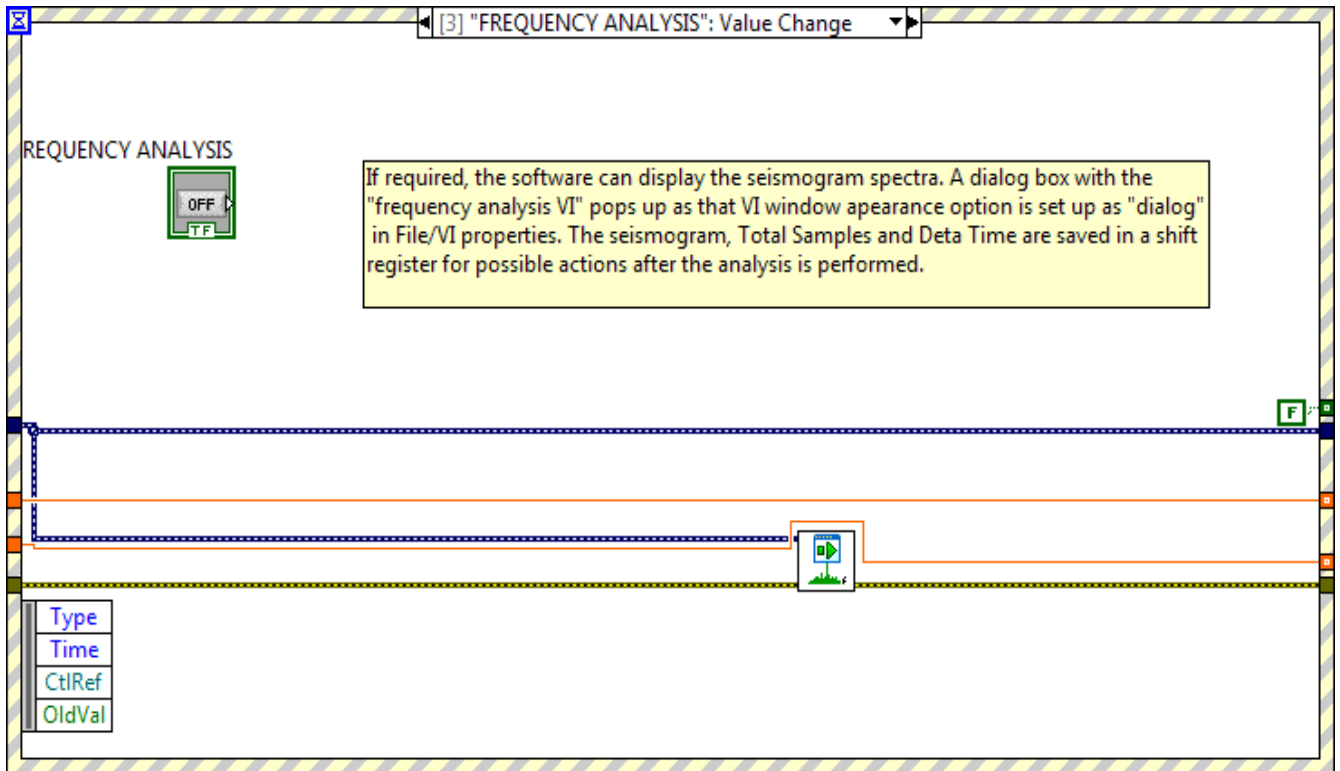


Figure A. 5: Seismic analysis VI .Frequency analysis event

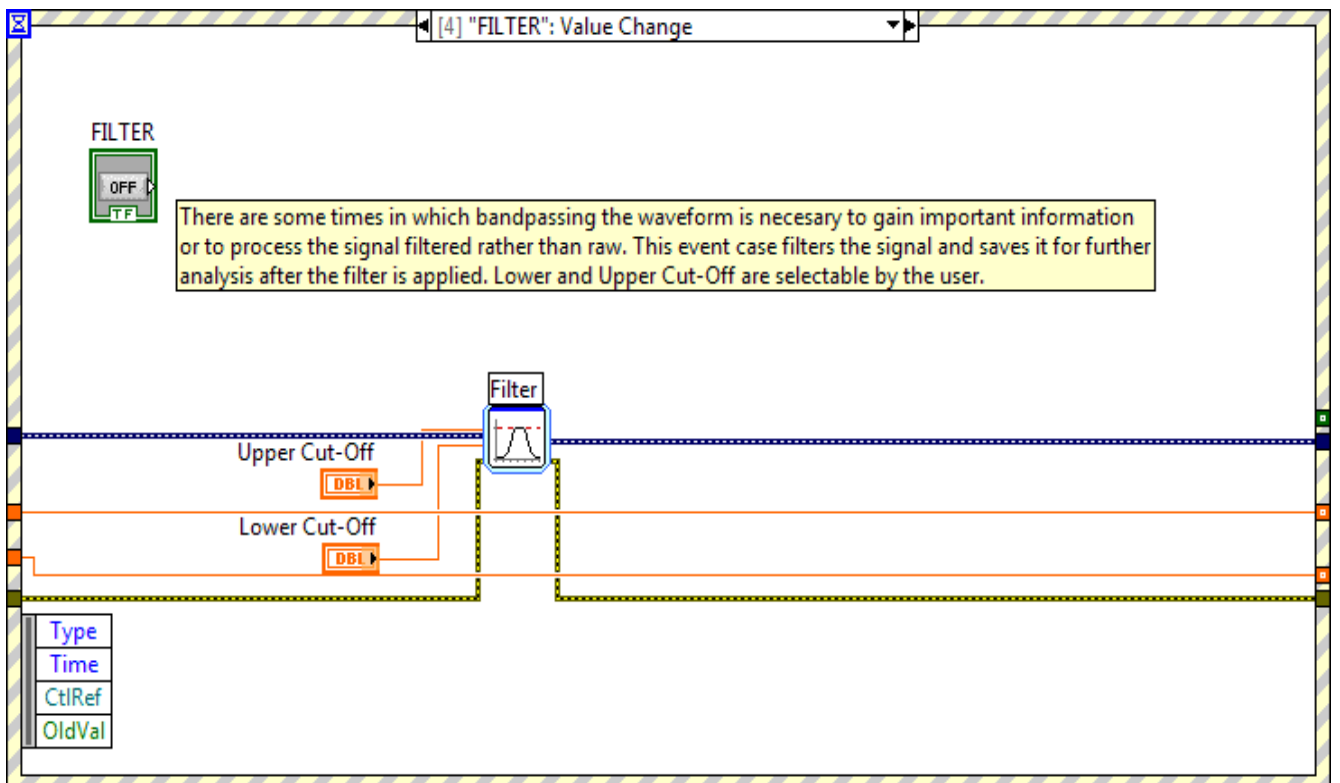


Figure A. 6:Seismic analysis VI.Filter event

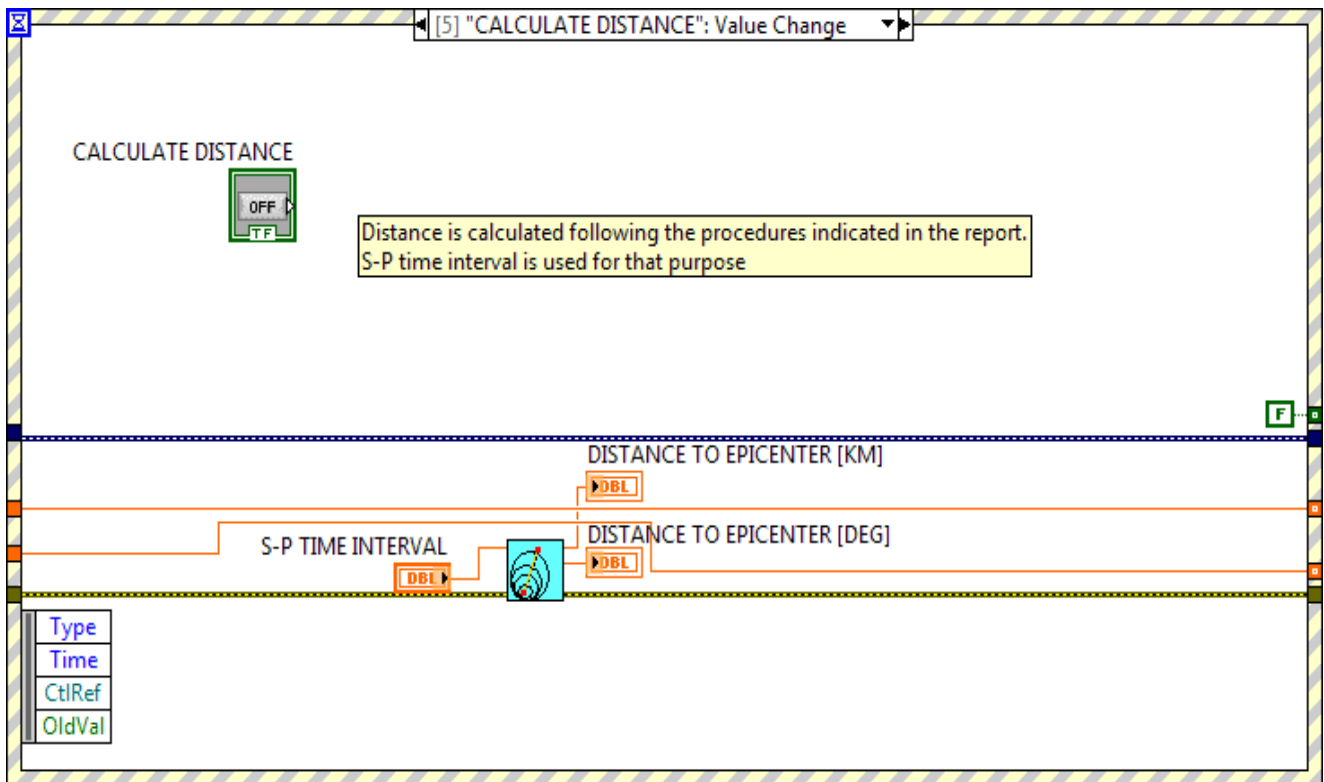


Figure A.7: Seismic analysis VI. Calculate distance event

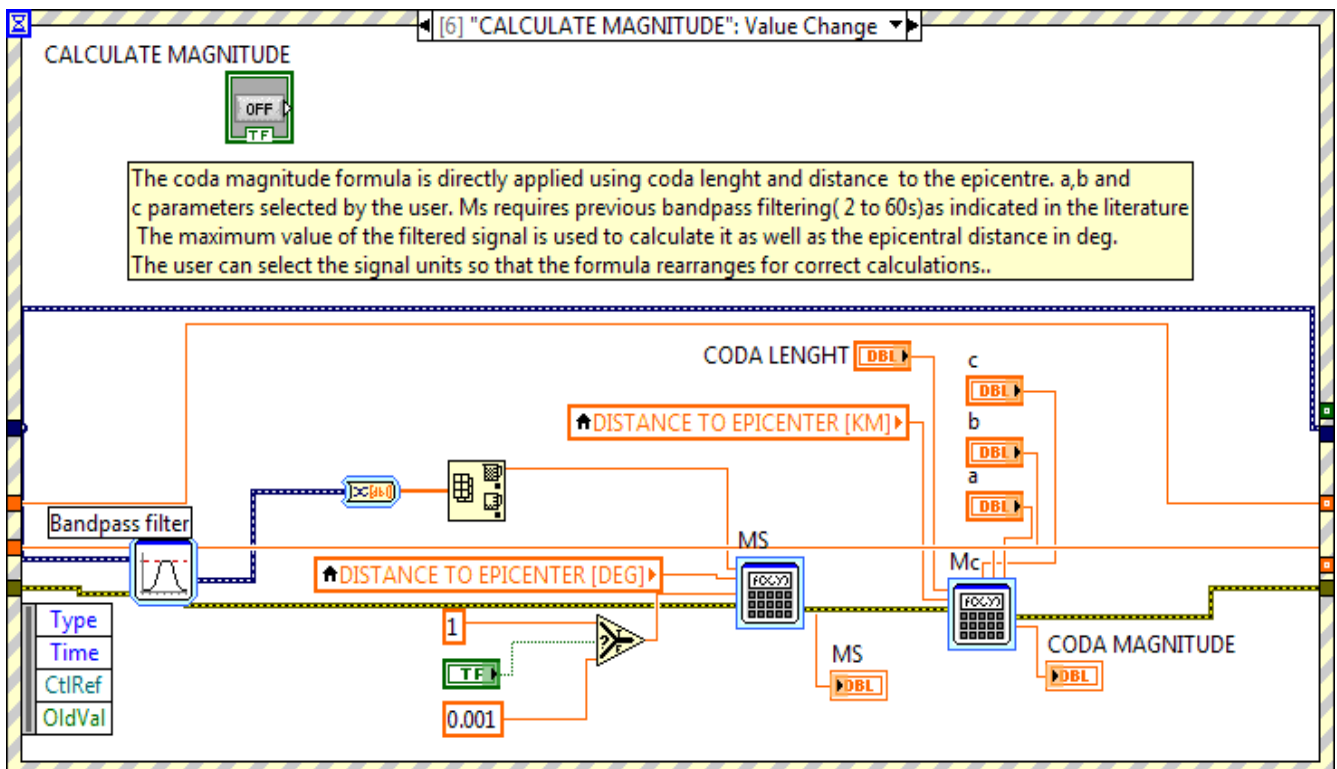


Figure A.8: Seismic analysis VI. Calculate magnitude event

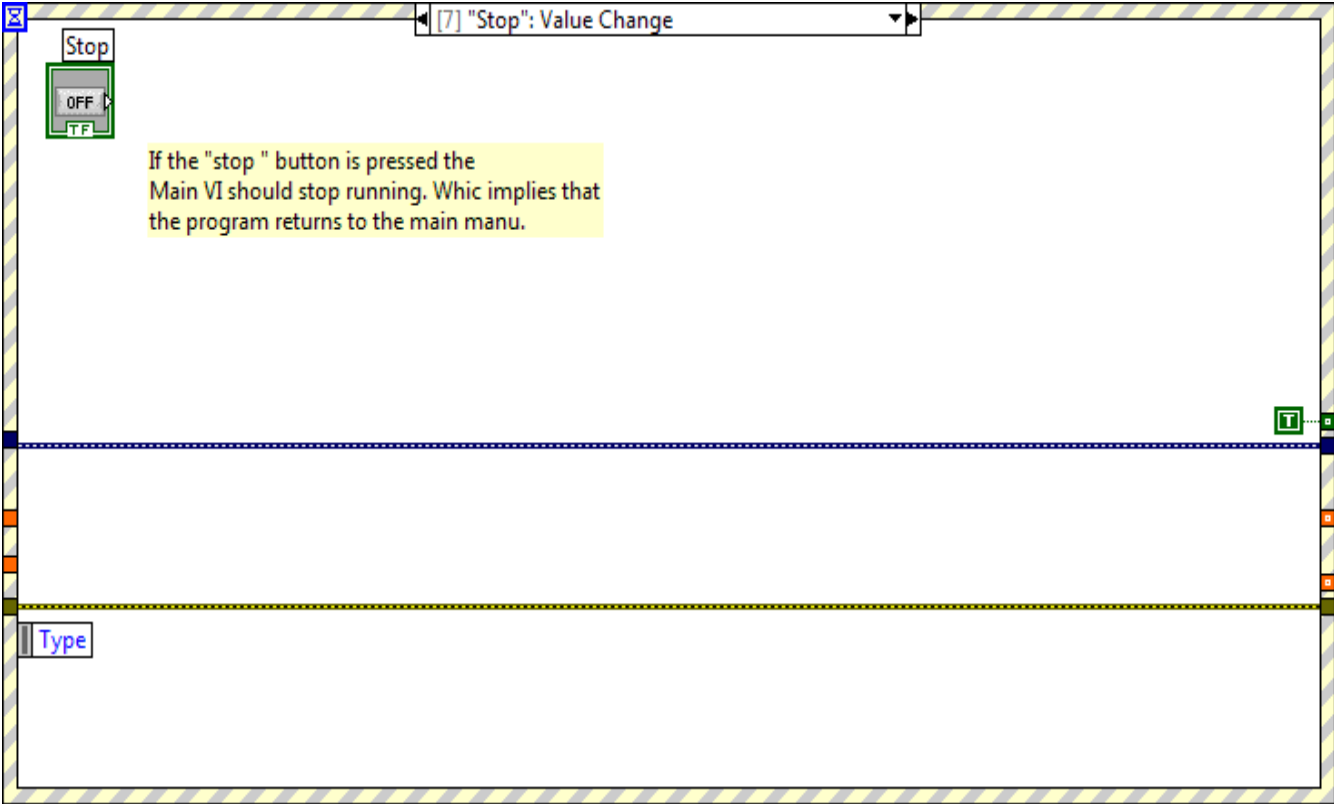


Figure A..9: Seismic analysis VI. Stop event.

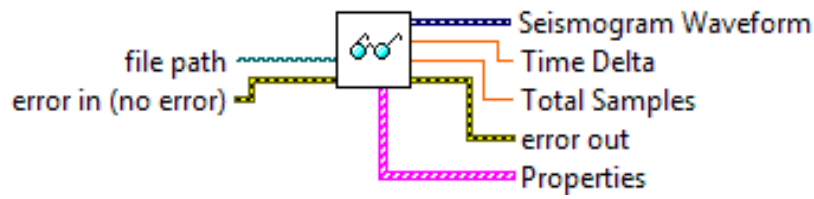


Figure A.10: Read SAC VI icon

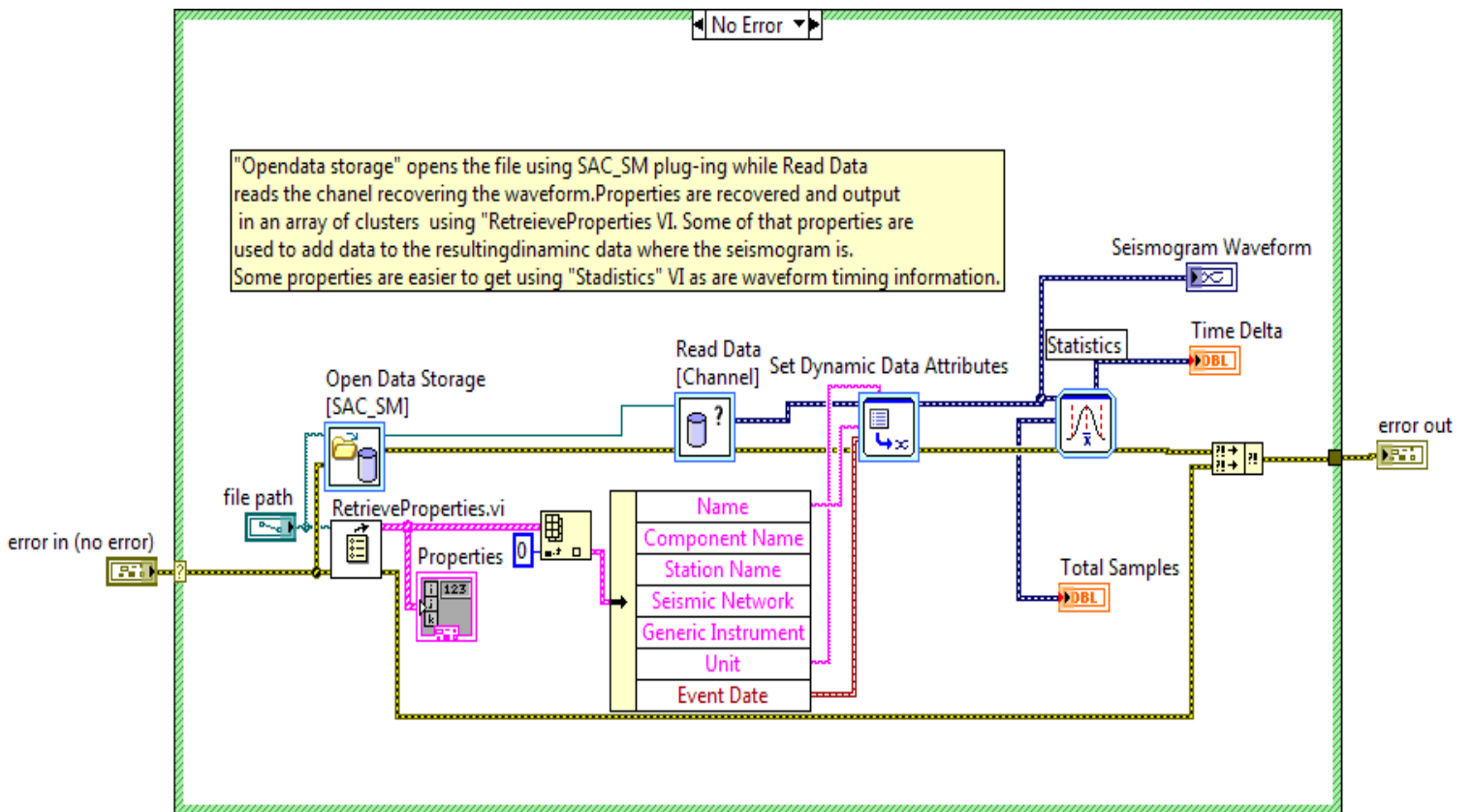


Figure A.11: ReadSAC VI block diagram

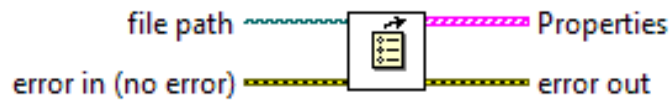
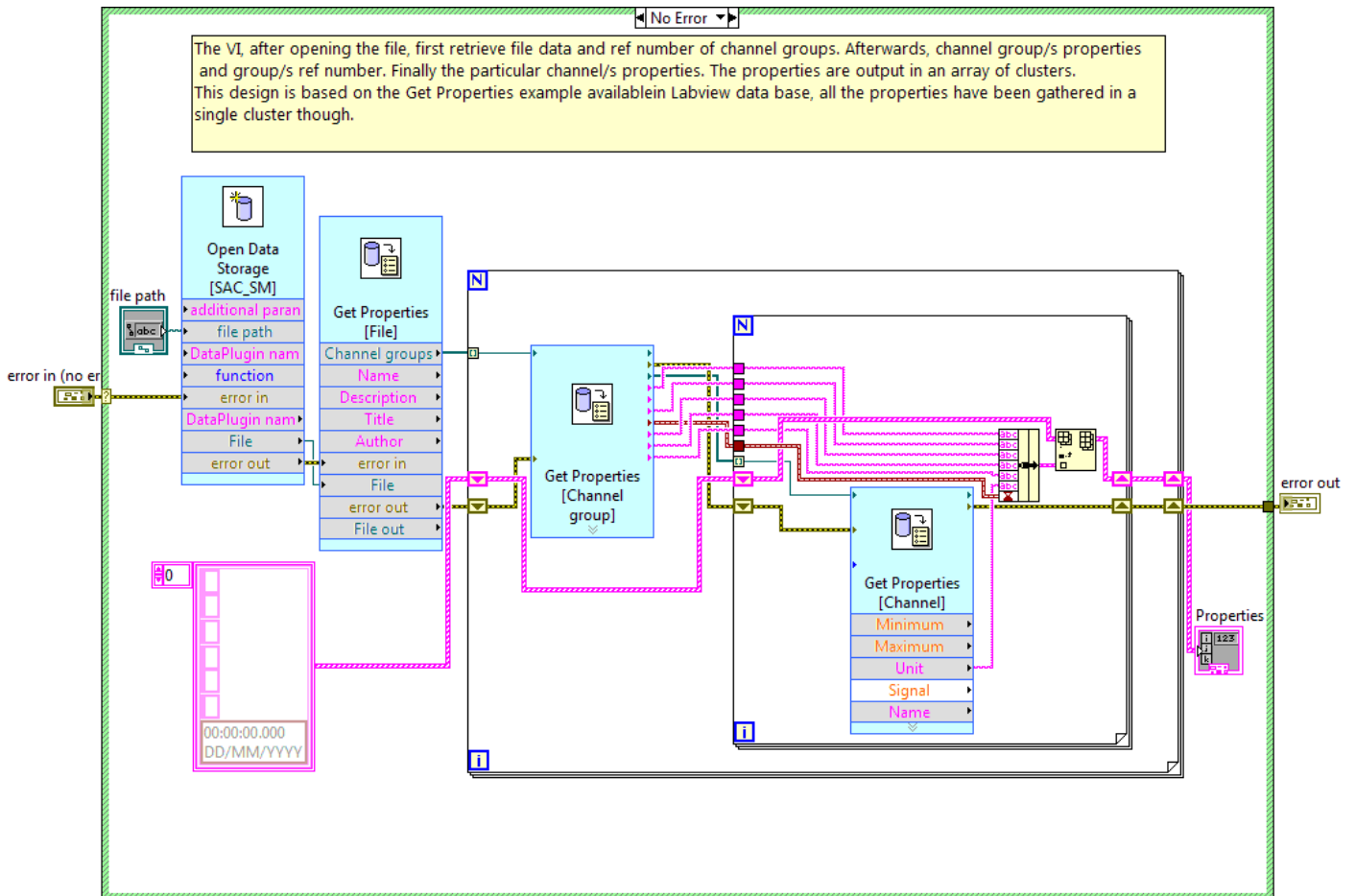


Figure A.12: Retrieve properties Icon



FigureA.11: Retrieve properties VI block diagram

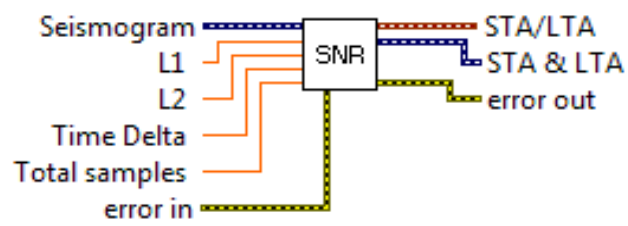


Figure A.3: STA LTA ratio icon

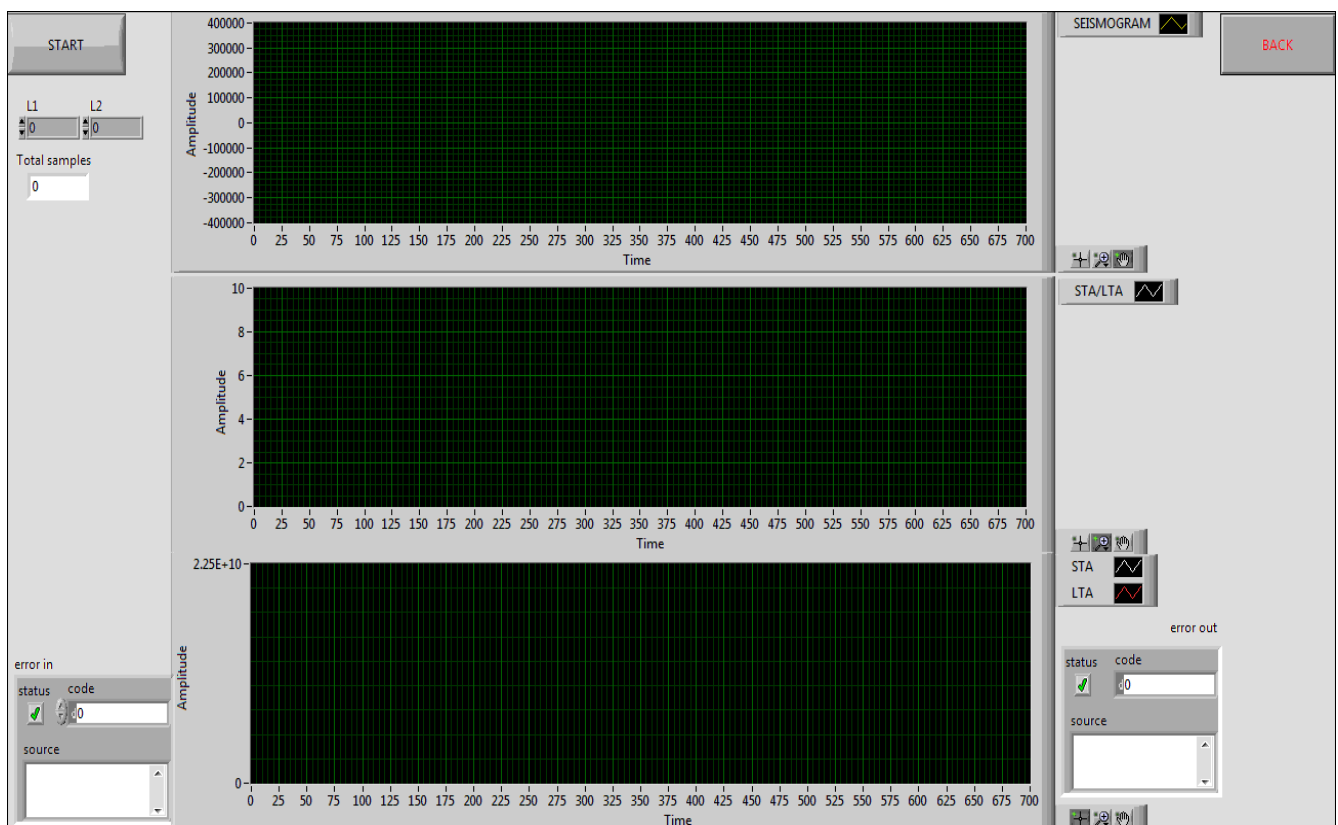


Figure A.12: STA LTA ratio front panel

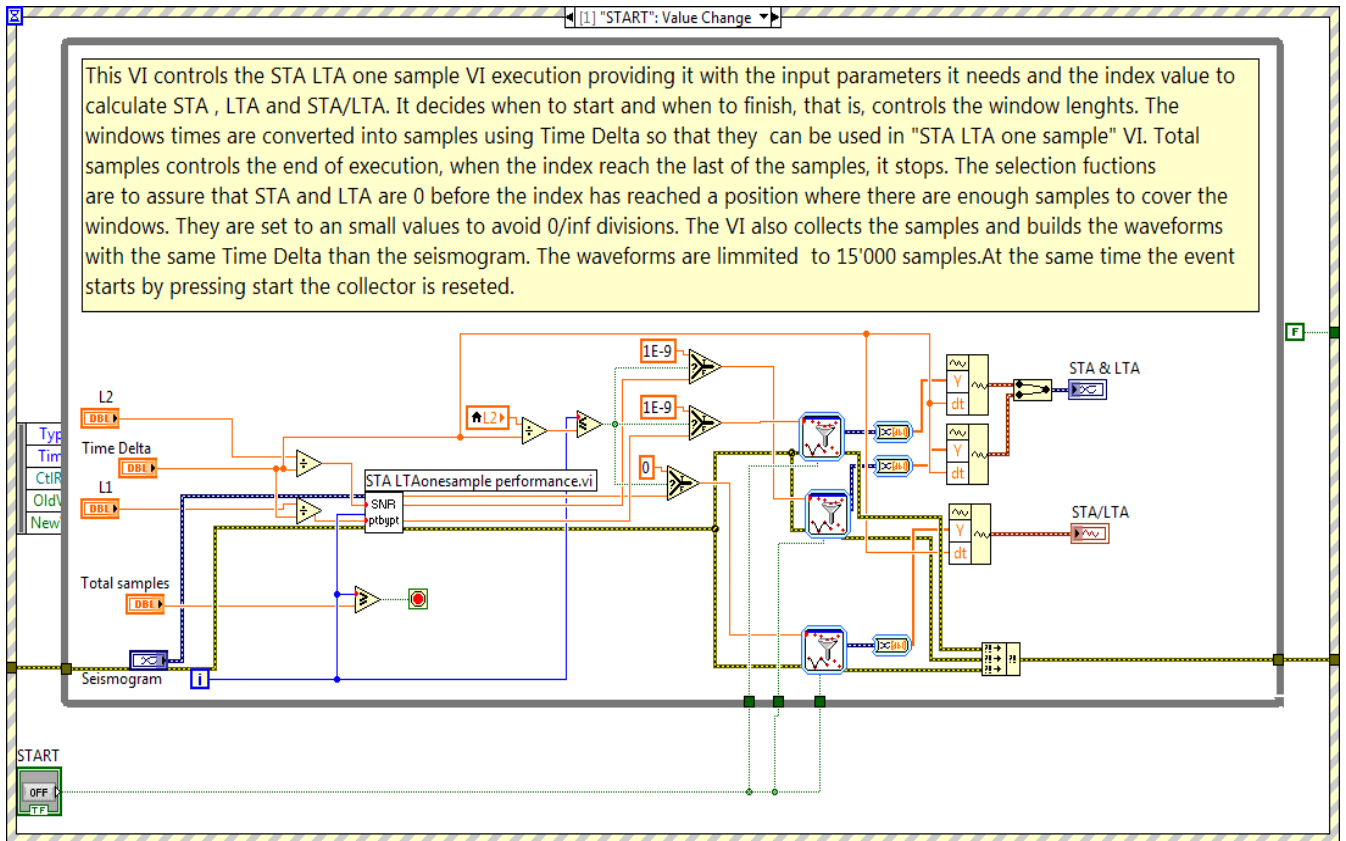
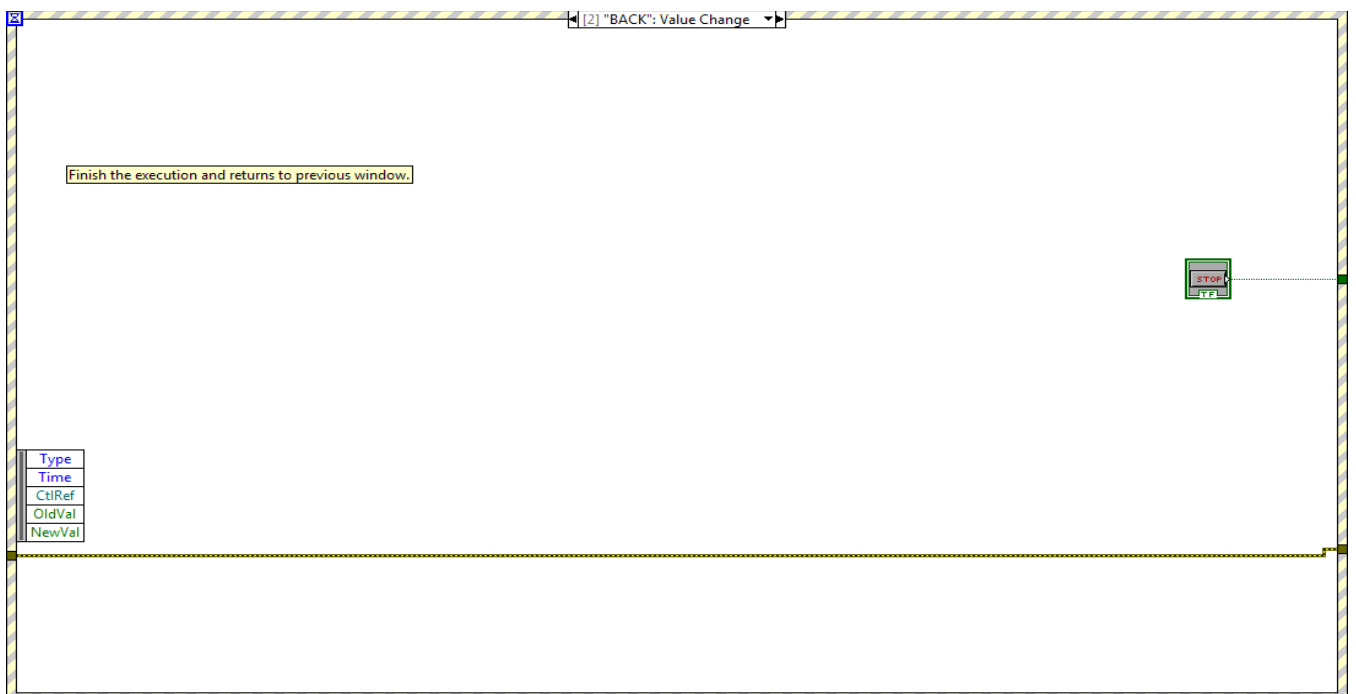
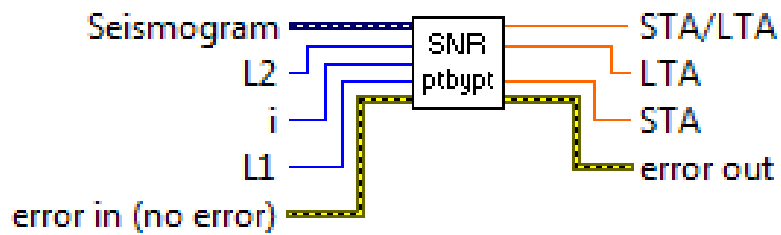


Figure A..13: STA LTA ratio VI Start event and global VI structure



FigureA.14:STA LTA ratio VI BACK event



FigureA.15: STA LTA one sample VI icon

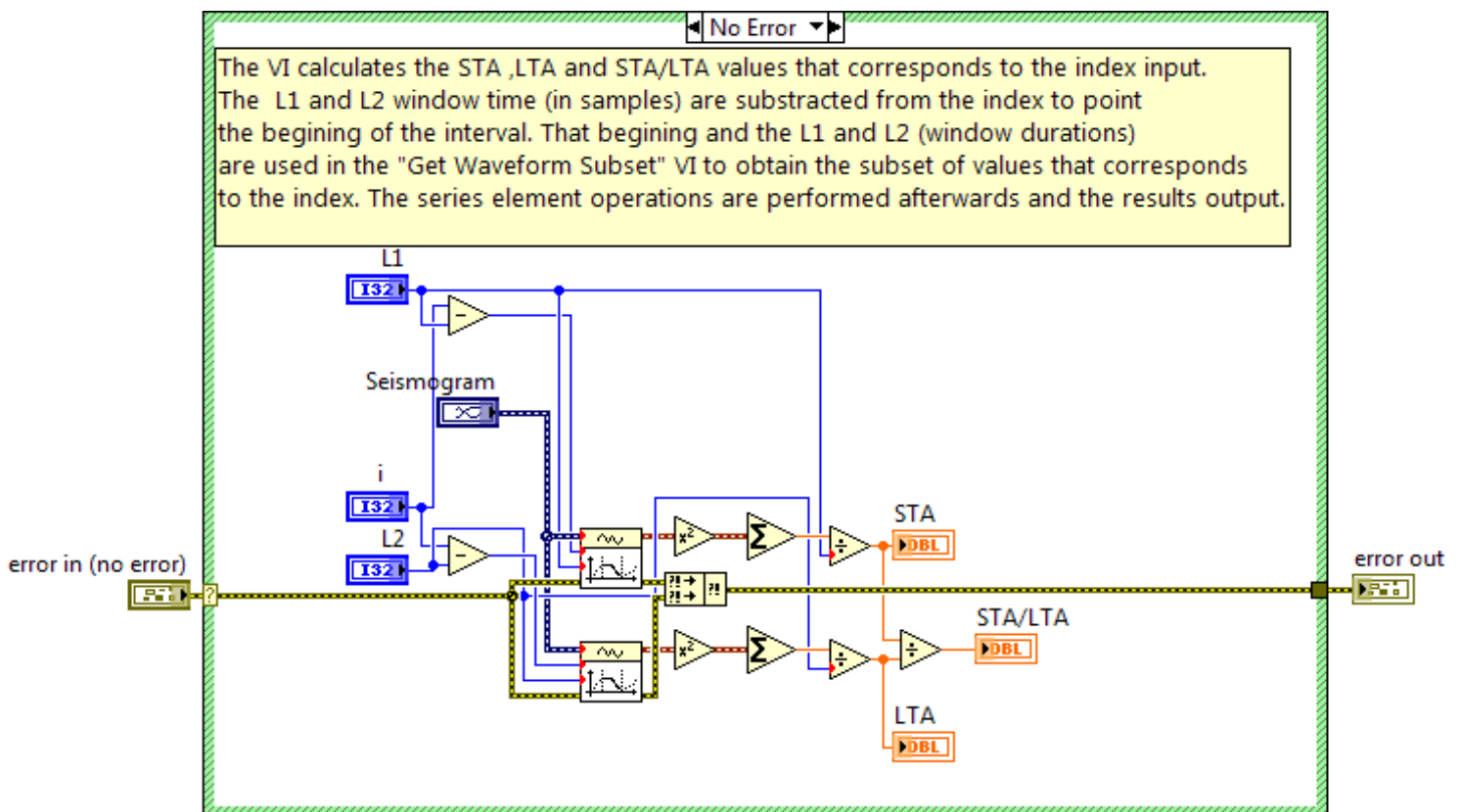


Figure A.16:STA LTA one sample block diagram

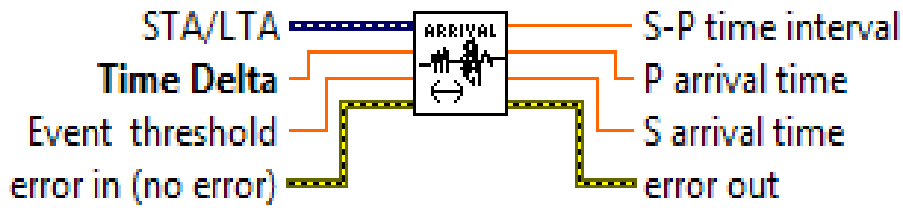


Figure A.17: Pick arrival times VI icon

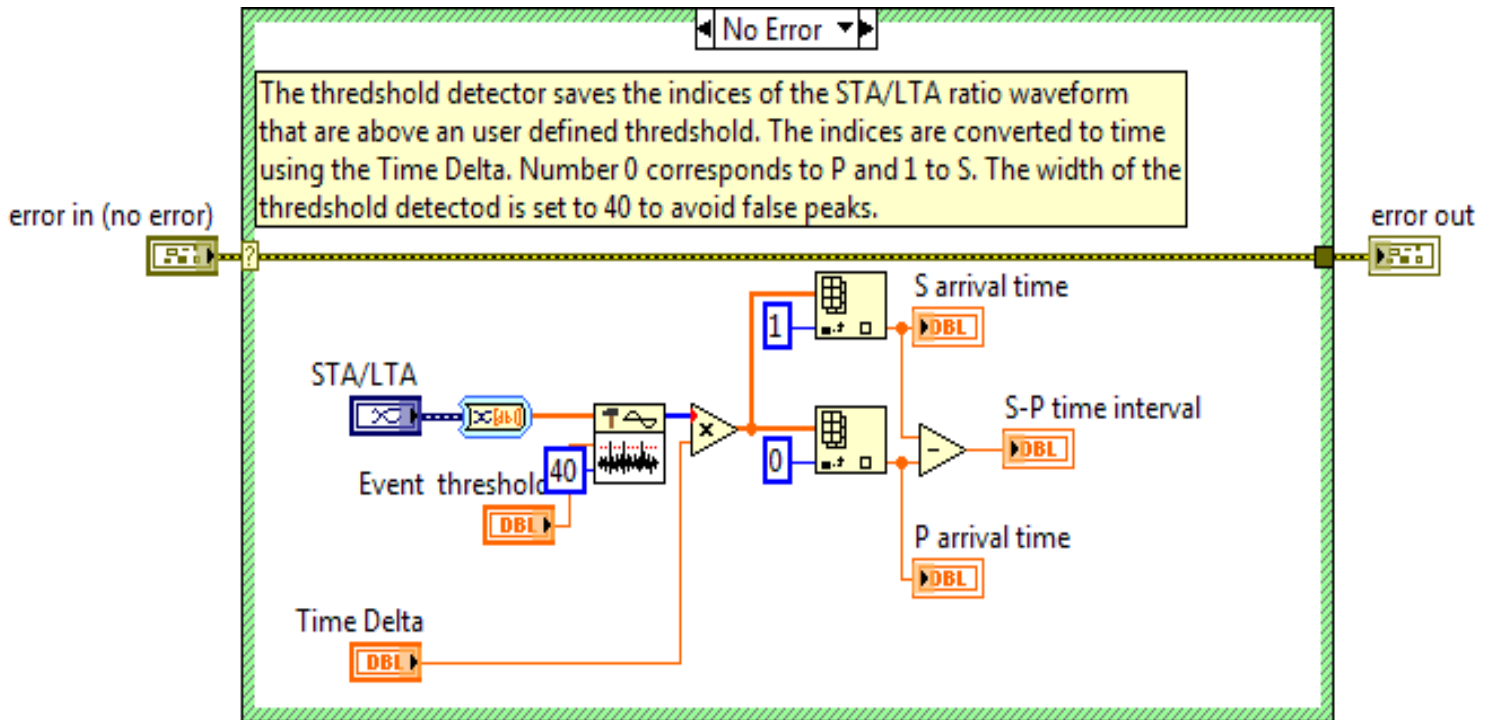
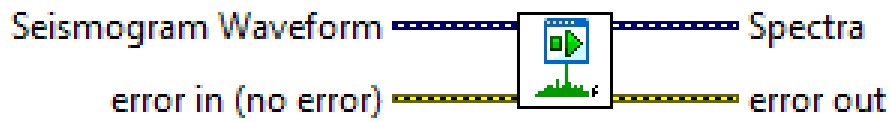
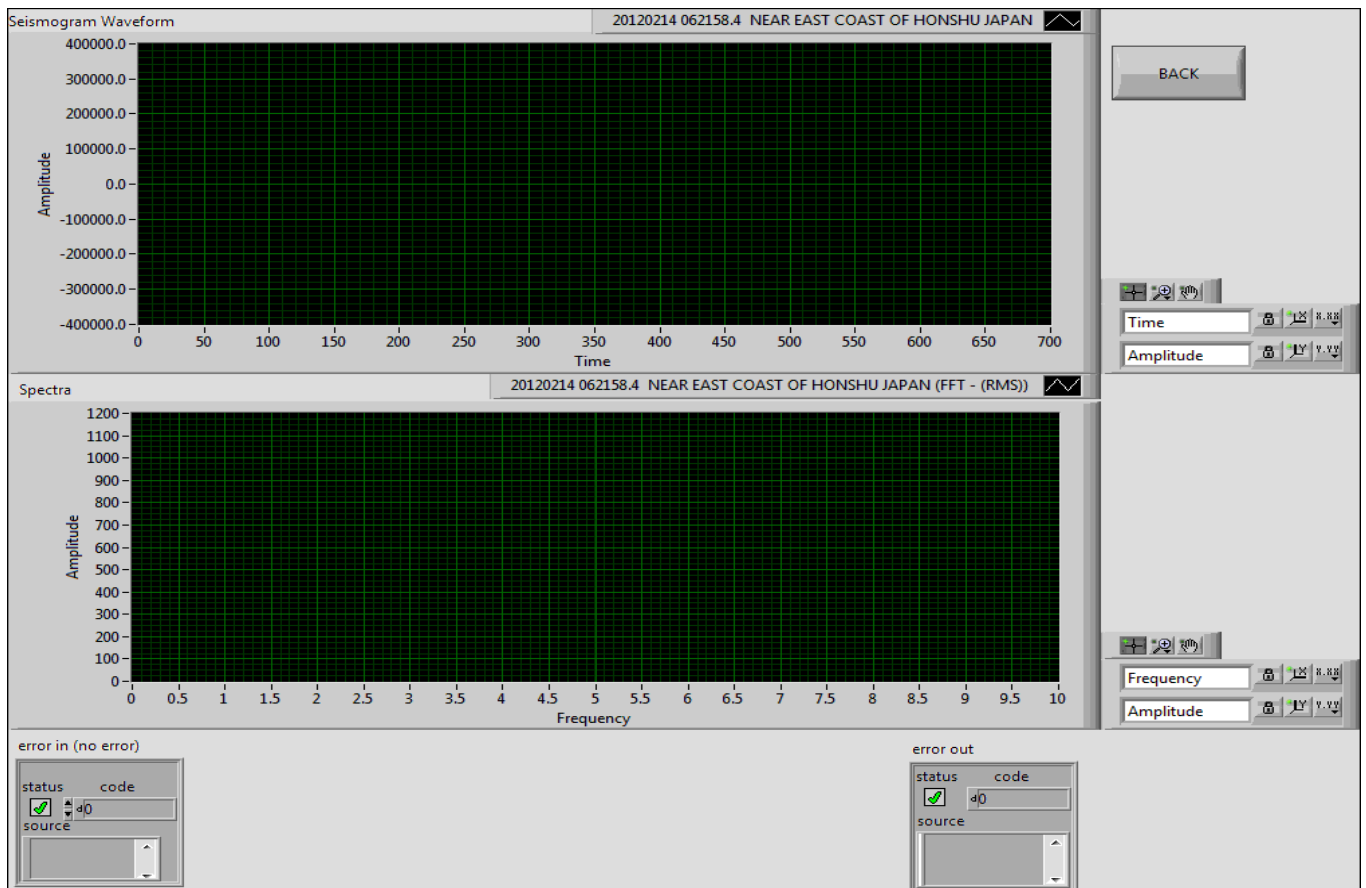


Figure A.18: Pick arrival times VI block diagram



FigureA.19: Frequency analysis VI icon



FigureA.20: Frequency analysis VI front panel

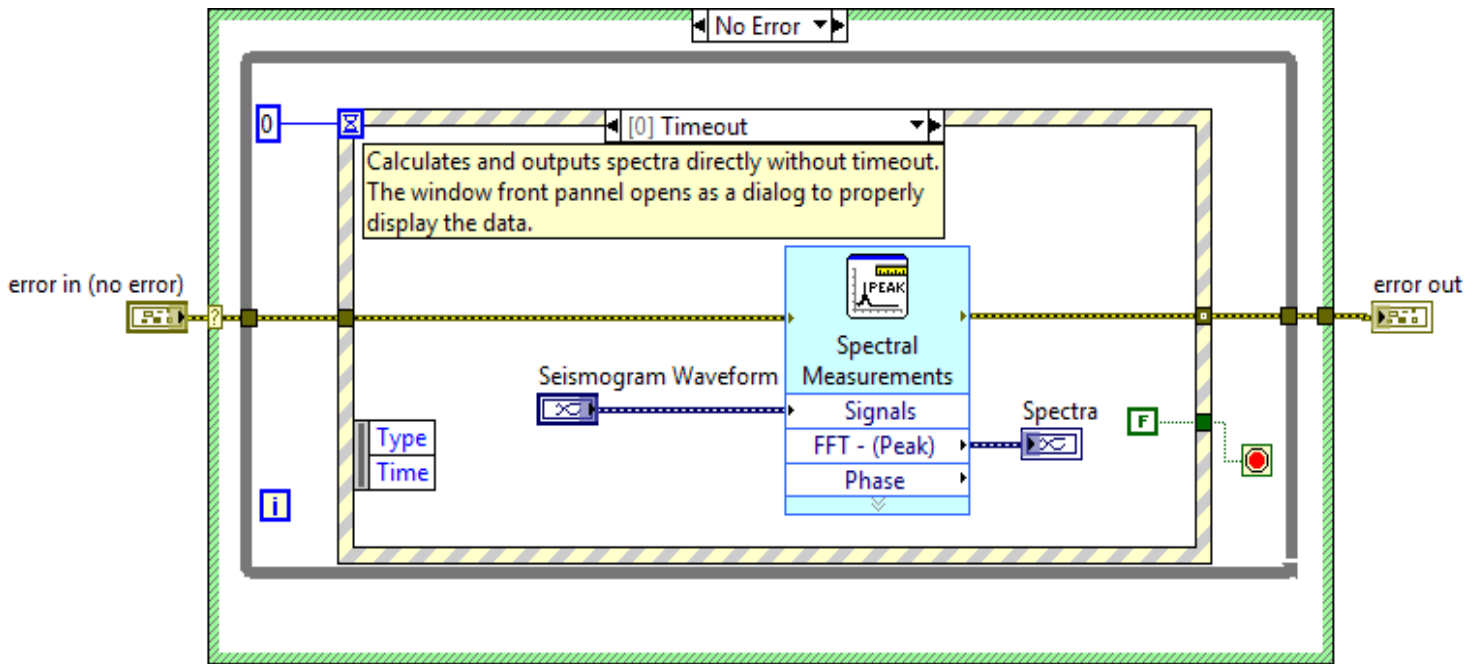


Figure A.21: Frequency analysis VI block diagram

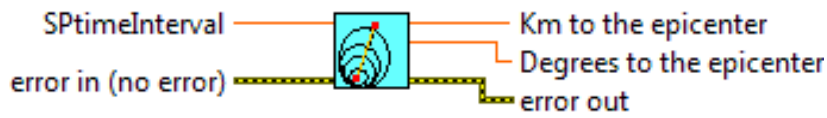


Figure A.22: Distance to the epicentre icon

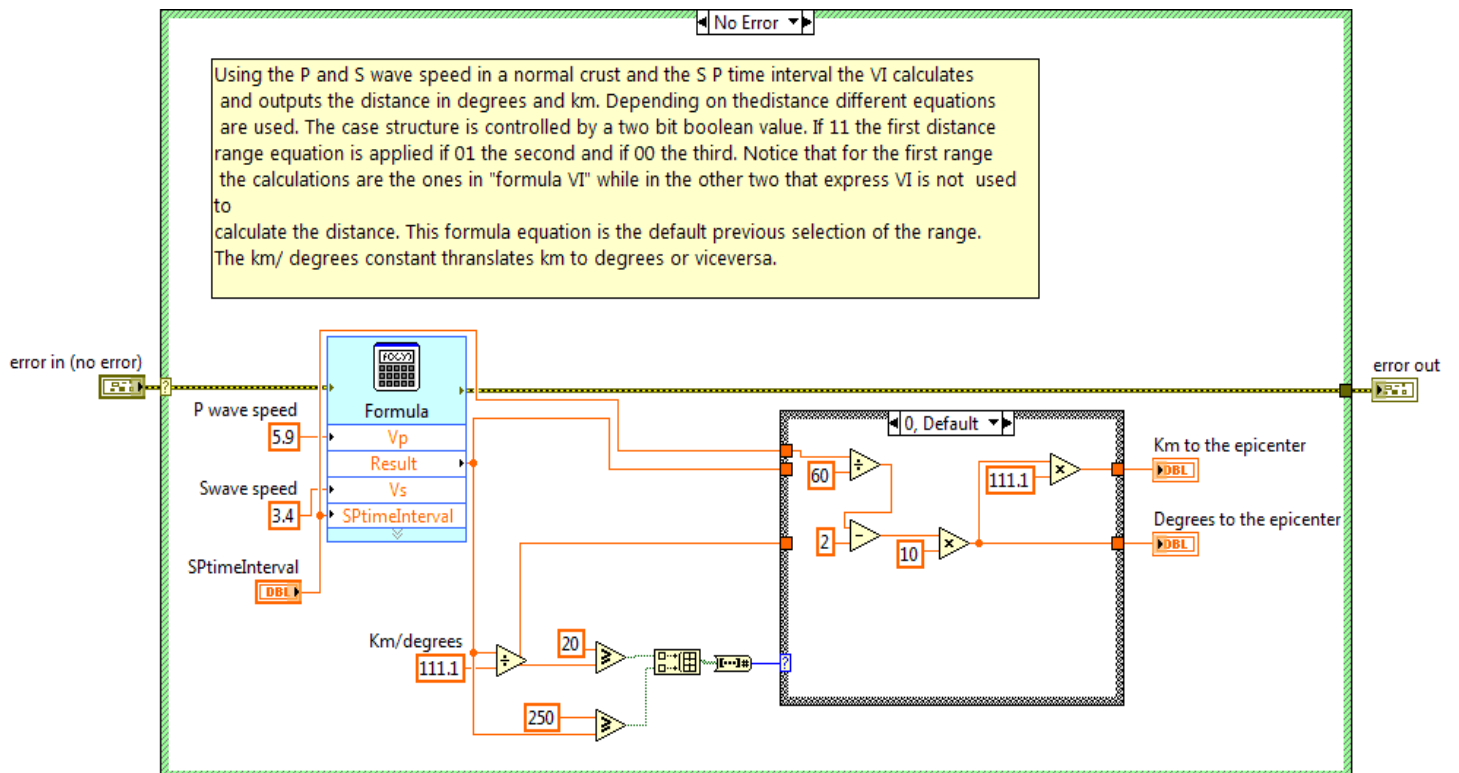


Figure A.23: Distance to the epicentre block diagram

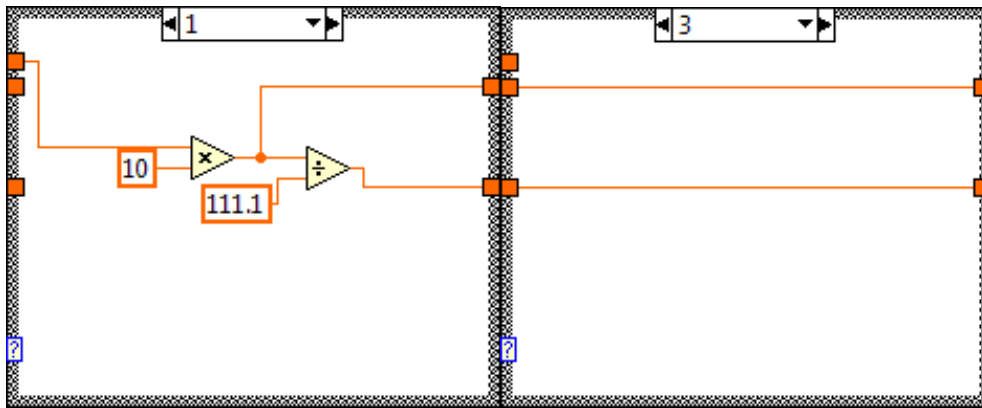


Figure A.24: Distance to the epicentre case structures

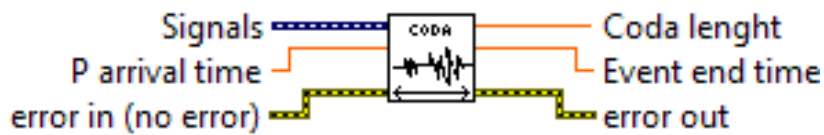


Figure A.25 Coda length meter

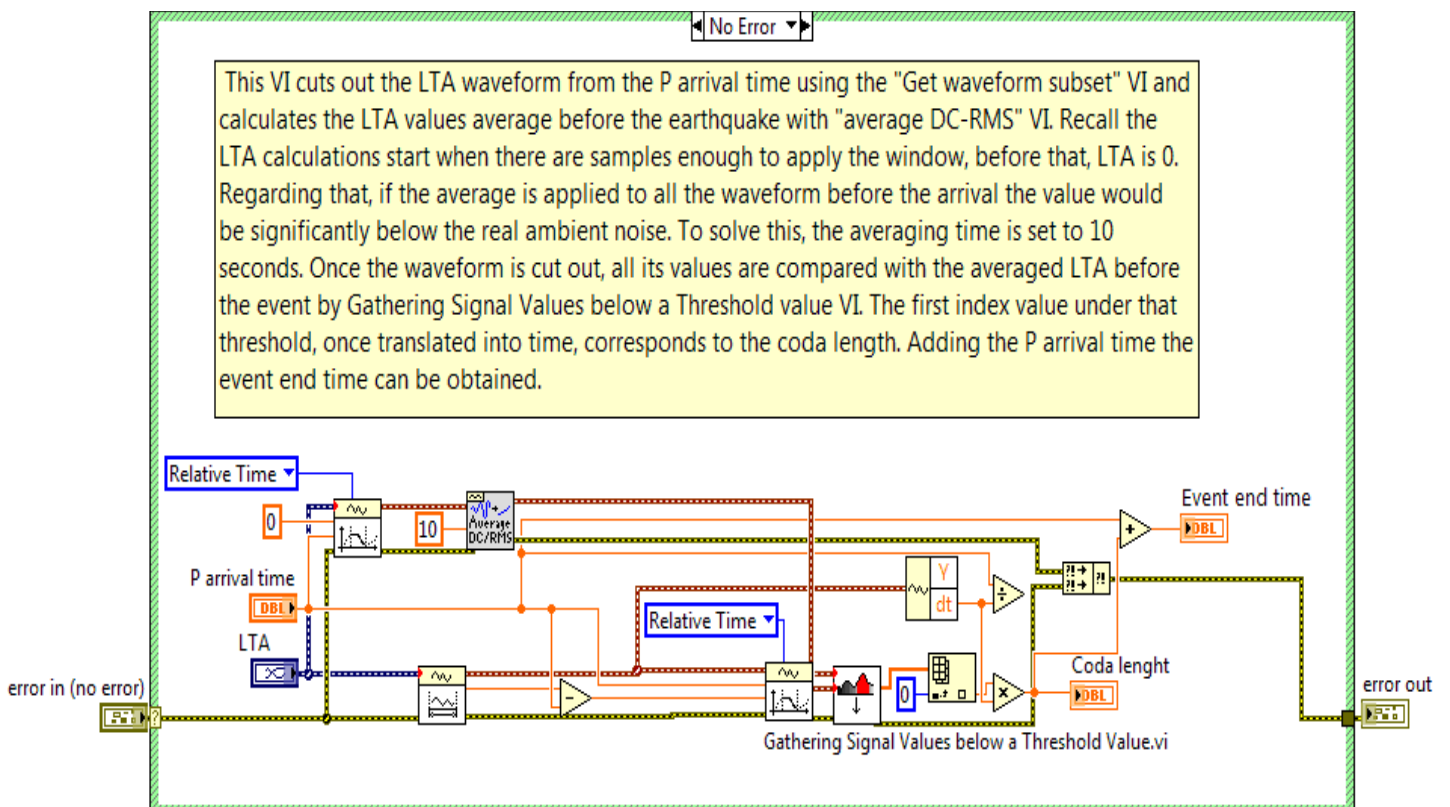


Figure A.26: Coda length meter VI block diagram

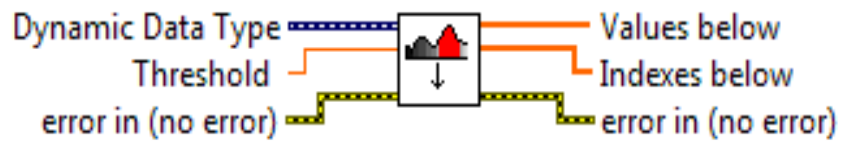


Figure A.27: Gather signals below a threshold VI icon

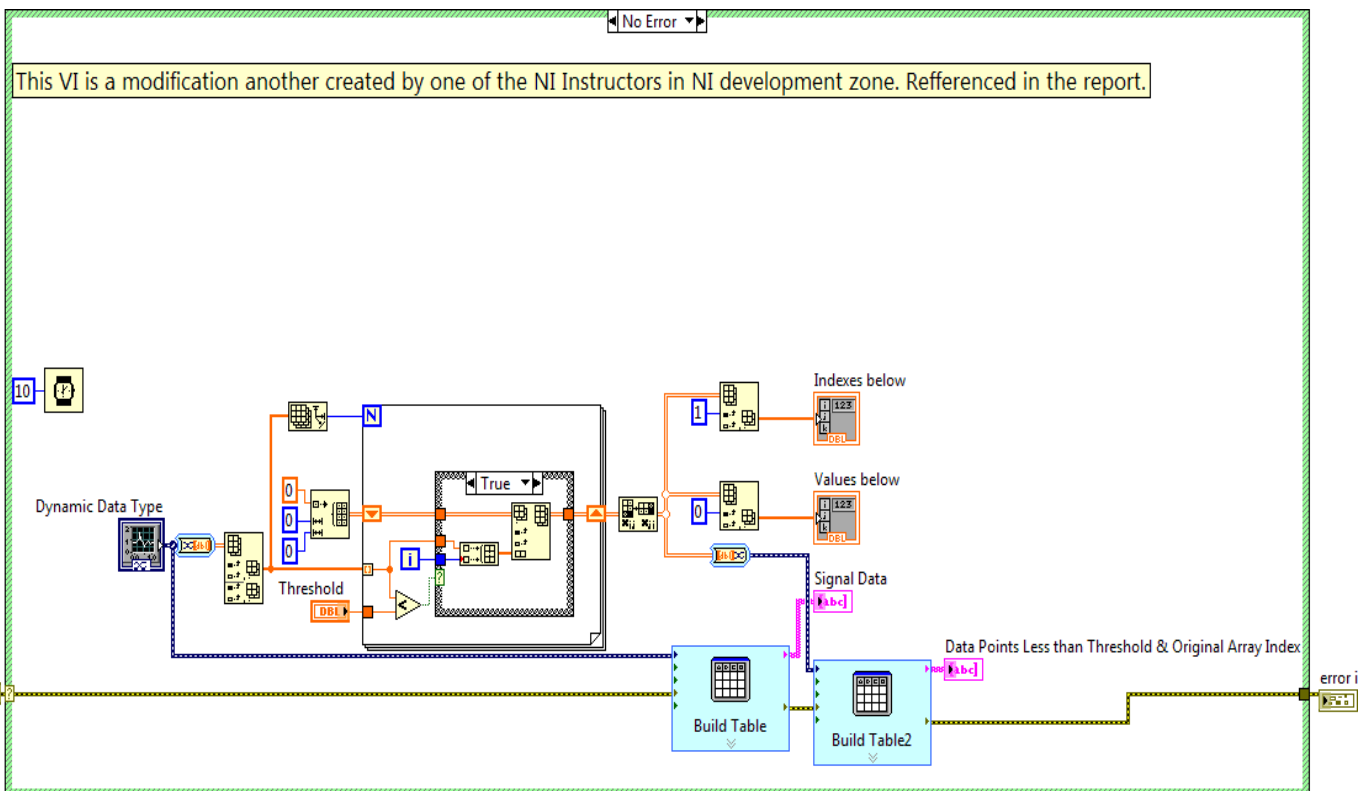


Figure A.28: Gather signals below a threshold block diagram (NI Instructors, 2011) .

Appendix B: Detailed Vibration DAQ software

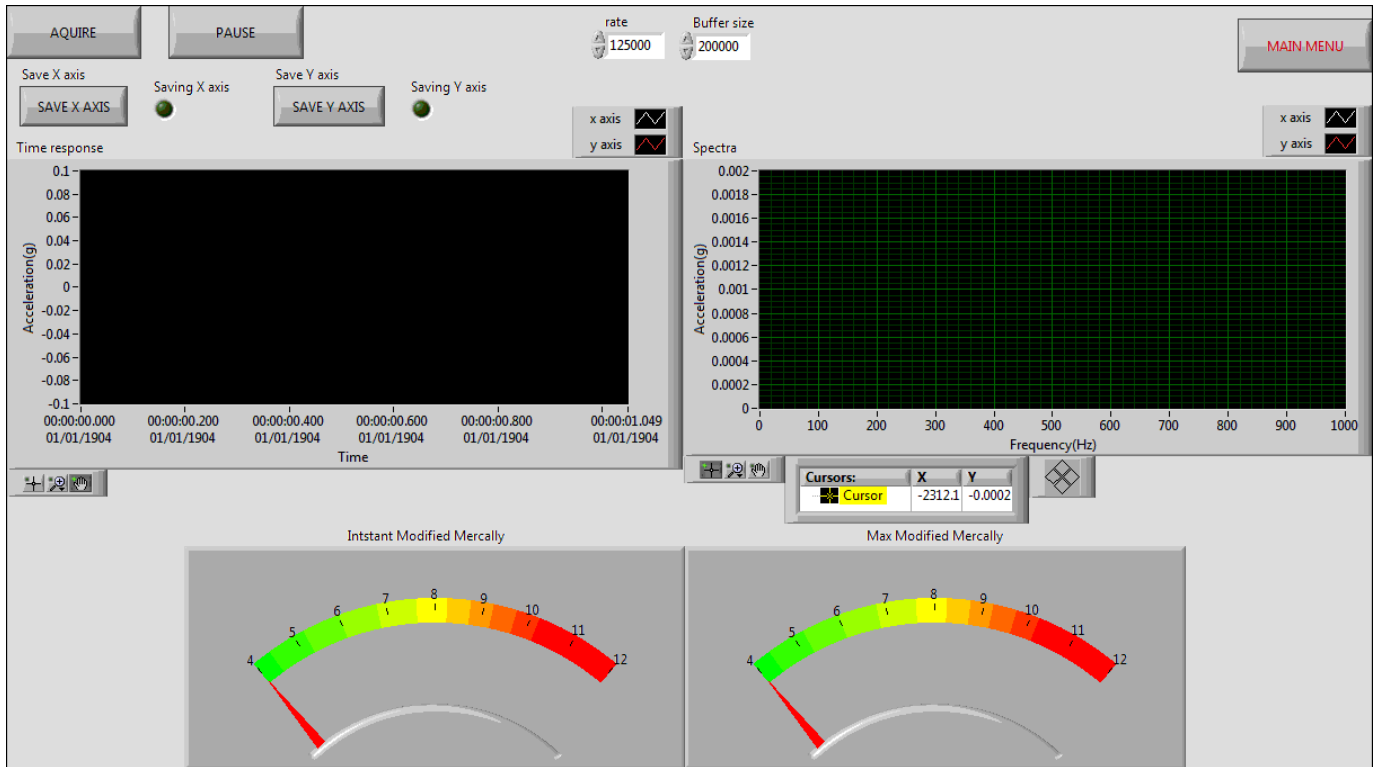


Figure B.1: Vibration DAQ VI front panel

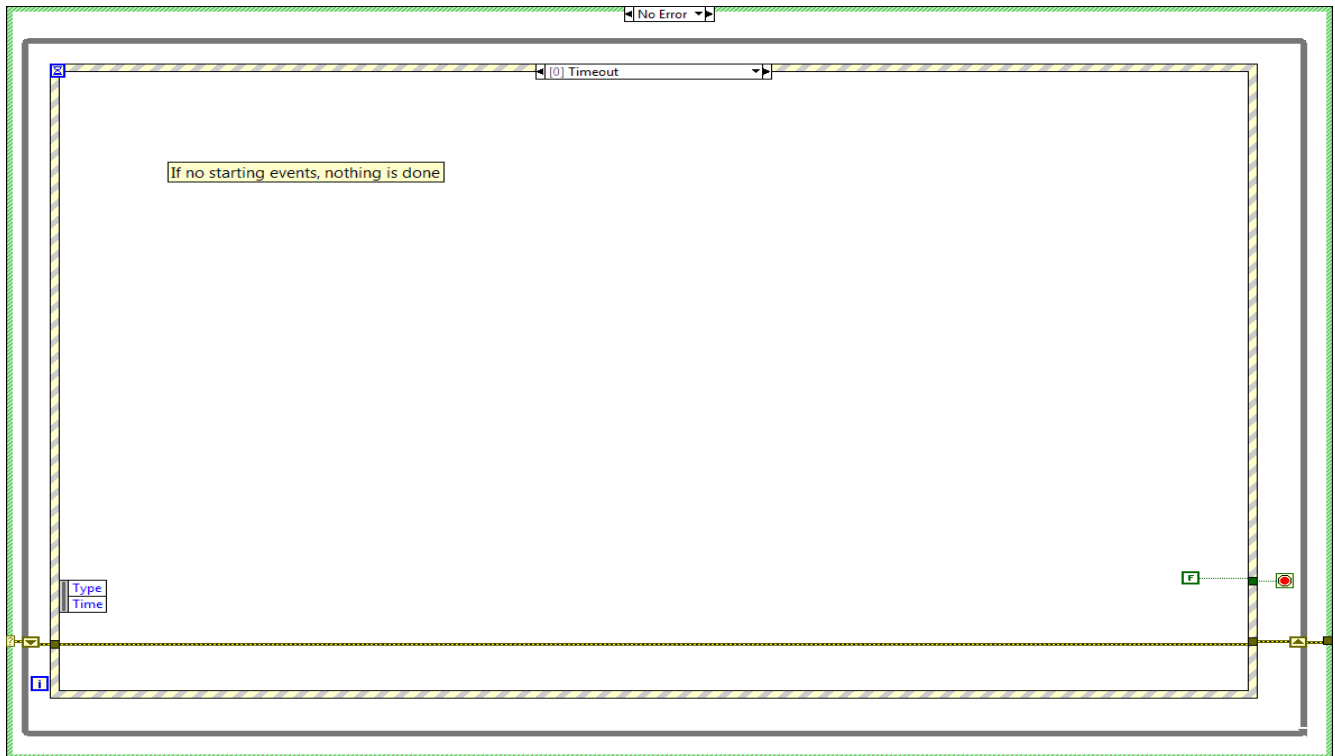


Figure B.2: Vibration DAQ event structure. Timeout.

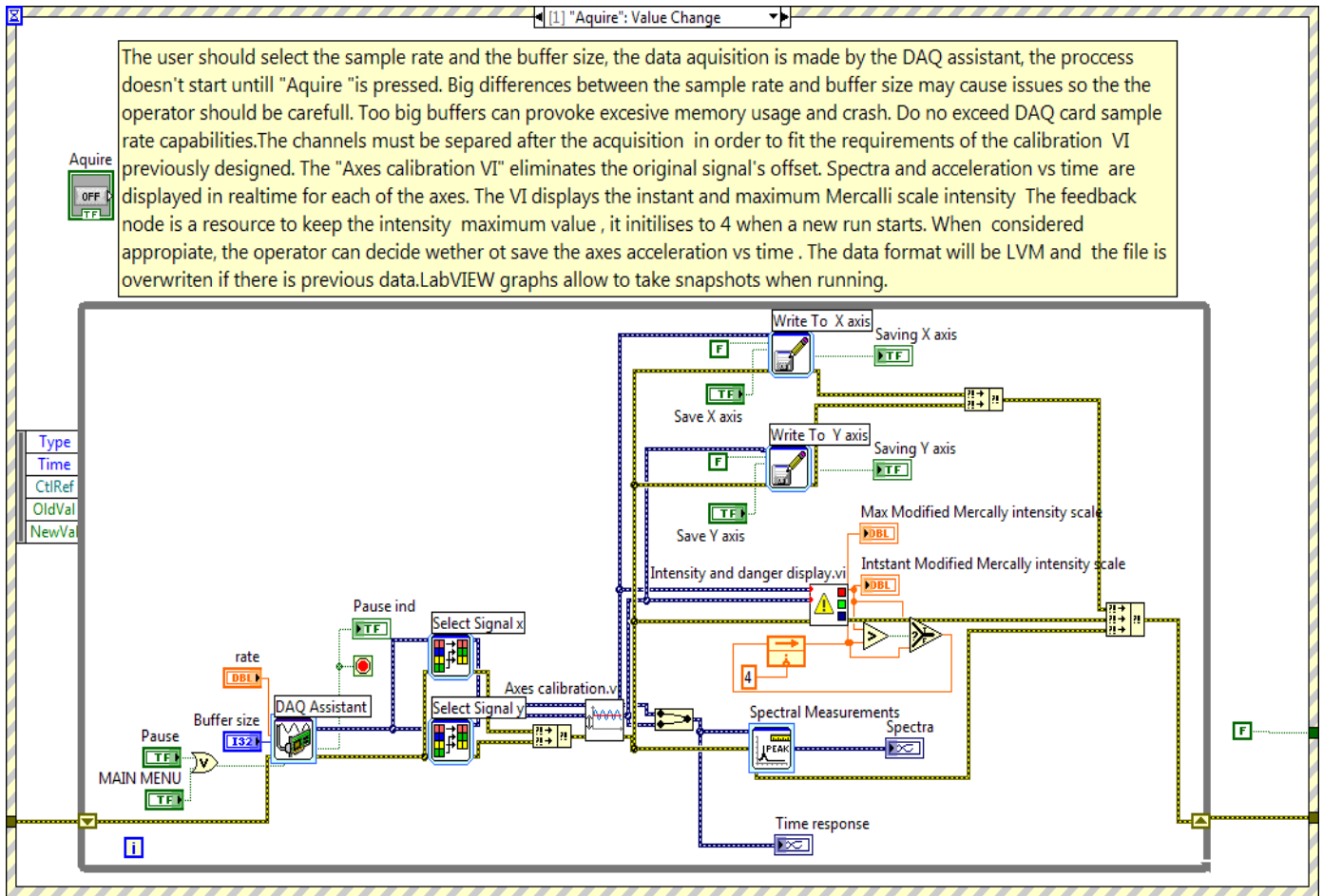


Figure B.3: Vibration DAQ VI. Acquire event

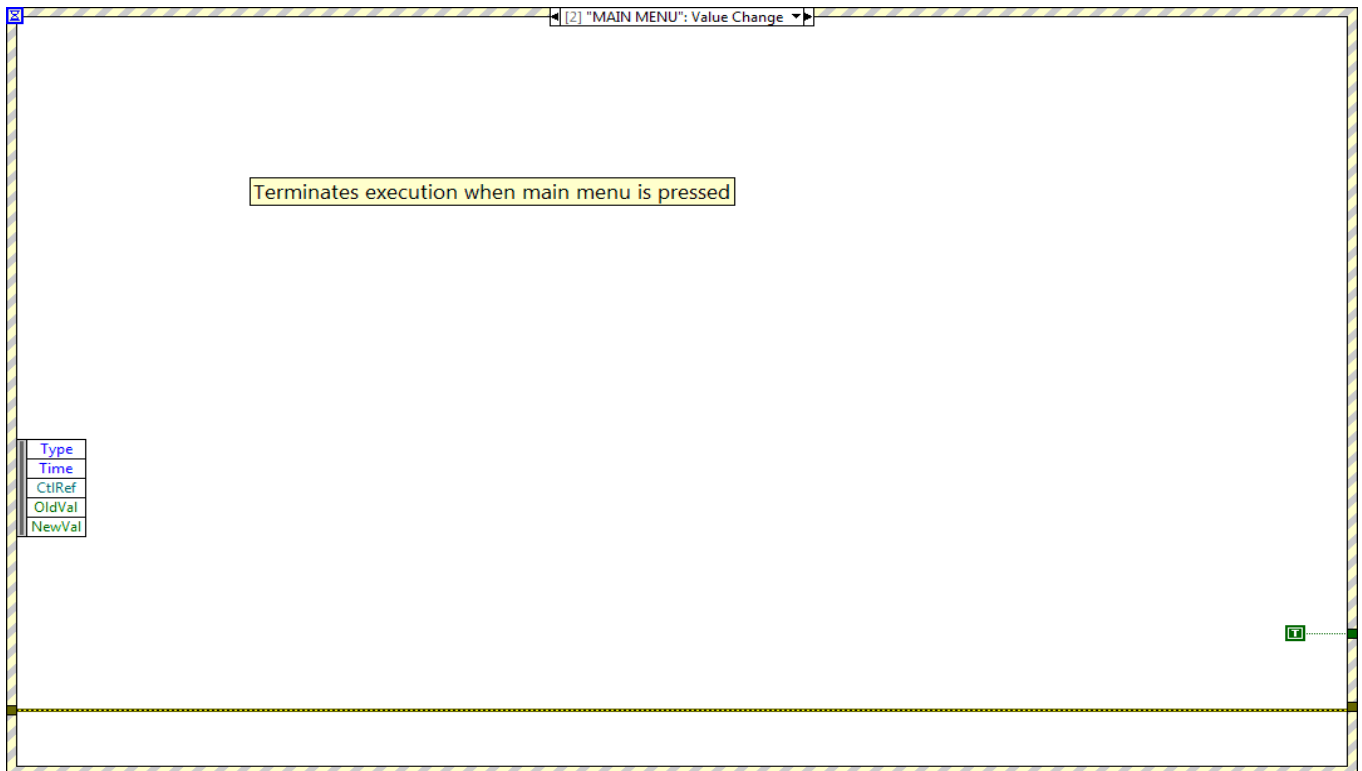
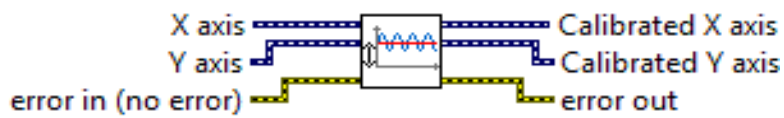


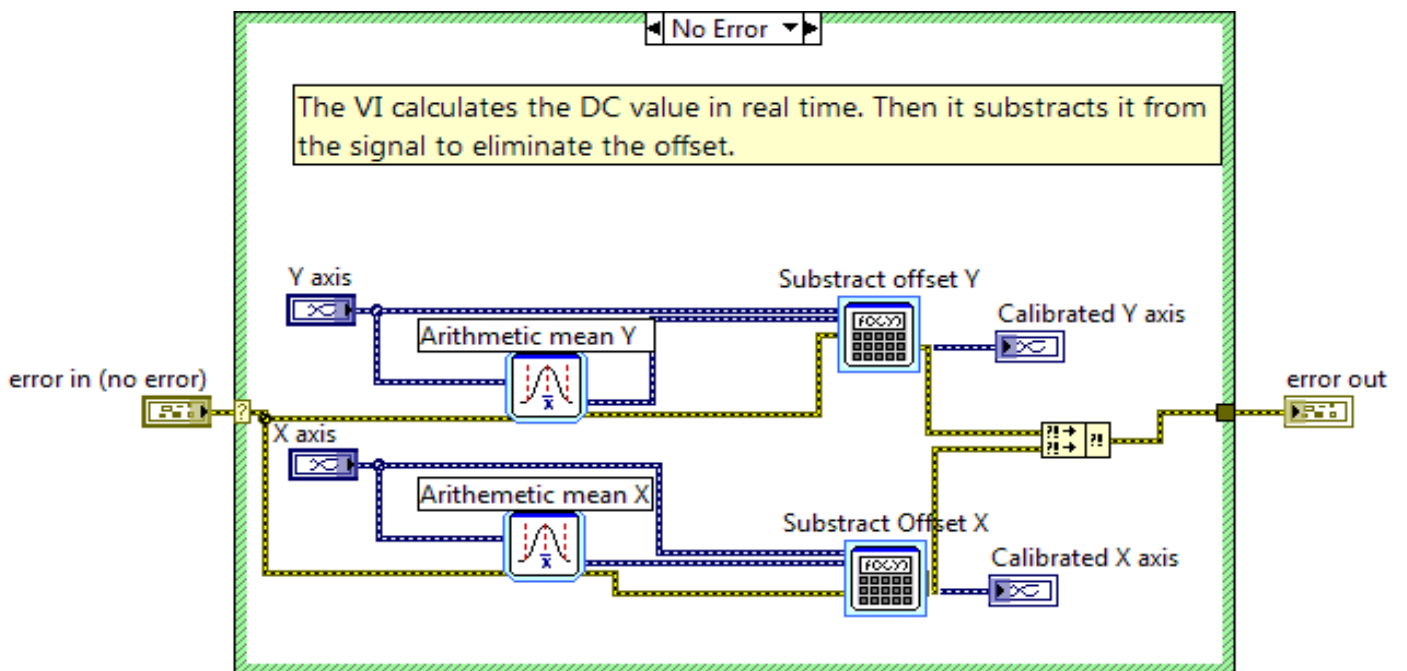
Figure B.4: Vibration DAQ VI Main menu event



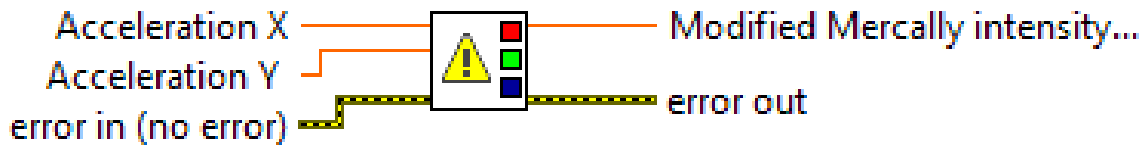
FigureB.5: Vibration DAQ VI pause event



FigureB.6: Axes calibration VI icon



FigureB.7: Axes calibration VI block diagram



FigureB.8: Intensity and danger display VI icon

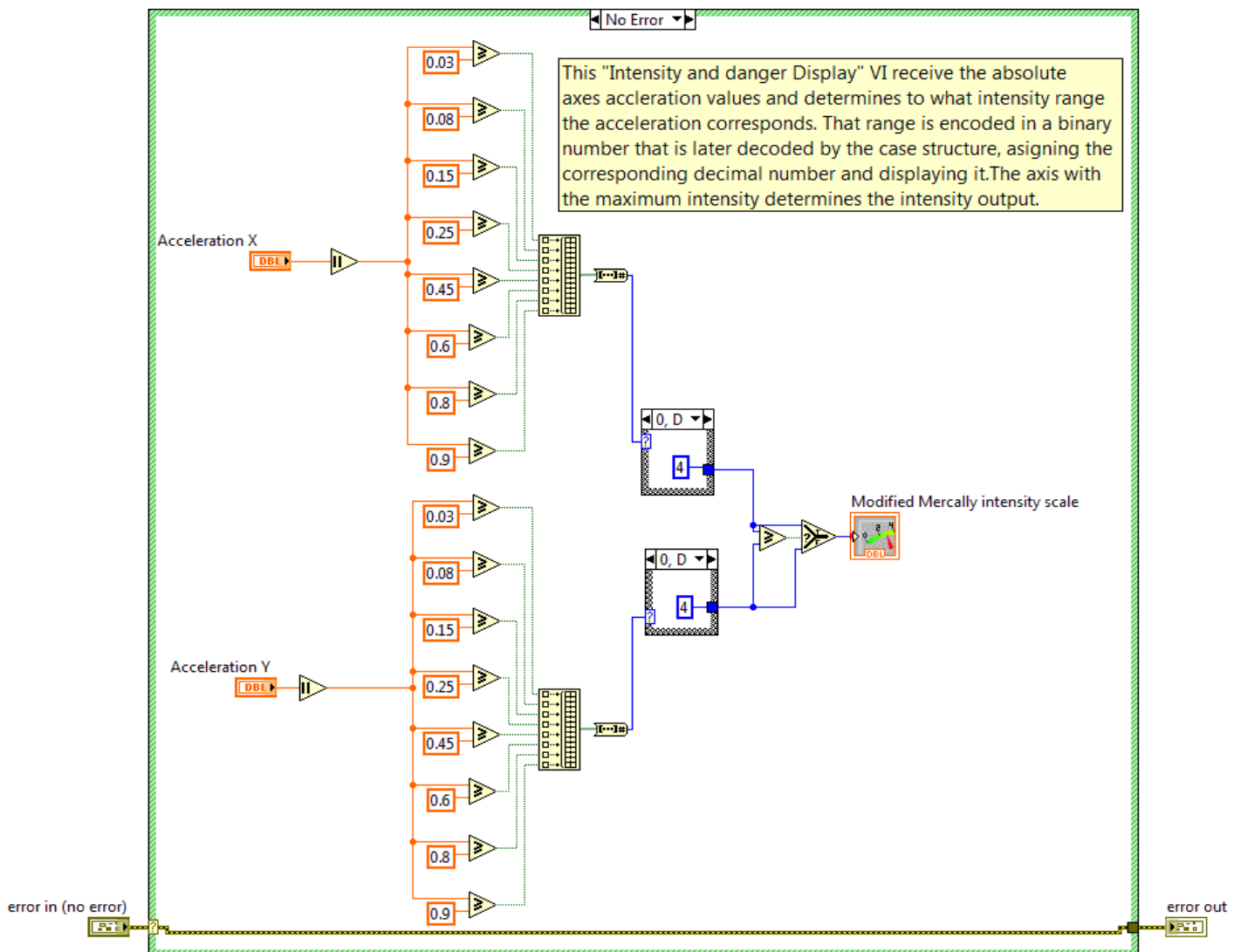
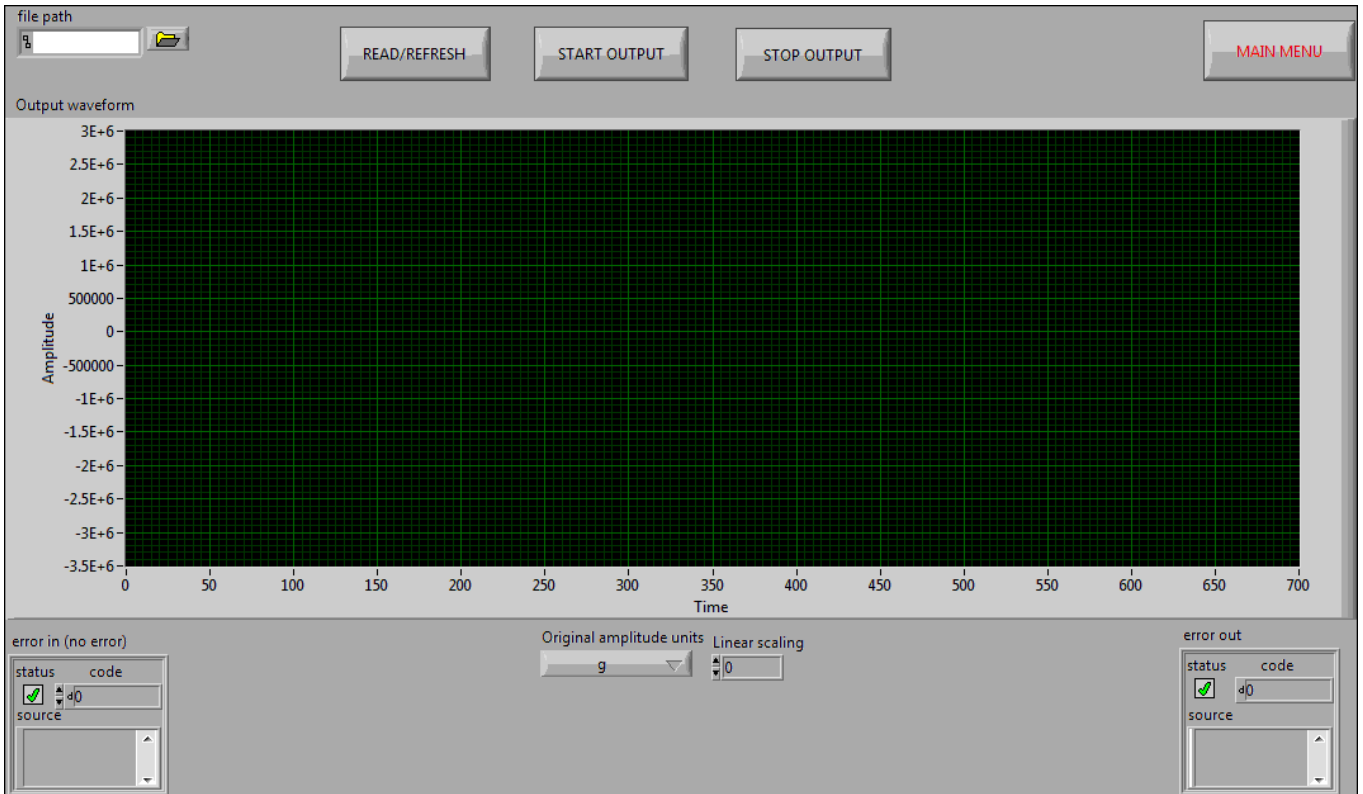
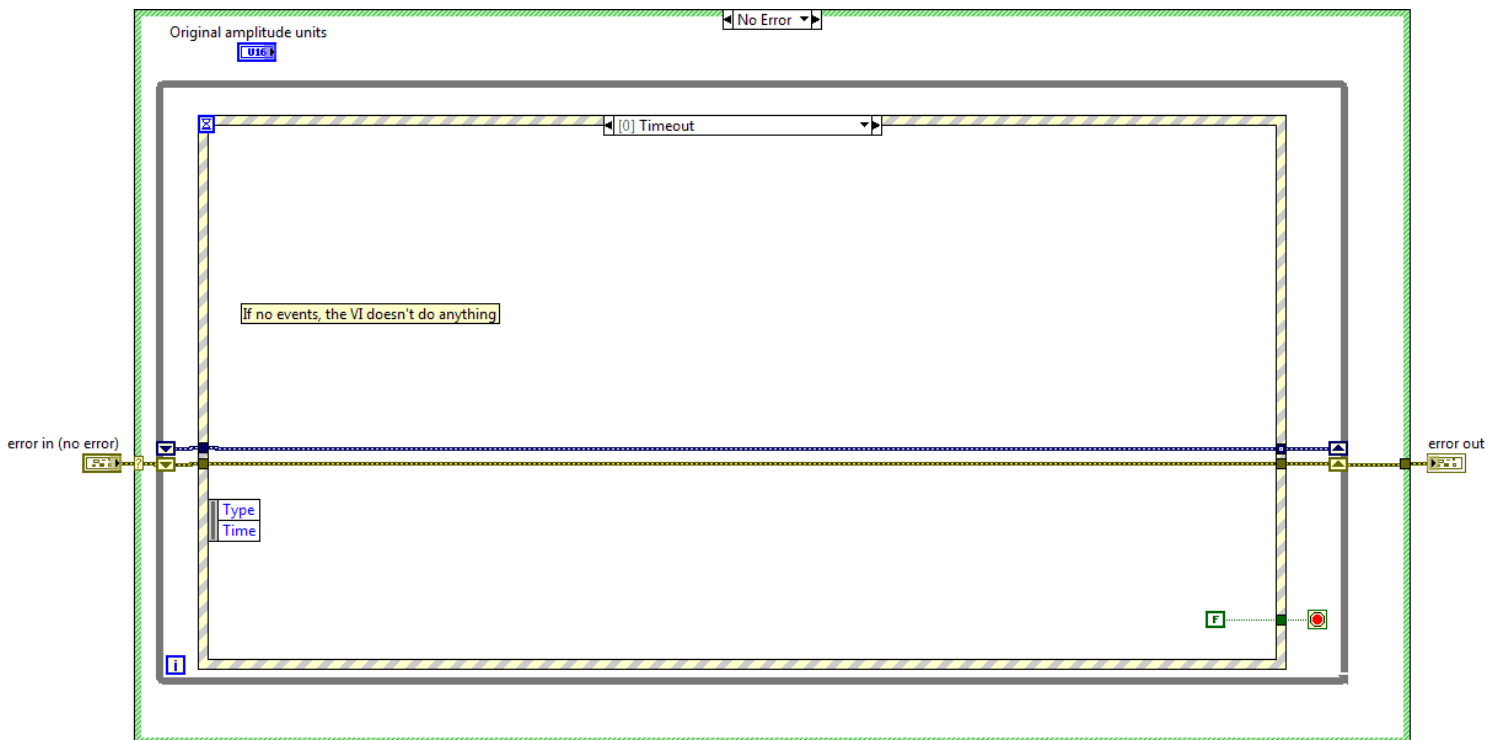


Figure B0.9: Intensity and danger display VI front panel

Appendix C: Detailed analogue output software



FigureC.1: Analogue output VI front panel



FigureC.2: Analogue output VI .Timeout event

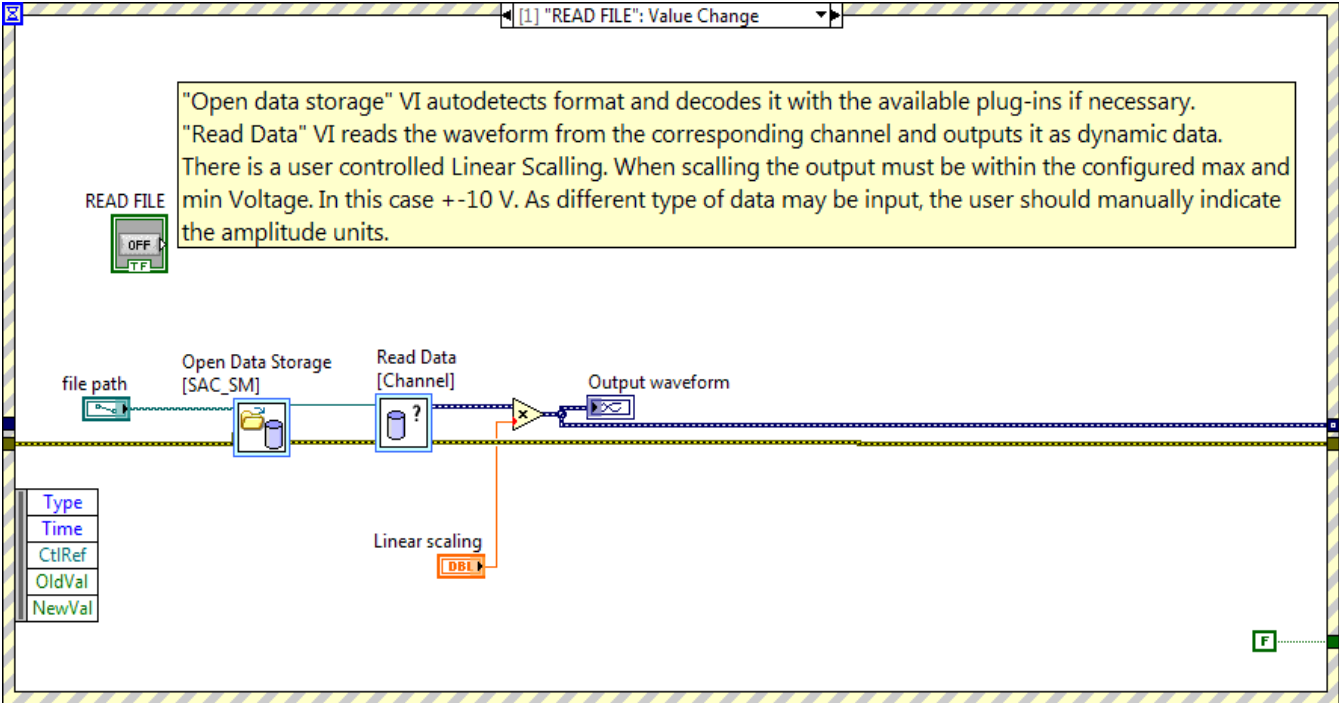


Figure C.3: Analogue output VI. Read file event.

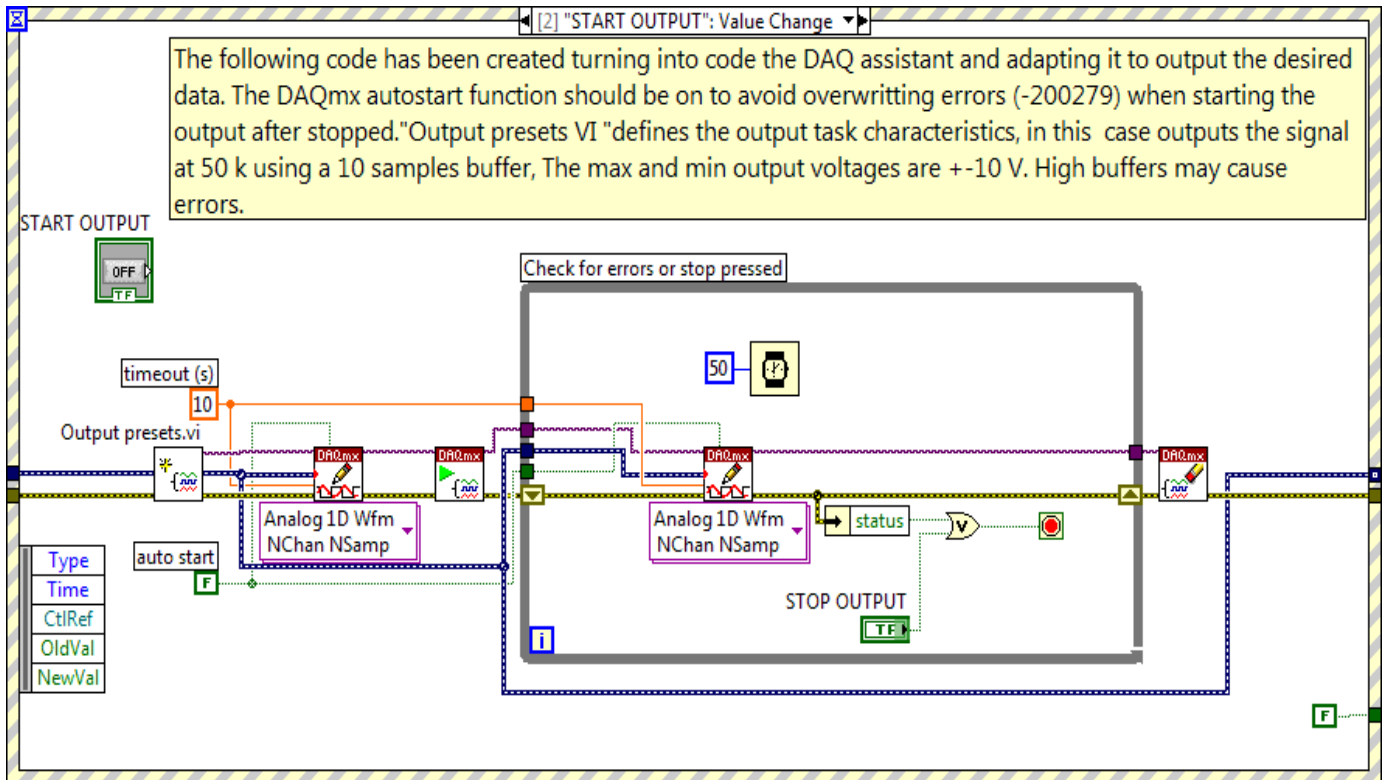


Figure C.4: Analogue output VI. Start output event.

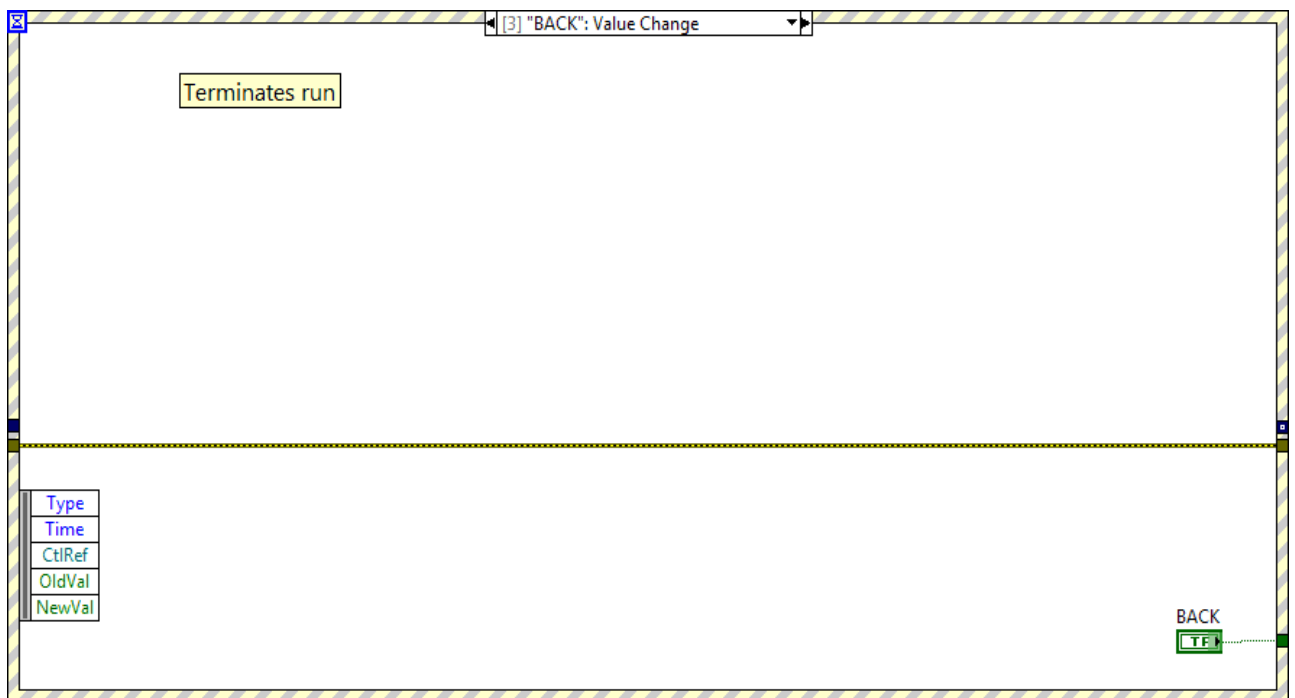


Figure C. 5: Analogue output VI. Back event

Appendix D: Brief Instructions for use

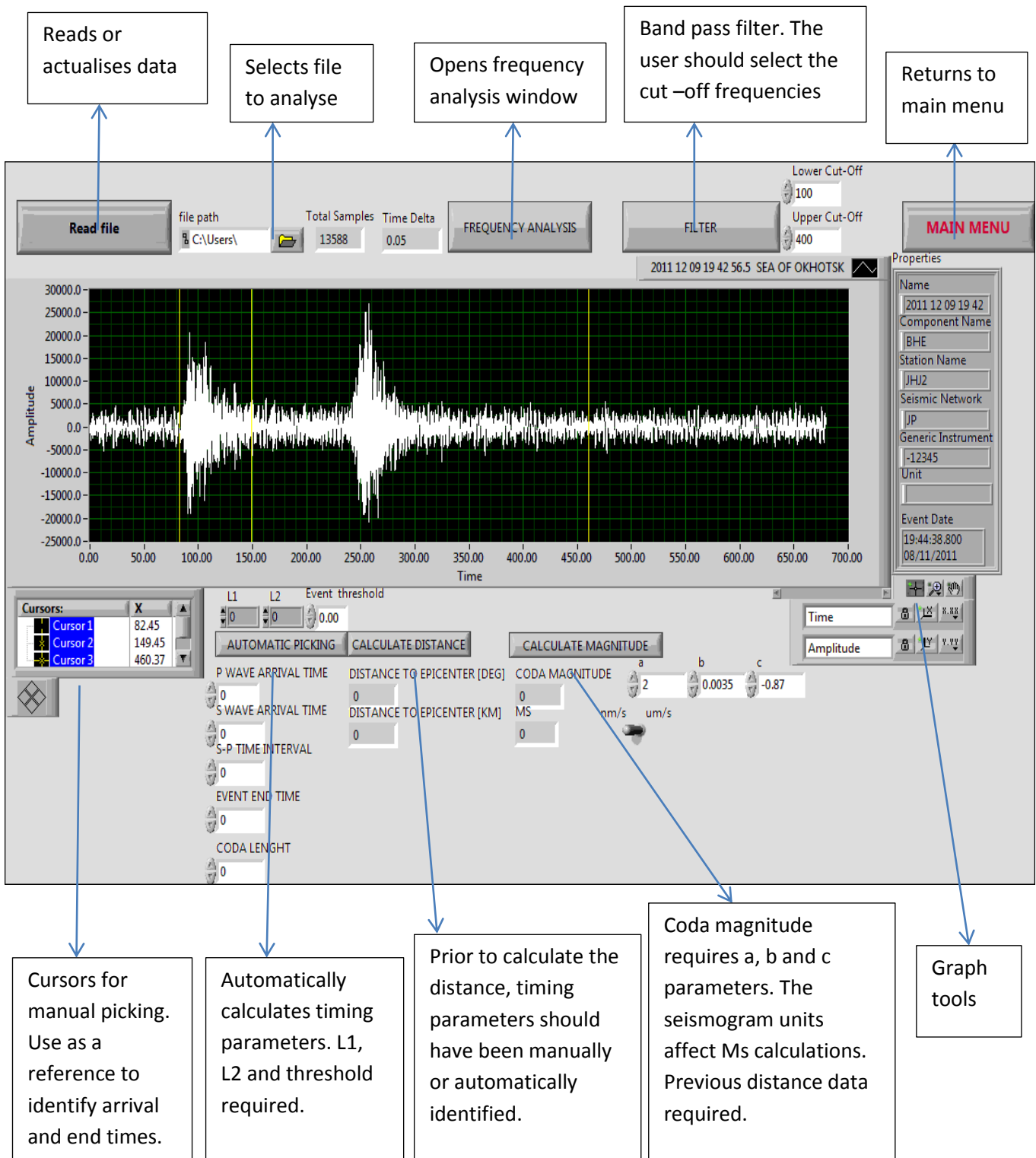


Figure D.1: Seismic analysis main window instructions

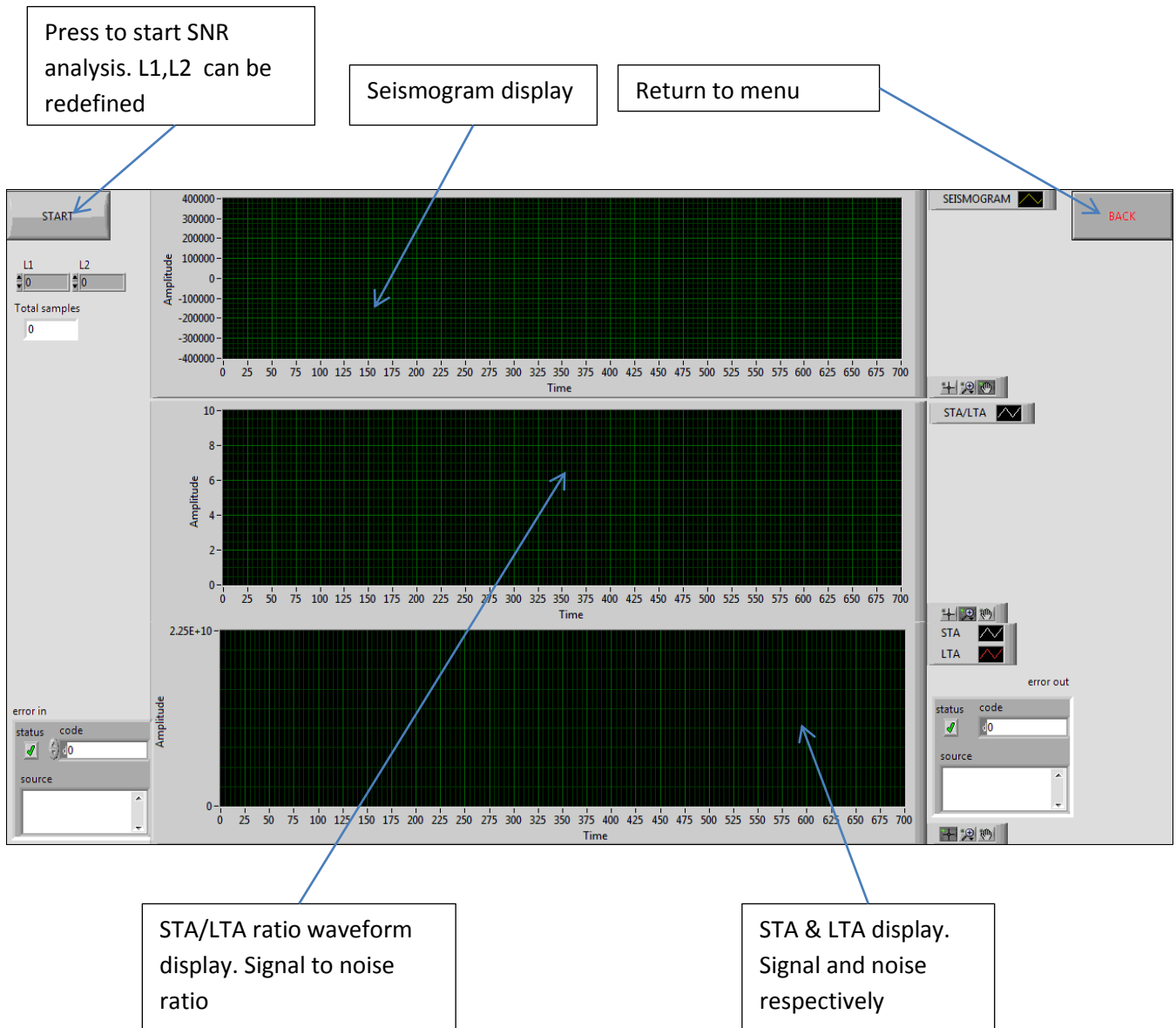


Figure D.2: STA LTA ratio VI front panel instructions

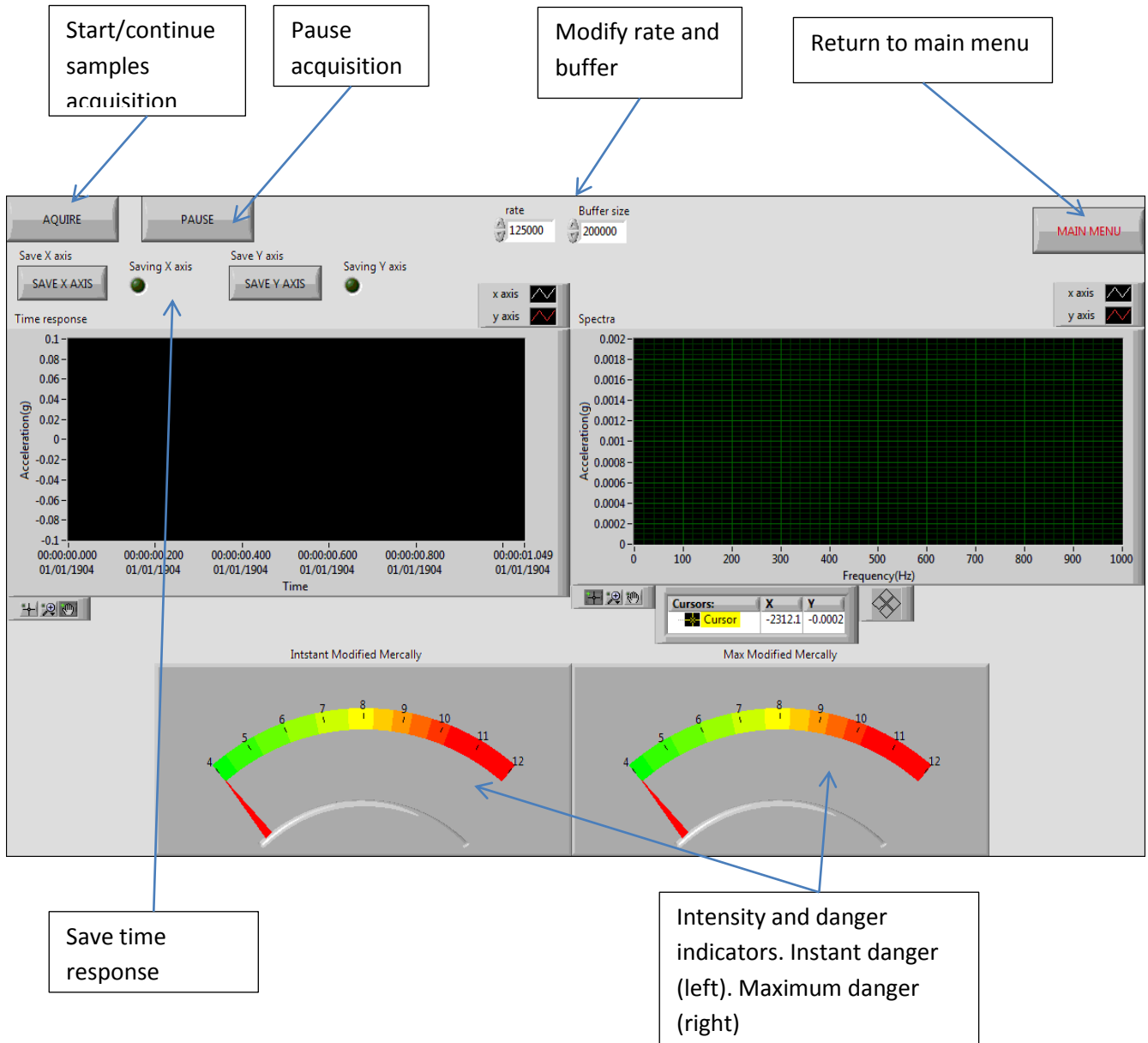


Figure D.3: Vibration DAQ VI instructions

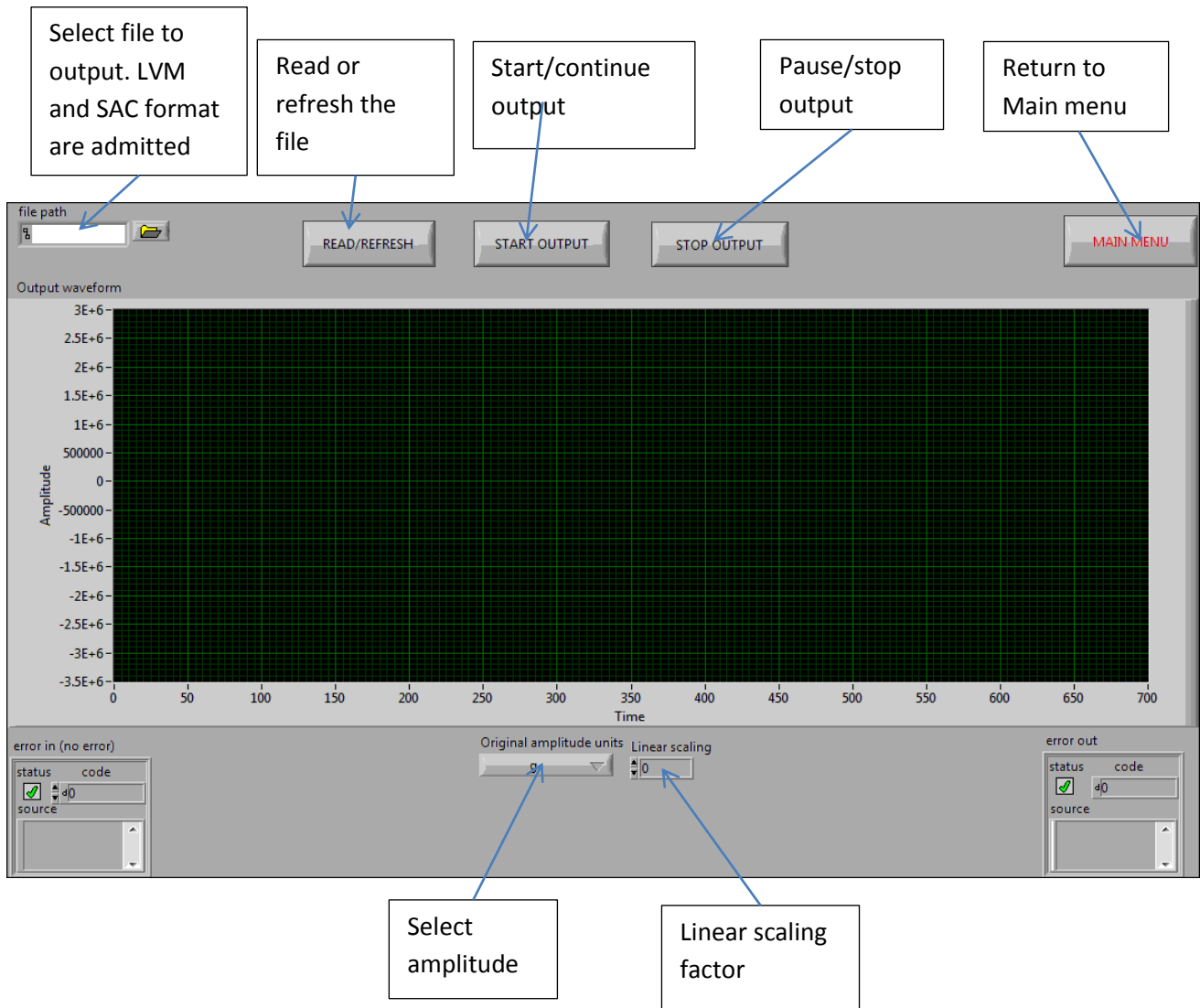
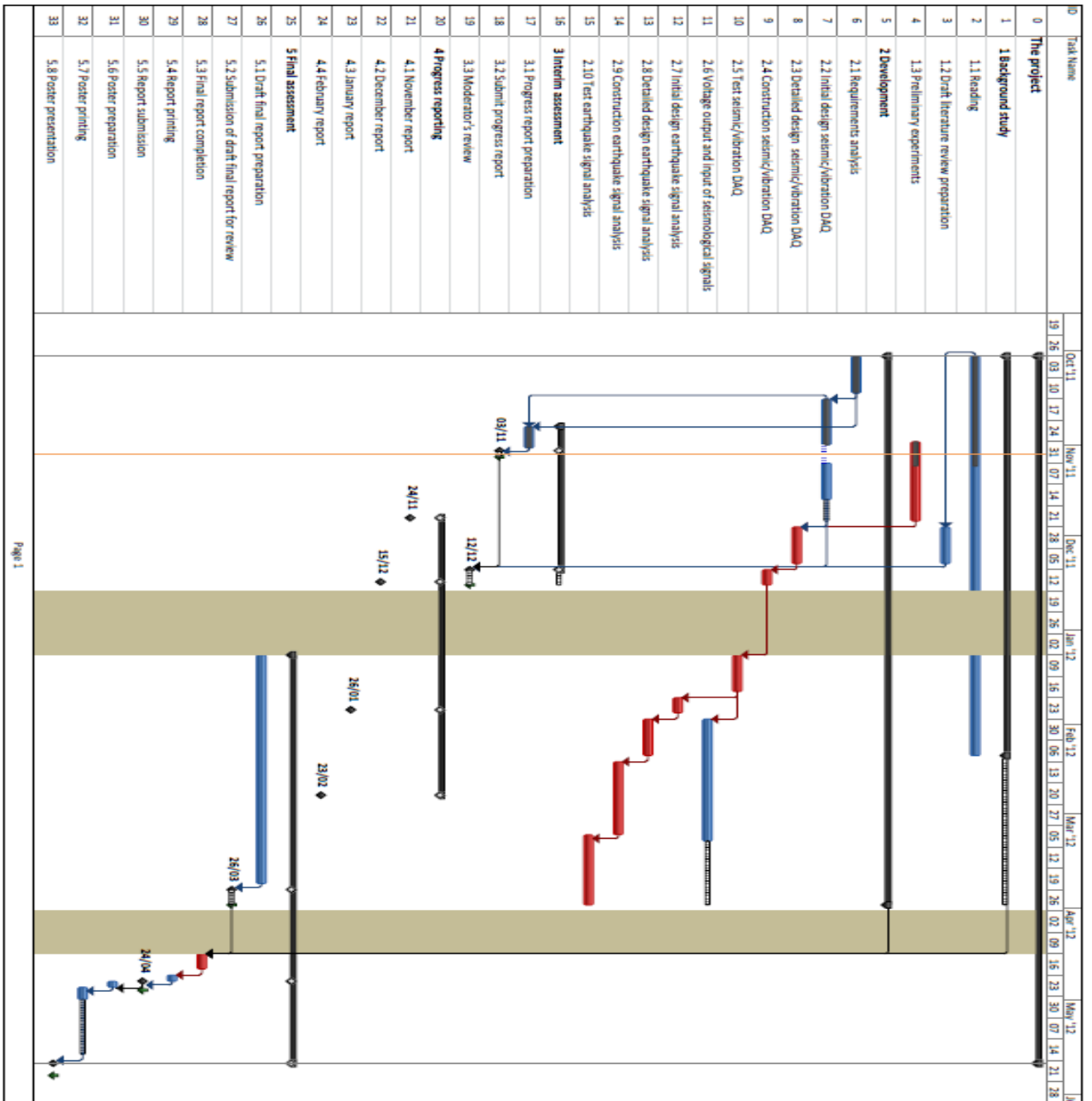


Figure D.4: Analogue output VI instructions

Appendix E : Planning documents

Gantt Diagram



Page 1

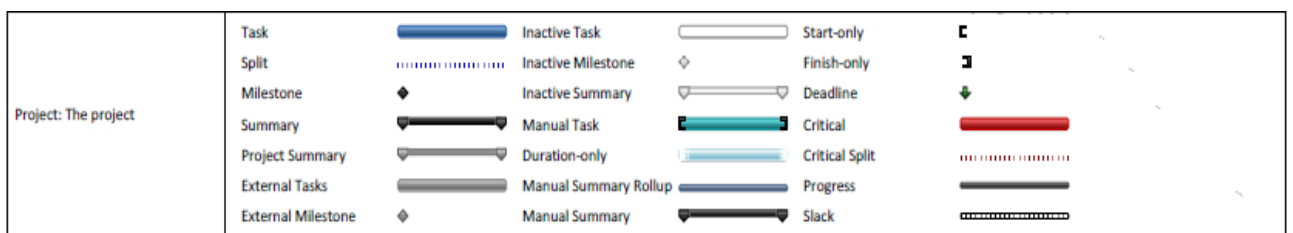


Figure D.1: Gantt diagram

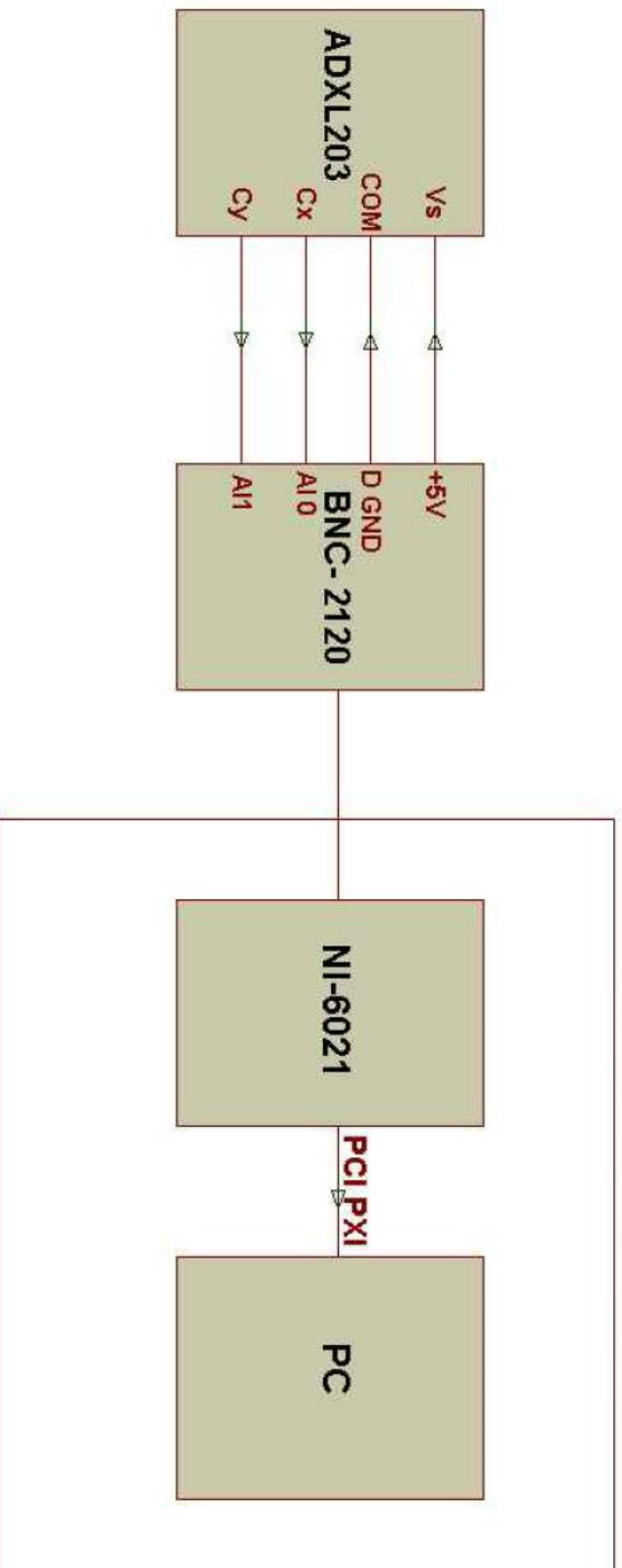
Risk register

Risk	Before mitigation			Mitigation plan	After mitigation			
	likelihood	consequence	risk level		likelihood	consequence	risk level	
Problems with Seismological Data management in Labview	Medium	Severe	2	Get different kinds of data formats and plugins; NI developer zone forum; labview internet resources	Medium	Moderate	5	Use of user designed plugins; develop a VI to adapt the data
Problems dealing with complex earthquake seismological data analysis	High	Moderate	3	Use of adequate algorithms for the level of knowledge on the issue; study of practical examples	Medium	Moderate	5	Selection of the most relevant and useful possible parameters.
Delay due to non-availability of DAQ hardware.	High	Severe	1	Design VIs to be able to operate with and without DAQ hardware.	High	Minor	6	Simulate signals in software.
Loss of data	Medium	Severe	2	Regular backup	Medium	Minor	8	Recover data from backup.
Non-availability of Seismic Data	Low	Severe	4	Different Data Sources	Low	Minor	9	Get the Data from another source
Generation/finding of suitable vibration for testing	Low	Moderate	7	Reasonable bandwidth resolution of the design to detect different types of vibration signals	Low	Minor	9	Manual generation of signals to analyse
Cheap suitable vibration accelerometer availability	Low	Moderate	7	Acquire enough knowledge about the device to be able to distinguish the relevant characteristics and widen the purchase options.	Low	Minor	9	Use of general purpose accelerometer.

Figure D.2: Risk register

Appendix F: DAQ Circuit and PCB plans

LABORATORY COMPUTERS



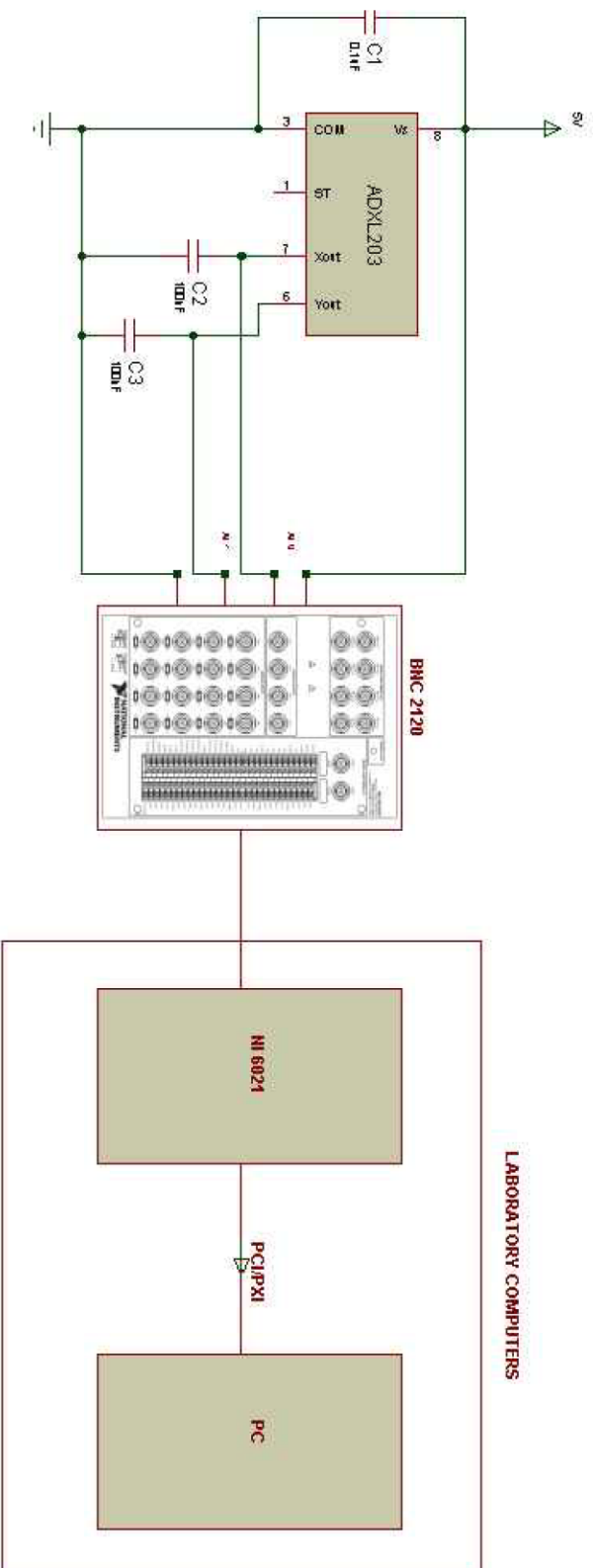
Issue	Date	Description of Modification	By
-	-	-	-
-	-	-	-
-	-	-	-
-	-	-	-
-	-	-	-
A	-	-	SG



Drawn By	Morano Martinez
Date Drawn	24/04/2012
Scale	No scale
Client	UCLAN
Clients Ref	

Block Diagram

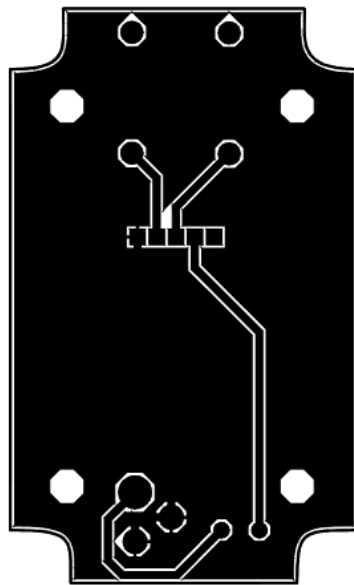
Drg. No.	A4	Issue	1
----------	----	-------	---



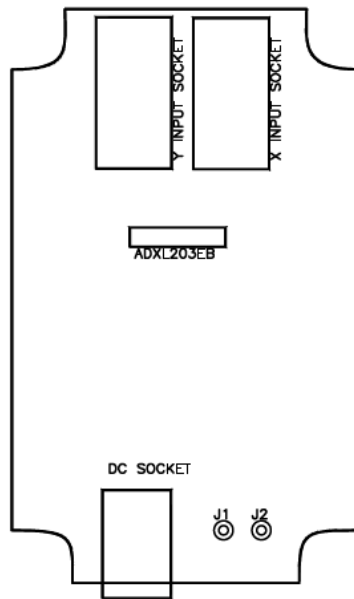
Issue	Date	Description of Modification	By
-	-	-	-
-	-	-	-
-	-	-	-
-	-	-	-
-	-	-	-
A	-	-	SG

		Drawn By	Martino Martinez
		Date Drawn	24/04/2012
		Scale	No scale
		Client	UCLAN
Client's Ref			

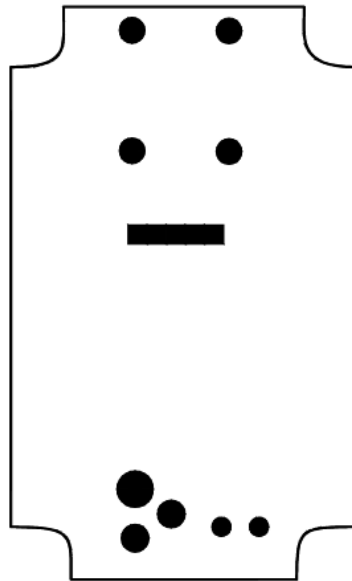
<h1>DAQ Schematic Circuit</h1>		Drq. No.	A4	Issue	2



-	-	-	-	Drawn By	Mariano Martinez	<p style="text-align: center;">PCB Bottom Copper</p>
-	-	-	-	Date Drawn	24/04/2012	
-	-	-	-	Scale	1:1	
-	-	-	-	Client	UCLAN	
A	-	-	SG	Clients Ref		
Issue	Date	Description of Modification	By			<p style="text-align: center;">  Issue 3 </p>



-	-	-	-	Drawn By	Mariano Martinez	<p style="text-align: center;">PCB Top Silk</p> 	<p style="text-align: center;">Issue 4</p>
-	-	-	-	Date Drawn	24/04/2012		
-	-	-	-	Scale	1:1		
-	-	-	-	Client	UCLAN		
A	-	-	SG	Clients Ref			
Issue	Date	Description of Modification	By	Clients Ref			



-	-	-	-	Drawn By	Mariano Martinez	<p style="text-align: center;">PCB Solder resist</p>
-	-	-	-	Date Drawn	24/04/2012	
-	-	-	-	Scale	1:1	
-	-	-	-	Client	UCLAN	
A	-	-	SG	Clients Ref		
Issue	Date	Description of Modification	By			
						Issue 6

Appendix G: DAQ hardware components list

Description	Manufacturer	Package	Quantity
Capacitor(100nF)	Multicomp	0805	2
Capacitor (0.1 μ F)	Multicomp	0805	1
ADXL203 MEMS accelerometer	Analogue Devices	5mm x 5mm x 2mm LCC	1
ADXL203EB Evaluation Board	Analogue Devices	-	1
C1553ATNAE Switch	Archoelectric switches	-	1
2.1 DC Jack	Dongguan HaoyuElectronics	-	1
MP-205 2.1 DC plug	Multicomp	-	1
4mm Banana jack	Multicomp	-	2
NI 6021DAQ card	National Instruments	-	1
BNC 2120 Connector socket	National Instruments	-	1
PCB	UCLAN	-	1
1591XXMS General purpose enclosure	Hammond Manufacturing		1
BNC Lead(BNC plug-4mm banana plug)	-	-	2
5 way 2.54 mm header	-	-	1
Double sided tape	-	-	1
Superglue	-	-	1

Table G.1 DAQ hardware component list

References

1. Central Weather Bureau. (2012). *FAQ for earthquake*. Retrieved 4 2012, from <http://www.cwb.gov.tw/V7e/knowledge/encyclopedia/eq004.htm>
2. U.S. Geological Survey. (2010, 3). *Explanation of Parameters*. Retrieved 12 2011, from Geologic Hazards Science Center: <https://geohazards.usgs.gov/deaggint/2002/documentation/parm.php>
3. Analog Devices. (2011). *ADXL103/ADXL203 Datasheets*. Retrieved 03 2011, from Analog Devices: http://www.analog.com/static/imported-files/data_sheets/ADXL103_203.pdf
4. Aszkler, C. (2005). *The Principles of Acceleration, Shock, and Vibration Sensors*. Retrieved 03 2011, from Sensemag: http://www.sensormag.com/sensors/acceleration-vibration/the-principles-acceleration-shock-and-vibration-sensors-574?page_id=4
5. Attri, R. K. (2004). *Developing of software for seismic & vibration analysis ussing C++*.
6. Attri, R. K. (2005). *Backend Framework and software approach to compute earthquake parameters from signals recorded from instrumentations system*. Working papers.
7. Barnes, J. R. (2011, December). *EMC/EMI/ESD Standards for Commercial Electronic Products*. Retrieved March 2012, from dBi Corporation: <http://www.dbicorporation.com/standard.htm#eu>
8. British Geological Survey. (2011). *Earthquakes*. Retrieved 10 2011, from British Geology Survey: <http://www.bgs.ac.uk/discoveringGeology/hazards/earthquakes/home.html>
9. British Geological Survey. (2012). *Earthquakes and data*. Retrieved 3 2012, from British Geological Survey: <http://www.bgs.ac.uk/schoolSeismology/schoolSeismology.cfc?method=viewQuakes>
10. Bukhari, A. R. (2000, 1). *Use Accelerometers For Vibration Measurement And Control*. Retrieved 11 2011, from Electronicdesign: <http://electronicdesign.com/article/test-and-measurement/use-accelerometers-for-vibration-measurement-and-c>
11. COSMOS. (2012). *Consortium of Organisations for Strong-Motion Observation System*.
12. De Silva, C. W. (2007). *Vibration monitoring, testing, and instrumentation*. CRC Press.
13. Endevco. (2006). *Guide to adhesively mounting accelerometers*. Retrieved 3 2012, from Endevco: http://www.endevco.com/resources/tp_pdf/TP312.pdf
14. European Strong-Motion Database. (2000). *European Strong-Motion Database*. Retrieved 3 2012, from http://www.isesd.hi.is/ESD_Local/frameset.htm
15. Han, L. (2010). *Microseismic Monitoring and Hypocenter Location*. UNIVERSITY OF CALGARY.
16. Haugen, F. (2008). *Tech teach*. Retrieved 12 2011, from Introduction to labVIEW: <http://techt teach.no/labview/lv85/labview/index.htm>

17. Havskov, J., & Ottemöller, L. (2010). *Routine Data Processing*. Springer.
18. IRIS. (2011). *IRIS Incorporated Resiarch Institution for Seismology*. Retrieved 11 2011, from <http://www.iris.edu/hq/>
19. Kayal, B. J. (2008). *Microearthquake Seismology and Seismotectonics of South Asia*. Springer.
20. Kennett, B. (2009). *Seismic Wave Propagation in Stratified Media*. ANU E Press.
21. Kris L. Pankow, J. C. (2007). *Use of ANSS Strong-Motion Data to Analyze Small Local Earthquakes*. Retrieved 11 2011, from Seismological research letters: <http://srl.geoscienceworld.org/content/78/3/369.extract>
22. Lent, B. (2009). *Simple Steps to Selecting the Right Accelerometer*. Retrieved 03 2009, from Sensemag: <http://www.sensormag.com/sensors/acceleration-vibration/simple-steps-selecting-right-accelerometer-1557>
23. Lynch, J. P. (2003). *Design and performance validation of a wireless sensing unit for structural monitoring aplication*. Stanford: Structural Engineering and Mechanics, Vol. 17, No. 3-4 (2004).
24. Martin, B., & Bono, A. (2010). *Transducers and intrumentations sistemas*. University of Zaragoza.
25. Munro, K. (2004). *Automatic event dection and picking of P wave arrivals*. CREWES.
26. Munro, K. A. (2005). *Analysis of microseismic event picking with applications to landslide and oil-field*. UNIVERSITY OF CALGARY.
27. National Instruments. (2007). NI602x Specifications.
28. National Instruments. (2008). BNC 2120 Instalation guide.
29. National Instruments. (2008). DAQ M series Manual.
30. National Instruments. (2008). DAQ System Overview. *NI 602X Manual*. National Instruments Corporation.
31. National Instruments. (2010). VI examples. National Instruments.
32. National Instruments. (2011). *Supported Data pluggins*. Retrieved 11 2011, from National Instruments Developer Zone: <http://zone.ni.com/devzone/cda/tut/p/id/4065>
33. National Instruments. (2012). *National Instruments support*. Retrieved 4 2012, from National instruments: <http://www.ni.com/support/>
34. NI Instructors. (2011, 9). *Gathering Signal Values Passed a Threshold Value VI*. Retrieved from <https://decibel.ni.com/content/docs/DOC-18091>
35. NIED. (1996). *K-NET*. Retrieved 11 2011, from K-NET: <http://www.k-net.bosai.go.jp/>

36. PREPA.R.E. (2008). *Measuring and Recording Intensity, Magnitude, Energy and Acceleration*. Retrieved 1 2012, from PREPA.R.E: <http://www.prepareinc.us/Chapter%20%20-%20Measuring%20and%20Recording%20-%20Intensity,%20Magnitude%20and%20Energy.pdf>
37. Renken, B. (1991). *Info-LabVIEW*. Retrieved 11 2011, from Info- LabVIEW: <http://www.info-labview.org/about.html>
38. Santoso, D. R. (2010). A simple instrumentation system for large structure vibration monitoring. *Indonesian Journal of Electrical engineering*.
39. SCEDC. (2011). *Southern California Earthquake Data Center*. Retrieved 04 2011, from <http://www.data.scec.org>
40. Turk et al, A. S. (2011). *Subsurface sensing*. John Wiley & Sons.
41. Turkel, S. (2000, August). *Controlling EMI Noise Problems*. Retrieved March 2012, from EC&M: http://ecmweb.com/mag/electric_controlling_emi_noise/
42. US Geological Survey. (2009). *The Modified Mercalli Intensity Scale*. Retrieved 1 2012, from <http://earthquake.usgs.gov/learn/topics/mercalli.php>
43. W.H.K Lee et al. (1972). *A method of estimating magnitude of local earthquakes from signal duration*. United States Department of Interior Geological Survey.
44. Wenzel, H., & Pichler, D. (2005). *Ambient vibration monitoring*. John Wiley & Sons LTD.